Towards a new view on metabolic networks: Automated reconstruction and large-scale computational analysis applied to *Dinoroseobacter shibae*

Von der Fakultät für Lebenswissenschaften

der Technischen Universität Carolo-Wilhelmina zu Braunschweig

zur Erlangung des Grades

eines Doktors der Naturwissenschaften (Dr. rer. nat.)

genehmigte

D i s s e r t a t i o n

von René Rex
aus Marburg

1. Referentin oder Referent: Prof. Dr. Dietmar Schomburg
2. Referentin oder Referent: Prof. Dr. Sándor Fekete
eingereicht am: 17.10.2012
mündliche Prüfung (Disputation) am: 19.12.2012

Druckjahr 2013

CONTENTS

1

INTRODUCTION

> *I cannot say whether things will get better if they change; what I can say is they must change if they are to get better.*
>
> — Georg Christoph Lichtenberg

Our knowledge about the biochemical reactions taking place in all kinds of living organisms and their underlying molecular machinery grew steadily during the last decades. The explosion of entries in genomic and biochemical databases is a clear indicator for this fact (Pagani *et al.*, 2012; Scheer *et al.*, 2011; Caspi *et al.*, 2012; Kanehisa *et al.*, 2012). However, as long as these pieces of information are not systematically put into context, the drawing of wider conclusions remains unfeasible. To address this problem, a new subfield combining computer science with systems biology emerged: Computational Systems Biology (Kitano, 2002). In this field, computational methods and concepts are applied to biological questions. On the one hand, these methods can be used to mine existing data sets for new insights and on the other hand, a new hypothesis can be tested or proposed using simulations of biological systems. This work is focused on the later aspect and especially on simulations of metabolic reactions taking place in a growing cell.

While the most accurate representation of chemical fluxes in an organism would be a set of time-dependent differential equations this approach denoted *dynamic modeling* is often impractical (Covert *et al.*, 2001). This is due to the fact that kinetic

parameters must be determined for each reaction in the model. A common technique to circumvent this obstacle is to limit the simulation to steady-state conditions (Burton, 1939). In this way, the kinetic parameters vanish and the problem becomes tractable – even on the genome-scale – by the means of linear optimization. Hence, the so-called *constrained-based modeling* has been used widely to study genome-scale metabolic networks of a multitude of organisms (Oberhardt *et al.*, 2009; Kim *et al.*, 2011).

Nevertheless, there is still a large gap between the number of sequenced genomes (2907 completed sequencing projects are reported by Pagani *et al.*, 2012) and the number of reconstructed metabolic networks (62 according to Kim *et al.*, 2011). The cause is that the reconstruction of a carefully curated genome-scale metabolic network is still a time-consuming process, which can take several months up to two years (Thiele and Palsson, 2010). Usually, a subsequent analysis of the model and its predictions is the next step after completing the reconstruction process. At this point, another gap becomes apparent. There is an overwhelming multitude of algorithms and software tools carrying out all kinds of simulations and analyses (Kim *et al.*, 2011) but most of them fall short if it comes to the interpretation of the numbers they produce. Hence, researchers often resort to cluttered spread sheets or manually laid out metabolic maps. To put it in a nutshell, the tools assisting in reconstruction of metabolic networks or in interpretation of the numbers they produce cannot keep pace with their data-producing counterparts.

This work paves the way for an automated reconstruction process for metabolic networks (Chapter 2), which significantly speeds up several steps of the laborious reconstruction process. Furthermore, this work introduces AMEBA, a software which identifies and interactively visualizes metabolic branch points and thus eases the interpretation of fluxes through metabolic networks (Chapter 3). Both methods were successfully applied to reconstruct and analyze the metabolic network of the marine

α-proteobacterium *Dinoroseobacter shibae* with respect to various environmental conditions (Chapter 4). In the same chapter, the usefulness of a large-scale computational analysis in contrast to the usual approach testing only a limited number of scenarios is demonstrated.

1.1 Terms and preliminaries

This section briefly introduces general terms from biology and computer science. A complete list of all terms and abbreviations used in this work can be found in the index starting on page 101.

1.1.1 *Biology*

All living organisms we see today have developed during the course of evolution from a common ancestor. The intermediate steps during this process can be used to define a hierarchical classification with several layers called taxa: the taxonomic tree. One of the first branches in the taxonomic tree separates the organisms without a cell nucleus (prokaryotes) from those with a nucleus (eukaryotes). This works is focused on prokaryotic organisms.

The largest part of a prokaryotic genome is organized in a structure commonly called prokaryotic chromosome. In contrast, plasmids are much smaller pieces of DNA, which can also be transfered from one to an other organism. If a gene occurs at multiple positions in the genome, all copies are called paralogous. Furthermore, if an organism has one or more genetic modifications compared to the wild type, it is called a mutant. To uniquely identify a gene, we use locus tags as an identifier throughout this work. A locus tag consists of two parts connected by an underline. It starts with a prefix, which often is

an abbreviation of the organism's name. The second part is the sequential number of this particular gene in the genome.

A large fraction of all genes in a prokaryotic genome code for proteins with a catalytic function commonly known as enzymes. Based on the chemical reaction an enzyme catalyzes, a systematic classification of the enzyme is given by its enzyme commission number (EC number). This number consists of four parts separated by a dot. If read from left to right, each part describes the reaction in increasing detail. However, the exact amount of chemical compounds, which are consumed and produced during a single reaction is only given by the stoichiometric factors in the reaction equation. Compounds which are not the main subject of a reaction but are also altered during the process (e. g., because they provide an electron) are called cofactors.

Throughout this thesis, the term *scenario* is used to describe the physiological state of an organism and its environment, which is described by the parameters of a simulation.

1.1.2 *Computer Science*

A relational database consists of a set of clearly structured tables, which can be used to store large data sets efficiently. Furthermore, the database enables an easy access of the data for further processing.

Linear programming is an optimization method which can be used to find the best values for a set of variables, which maximize or minimize a given linear objective function. Usually, the variables are subject to constraints given as equalities or inequalities, which must be fulfilled additionally. If interpreted geometrically, these constrains describe a polytope, a convex geometric object consisting of edges and faces. In this work, we use a freely available implementation of a linear problem solver to handle such optimization problems.

2

A METHOD FOR SEMI-AUTOMATED RECONSTRUCTIONS OF GENOME-SCALE METABOLIC NETWORKS

> *The machine does not isolate man from the great problems of nature but plunges him more deeply into them.*
>
> — Antoine de Saint Exupéry

2.1 Introduction

Genome-scale metabolic models summarize the knowledge about an organism and thus allow predictions about its features and capabilities (Lacroix *et al.*, 2008; Durot *et al.*, 2009). Hence, the reconstruction of an accurate metabolic network is a valuable but also time-consuming task, which involves several distinct steps (Thiele and Palsson, 2010). The process includes the identification of metabolic enzymes in the genome and the assembly of a draft reconstruction. Next, the reachability of all biomass compounds has to be tested and gaps in the corresponding synthesis pathways need to be filled if necessary. Finally, the resulting network should be validated against experimental data.

Such models can be used to simulate and predict the organisms' response to genetic alterations or to changed environmental conditions and thus guide wet-lab experiments (Oberhardt

et al., 2009). Furthermore, a model assists in the interpretation of experimental data by serving as an easily accessible reference and as a testbed for hypotheses generated from experimental results. Another field of application for genome-scale metabolic models is metabolic engineering. In this field, the model can give important hints which modifications may lead to the desired result – e. g., the overproduction of a certain compound (Kjeldsen and Nielsen, 2009). Even the reconstruction process itself yields valuable knowledge because filled gaps in essential metabolic pathways indicate that there might exist homologous genes in the genome still lacking an annotation (Henry *et al.*, 2010). Finally, from a partial automation of the reconstruction process, additional advantages arise: 1) acceleration of the total process and 2) avoidance of errors caused by oversight. This is especially true if multiple networks of related organisms should be reconstructed. In this case, the automation additionally guarantees reusability.

In recent years, two platforms for an automated reconstruction were proposed. The first one named *SEED Model* is purely web-based (DeJongh *et al.*, 2007; Henry *et al.*, 2010). SEED Model covers several steps of the reconstruction process including genome annotation, creation of gene-protein-reaction associations, and gap-filling using mixed integer linear programming. The pool of biochemical reactions used for reconstruction of metabolic networks in SEED Model stems from KEGG (Kanehisa *et al.*, 2012) and various published genome-scale metabolic models. In contrast, the second platform *Pathway Tools* combined with its extension *MetaFlux* (Karp *et al.*, 2010; Latendresse *et al.*, 2012) is a stand-alone application based on the MetaCyc database (Caspi *et al.*, 2012). Furthermore, Pathway Tools depends on a preexisting genome annotation which can be imported into a pathway/genome database. Pathways existing in the organism in question are predicted by the software based on known metabolic pathways stored in MetaCyc. MetaFlux also uses mixed integer linear programming to identify and fill gaps in the metabolic network. An important prerequisite for

the generation of any predictive model is consistent and complete data. Regarding genome annotations, the method presented in this work takes advantage of the aggregated genome annotations provided by the EnzymeDetector database (Quester and Schomburg, 2011). This database aggregates annotations from different sources and assigns a relevance score to each entry indicating the level of confidence. Hence, the EnzymeDetector database can be used as firm ground to build a metabolic model.

In this chapter, an approach to automatically reconstruct a draft version of a metabolic network based on a given genome annotation is described. Furthermore, a method to extract a high-quality genome annotation from the EnzymeDetector database is introduced.

2.2 Input databases

2.2.1 *EnzymeDetector: enzyme function prediction and annotation database*

The EnzymeDetector database integrates genome annotations from different resources and results of a BLAST search (Quester and Schomburg, 2011; Camacho *et al.*, 2009). Furthermore, each entry has been assigned a so-called relevance score indicating the level of confidence in the source. This score represents either a subsumption of the quality indicators of the BLAST hit or a rating of the source database based on a statistical scoring scheme. If multiple sources annotate the same enzyme for one gene, all corresponding scores are summed up. As of July 2012, the web interface lists aggregated genome annotations of 1301 prokaryotic strains. However, the query method presented in this chapter accesses the annotations directly via the back-end of a relational database system.

2.2.2 *MetaCyc: biochemical reaction and pathway database*

MetaCyc is an on-line resource with a a strong emphasis on metabolic pathways and their distribution over the taxonomic tree (Caspi *et al.*, 2012). Moreover, the database provides information on enzymes and biochemical reactions based on literature citations. The version 16.0 used in this work contains 7893 enzymes, 10262 reactions, and 1842 pathways. All data is freely accessible and provided as flat files in a plain text format. To increase the accessibility of the data during the automated generation, these flat files were parsed and the resulting tables were stored in a relational database system.

2.2.3 *BRENDA: manually curated database on enzymes and their reactions*

The Braunschweig Enzyme Database (BRENDA) holds detailed information on enzymes, ligands, cofactors, and kinetic parameters (Scheer *et al.*, 2011). Most entries are obtained from primary literature and are manually curated. Hence, the BRENDA is a reliable resource for the reconstruction and the manual review of a metabolic network.

2.3 New methods assisting in the reconstruction process

2.3.1 *Querying the EnzymeDetector database*

To obtain a consistent genome annotation from the EnzymeDetector database, one needs to establish a unique relation between a gene and an enzyme function. However, often multiple enzymes are associated with a gene by a non-zero relevance score. Hence, a strategy is needed to select the most likely enzyme the gene is coding for. For the approach pre-

sented here, a low threshold l and high threshold h satisfying $l \leq h$ is required. Both values are organism-specific and reflect how well-studied the organism is. This is due to the fact that well-studied organisms have higher relevance scores on average (Quester and Schomburg, 2011). In the subsequent analysis only genes with a relevance score $s > l$ are taken into account. This prevents the inclusion of low-quality or erroneous entries originating from a single source. If a gene is associated with only one enzyme at this point, the association is clear and the matter is settled. The genes with multiple entries require closer inspection. In rare cases, all entries associated with one gene do not overlap and hence do not contradict each other. In such a case, all entries can be kept. An example for a non-overlapping annotation in *D. shibae* can be seen in Table 2.1. Here, the gene Dshi_2437 codes for both enzymes catalyzing the first two steps of the L-Rhamnose degradation pathway. However, if entries overlap, only one can be kept. To decide whether one entry is clearly the best one, we sort all entries for each gene by their score and calculate the ratio of the second highest score divided by the highest score. If this ratio is less than $\frac{2}{3}$, the first entry is considered to be the correct one and all others are dropped. Otherwise, only high-quality entries with a score $s > h$ are kept. In some cases, this method may lead to an ambiguous annotation or no annotation at all. Hence, a manual review of this part of the annotation is needed, but only in very few cases. Concerning the reconstruction protocol (Thiele and Palsson, 2010), the method proposed here covers Step 1 (genome annotation) and contributes to the confidence scoring system (Step 15). The next chapter of this thesis contains an application of the method for the reconstruction of the metabolic network of *D. shibae*.

2.3.2 *Semi-automated reconstruction of metabolic networks*

An overview of the semi-automated reconstruction process leading to a preliminary metabolic network can be seen in Figure 2.1. The first step is to add reactions which can potentially

Table 2.1: Example of a non-overlapping annotation in *D. shibae*

Locus tag	EC	Enzyme name	Start	End	Total score
Dshi_2437	5.3.1.14	L-Rhamnose isomerase	1	412	28
Dshi_2437	2.7.1.5	L-Rhamnose kinase	476	883	8

take place in the organism in question. There are three ways to add reactions to the new metabolic network: by 1) EC number, 2) gene product name, and 3) manually specifying a reaction. Usually, the first way is the most common one because the starting point for a metabolic reconstruction often is a set of enzymes (represented by their EC numbers) stemming from a genome annotation. However, in some cases the enzyme catalyzing a reaction has not been identified or has no EC number assigned, yet. Hence, the second way can be used to add reactions which are associated with their corresponding gene or gene product directly. Finally, option three can be used to add novel or hypothetical reactions which are not associated with any location in the genome. Optionally, the first two ways can be refined by setting a target taxon. If set, only reactions known to occur in the selected taxon or any subtaxa are taken into account for the reconstruction of the metabolic network. All connections between a reaction and an enzyme, a gene or a taxon are established using the information from the MetaCyc database (Caspi *et al.*, 2012). If the cofactor in use is unclear for a reaction (e. g., $NAD(P)^+$) all variants are created automatically.

Another important question regrading biochemical reactions is whether they are reversible or irreversible under the conditions studied. This is especially true for energy-consuming reactions. Therefore, our method applies two thermodynamic rules of thumb to adjust reactions directions if necessary. The first one ensures that the energy-rich compound ATP is only

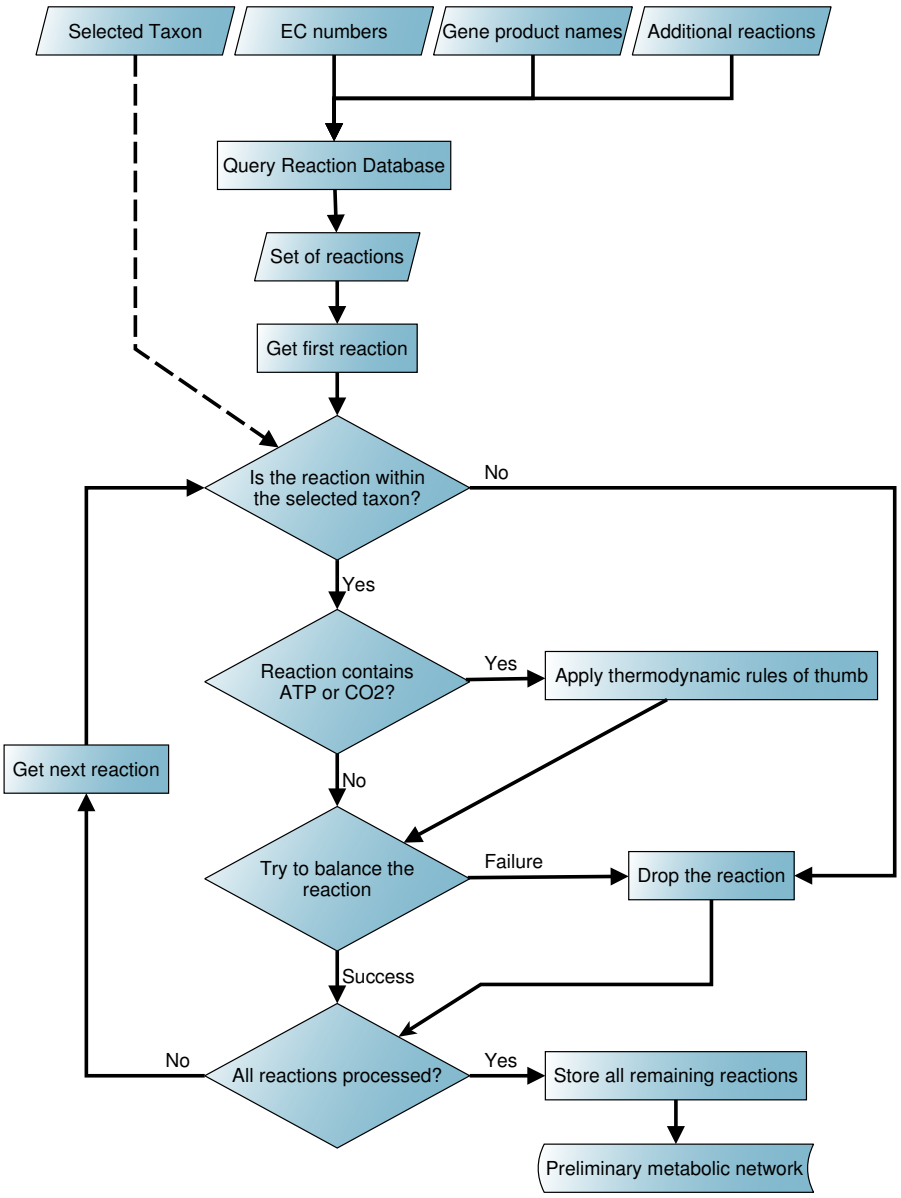

Figure 2.1: Flowchart of the semi-automated reconstruction process. Optional input is indicated by a dashed line. The addition of spontaneous reactions is not shown.

produced by enzymes which are known to form ATP (Table 2.2). The second rule deals with the fixation of CO_2. Only reactions associated with an enzyme for which CO_2 fixation is described in the literature are allowed to consume CO_2 (Table 2.3). If necessary, the direction of reactions not following these rules is adjusted automatically. Furthermore, a couple of reactions frequently encountered during metabolic reconstructions

have been corrected permanently based on experimentally determined reversibility information obtained form the BRENDA (Scheer *et al.*, 2011).

Moreover, the stoichiometry of the reactions is computationally balanced if needed. This is done by setting up a mixed integer linear problem based on the stoichiometric factors and the molecular formulas of the reactants, which minimizes the sum of absolute adjustments of the stoichiometric factors needed to balance the reaction. At this point, all reactions containing generic reactants are ruled out because they do not have a molecular formula. Exceptions are certain protein classes like thioredoxins, ferredoxins or cytochromes, which serve as an electron carrier.

At last, reactions taking place even in absence of a catalyzing enzyme are added automatically. These spontaneous reactions are included if all educts of the reaction are already part of the metabolic network reconstructed up to now. To account for consecutive spontaneous reactions, this step is repeated until no new reactions are added. All reactants in the metabolic network can be identified using any synonym stored in the MetaCyc database or by specifying their corresponding IUPAC International Chemical Identifier (InChI[1]).

2.4 Conclusion

The final output of the automated reconstruction process is a preliminary metabolic network consisting of reactions, which have been checked for stoichiometric, thermodynamic, and taxonomic plausibility. Altogether, the process significantly speeds up several steps of the reconstruction protocol (Thiele and Palsson, 2010): candidate metabolic functions (Step 2), generic reaction terms / substrate and cofactor usage (Step 6), reaction stoichiometry (Step 9), reaction directionality (Step 10), metabolite identifiers (Step 14), and spontaneous reactions (Step 19). Not

1 http://www.iupac.org/inchi/

Table 2.2: ATP forming enzymes obtained from the BRENDA.

EC Number	Enzyme name
2.7.1.159	inositol-1,3,4-trisphosphate 5/6-kinase
2.7.1.40	pyruvate kinase
2.7.11.15	beta-adrenergic-receptor kinase
2.7.11.19	phosphorylase kinase
2.7.2.2	carbamate kinase
2.7.2.3	phosphoglycerate kinase
2.7.3.3	arginine kinase
2.7.4.1	polyphosphate kinase
2.7.4.3	adenylate kinase
2.7.4.6	nucleoside-diphosphate kinase
2.7.6.1	ribose-phosphate diphosphokinase
2.7.7.28	nucleoside-triphosphate-aldose-1-phosphate nucleotidyltransferase
2.7.9.1	pyruvate, phosphate dikinase
3.6.1.17	bis(5'-nucleosyl)-tetraphosphatase (asymmetrical)
3.6.1.9	nucleotide diphosphatase
3.6.3.14	H+-transporting two-sector ATPase
3.6.3.6	H+-exporting ATPase
3.6.3.7	Na+-exporting ATPase
3.6.3.9	Na+/K+-exchanging ATPase
3.6.4.10	non-chaperonin molecular chaperone ATPase
4.1.1.49	phosphoenolpyruvate carboxykinase (ATP)
6.2.1.13	Acetate-CoA ligase (ADP-forming)
6.2.1.5	Succinate-CoA ligase (ADP-forming)

Table 2.3: Enzymes capable of CO_2 fixation obtained from the BRENDA.

EC Number	Enzyme name
1.2.7.1	pyruvate synthase
1.2.7.2	2-oxobutyrate synthase
1.2.7.3	2-oxoglutarate synthase
1.2.7.4	carbon-monoxide dehydrogenase (ferredoxin)
2.7.2.2	carbamate kinase
4.1.1.21	phosphoribosylaminoimidazole carboxylase
4.2.1.1	carbonate dehydratase

covered is the identification of candidate reactions for gap filling (Steps 46 and 47). However, the preliminary model can be used as basis for either a manual gap-filling or the usage of an existing automatic approach. In addition, manual adaptations to organism-specific preferences and conditions are still needed. For instance, the usage of cofactors should be adjusted if experimentally verified data is available. Except for the periplasmic and the cytoplasmic space, the preliminary model does not account for different compartments inside the cell. Hence, the usefulness for eukaryotic organisms is currently limited. Moreover, boundary reactions, which allow compounds to enter or leave the system, and transport reactions, which transport compounds through the cell membrane, need to be added manually. If the model is intended to be used for simulating the organisms' metabolism (e. g., in a constrained-based approach), additional parameters need to be specified. Most importantly, this includes uptake rates of the main nutrients and a precise biomass composition to simulate growth. Chapter 4 deals with the complete reconstruction process and the simulation of the metabolic network of *D. shibae*.

3

IDENTIFICATION AND VISUALIZATION OF METABOLIC BRANCH POINTS

> *With four parameters I can fit an elephant, and with five I can make him wiggle his trunk.*
>
> — John von Neumann

3.1 Introduction

A comprehensive visualization of a metabolic network opens the door for a detailed analysis of its features and greatly eases the interpretation of data stemming from experiments or simulations. The most straightforward approach to represent a metabolic network is a graph made of nodes and edges (Lacroix *et al.*, 2008). Traditionally, such a graph is visualized using a static map consisting of manually composed pathways (Kanehisa *et al.*, 2012; Caspi *et al.*, 2012). A more recent strategy is to create automatically laid out graphs for each network individually (Bourqui *et al.*, 2007; Pey *et al.*, 2011; Heath *et al.*, 2011).

High-throughput techniques and advanced simulations of biological systems produce vast amounts of data. To draw non-trivial conclusions, this data must be organized and integrated. Using different colors, shapes, line widths and labels, graph representations of metabolic networks are able to account for

several data sources simultaneously. Hence, graphs are often the method of choice to get a visual impression of the interactions among the biological subsystems studied.

On the one hand, map-based approaches provide a familiar view on well-known metabolic pathways. On the other hand, the advantage of customized layout algorithms clearly lies in their flexibility. This is due to the fact that the structure of the graph can be altered to tailor the visualization for a specific question. While pathway databases receive mainly incremental updates, which add novel pathways and reactions, a lot of research is conducted targeting an individualized representation of metabolic networks. All layout algorithms customized for biological networks aim to arrange the nodes of the corresponding graph in a way which eases the interpretation of the network. A popular approach is to guide the arrangement by extrinsic information like textbook pathway associations or atom-mapping data (Bourqui *et al.*, 2007; Heath *et al.*, 2011). Besides guiding the layout algorithm directly, this information can be used to reduce the complexity of the problem. For instance, the interactions of the nodes could be limited to primary metabolites or to molecules exchanging carbon atoms (Bourqui *et al.*, 2007; Pey *et al.*, 2011). As an effect, the final graph contains fewer edges and thus is more readable. Moreover, the reduction eases the approximation of NP-hard problems (e. g., graph planarization) usually encountered during the computation of the layout (Liu and Geldmacher, 1977; Bourqui *et al.*, 2007). To further improve the informative value of the graph, techniques have been proposed to highlight some nodes displaying certain features. One approach is to magnify metabolites which participate in more pathways than others (Pey *et al.*, 2011). Another method indicates reactions at which the metabolic flux branches (Heath *et al.*, 2011).

Nevertheless, none of the approaches mentioned above is widely used up to now. This is probably due to drawbacks, which have not been addressed successfully yet. For instance, static maps neglect the complex interactions between pathways

because they rely on textbook definitions. Furthermore, a map is only usable for those parts of a metabolic network which can be associated with nodes on the map. Novel or custom reactions cannot be handled. In contrast, an automatic layout algorithm takes into account every reaction and each interaction of the network. However, when applied to genome-scale networks, layout algorithms lead to cluttered and confusing graphs in most cases. Moreover, the extrinsic information needed as additional input may not be available for all nodes. Another drawback is the runtime of several minutes, which prohibits an interactive usage of the algorithms.

This chapter introduces the advanced metabolic branch point analysis (AMEBA). AMEBA employs a generalized definition of metabolic branch points to reduce the number of nodes displayed of a network while retaining as much information as possible. Although the algorithm does not rely on extrinsic information, it can be guided additionally by expert knowledge. Furthermore, the runtime of less than a second – even for genome-scale metabolic networks – enables an interactive usage.

3.2 Methods

3.2.1 *Bipartite graph representation of a metabolic network*

Throughout this chapter, metabolic networks are represented as bipartite graphs . Such a graph has two types of nodes, which are reactions and metabolites in our case. If in a graph any node of one type is not directly connected to a node of the same type, the graph is called bipartite. Hence, reactions are only connected via metabolites and vice versa. An example for a bipartite graph can be seen in panel A of Figure 3.2. In this graph, all nodes starting with the capital letter "R" represent reactions while all other indicate metabolites.

3.2.2 *Split-ratio analysis*

If a steady-state condition is imposed on a metabolic network, the sum of the fluxes producing an internal metabolite i is equal to the sum of consuming fluxes. Here, we denote the total flux through metabolite i by ϕ_i. An alternative name used in the past is flux sum (Kim *et al.*, 2007). Given the stoichiometric matrix S and the flux vector v the split-ratio

$$\rho_{ij} = S_{ij} \cdot v_i$$

is the fraction of metabolite i produced (if positive) or consumed (if negative) via reaction j. To calculate the total flux through metabolite i these fluxes need to be divided into producing and consuming fluxes:

$$\begin{aligned} P_i &= \{j | \rho_{ij} > 0\} \\ C_i &= \{j | \rho_{ij} < 0\} \end{aligned}$$

Now, the flux through metabolite i is:

$$\phi_i = \sum_{j \in P_i} \rho_{ij} = -\sum_{j \in C_i} \rho_{ij}.$$

Division of the relative shares by the total flux yields the relative split-ratios

$$\rho^*_{ij} = \frac{\rho_{ij}}{\phi_i}.$$

3.2.3 *Identification of metabolic branch points*

The intuitive definition of a metabolic branch point is a node in a metabolic network where the flux splits into multiple smaller fluxes. For instance, a metabolite could be produced by a single reaction and consumed by two other reactions. This is the case for chorismate, which is a branch point in the biosynthesis of aromatic amino acids (Gibson *et al.*, 1962; Figure 3.1). AMEBA

was developed to generalize the approach of split-ratio analysis to the whole metabolic network and visualize the extended metabolic context of a selected metabolite or reaction. The analysis starts with the complete bipartite reaction graph. If a flux distribution is given, all reactions carrying no flux are omitted. However, as the complete graph is much too complex for a meaningful interpretation, the graph is reduced according to user-supplied parameters.

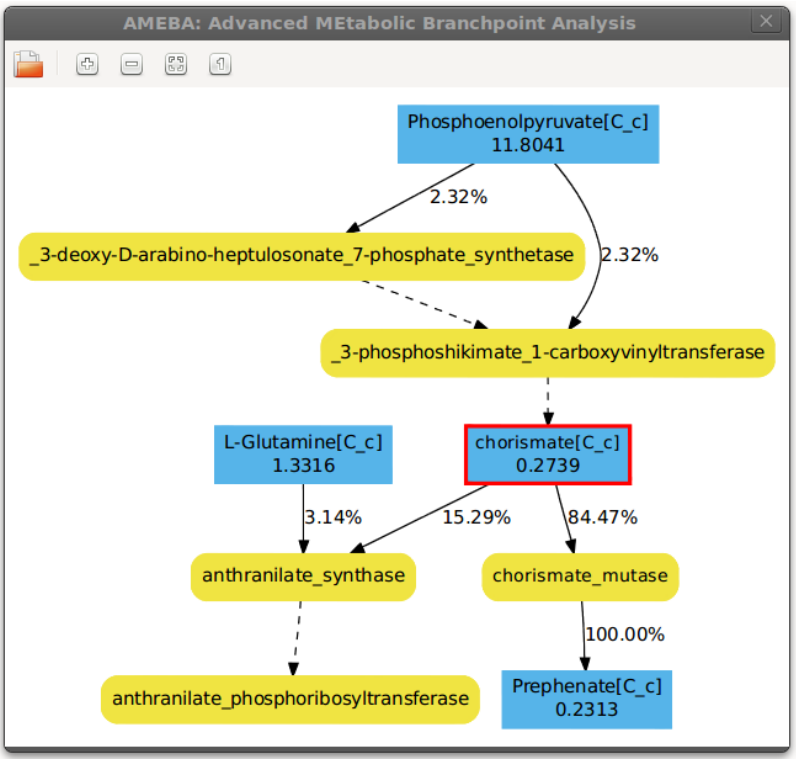

Figure 3.1: Screenshot of the AMEBA implementation displaying the metabolic branch point chorismate in the metabolic network of *E. coli*. Reactions are shown in yellow (round boxes) while metabolites are shown in blue (angular boxes). The percentages shown at the edges are the relative split ratios.

First, the user selects one or more nodes as the hub of the analysis. Optionally, the user can provide a list of nodes to be excluded and a list of nodes to be disconnected. Excluded nodes are completely removed from the graph, while disconnected nodes are split into separate instances for each occurrence of the metabolite or reaction in the network. Typically, the first list

would be used to exclude metabolites that are ubiquitous, but not relevant in most contexts (e.g. H_2O or protons). The second list can be used to prevent crowding of the graph by promiscuous compounds such as currency metabolites (e.g. ATP or NADH). Moreover, the user can specify a maximum distance to the selected hub nodes. Nodes beyond this limit will not be shown in the final graph. If the resulting graph is disconnected, only the largest connected component is displayed.

The steps of the algorithm are illustrated in Figure 3.2. AMEBA starts with the calculation of the split ratios for all metabolites based on the given flux distribution. Subsequently, the bipartite reaction graph is built, and the edges are labeled with their corresponding split ratios. Panel A of Figure 3.2 shows the initial state of an example graph representing the metabolic context of reaction R1, with edge labels omitted for clarity. Next, the respective nodes specified by the user are removed and disconnected (Figure 3.2 panel B). At this point, the complexity of the graph is further reduced by bridging transitory nodes (Figure 3.2 panel C). Specifically, each node that has exactly two neighbors is replaced by a dashed edge. This step is repeated until no such nodes remain. Disconnected nodes are not taken into account when the number of neighbors is determined. Finally, all nodes beyond the specified maximum distance are removed (Figure 3.2 panel D). Besides the selected node, the remaining graph contains only nodes at which the metabolic flux branches – metabolic branch points (Figure 3.2 panel E).

3.2.4 *Implementation details*

AMEBA has been implemented in the Python programming language version 2.7 (http://python.org). Metabolic models are handled using the data structures of metano (Riemer *et al*, manuscript in preparation, http://metano.tu-bs.de). Furthermore, the implementation uses NetworkX (Hagberg *et al.*, 2008) for graph operations and Graphviz (Ellson *et al.*, 2004)

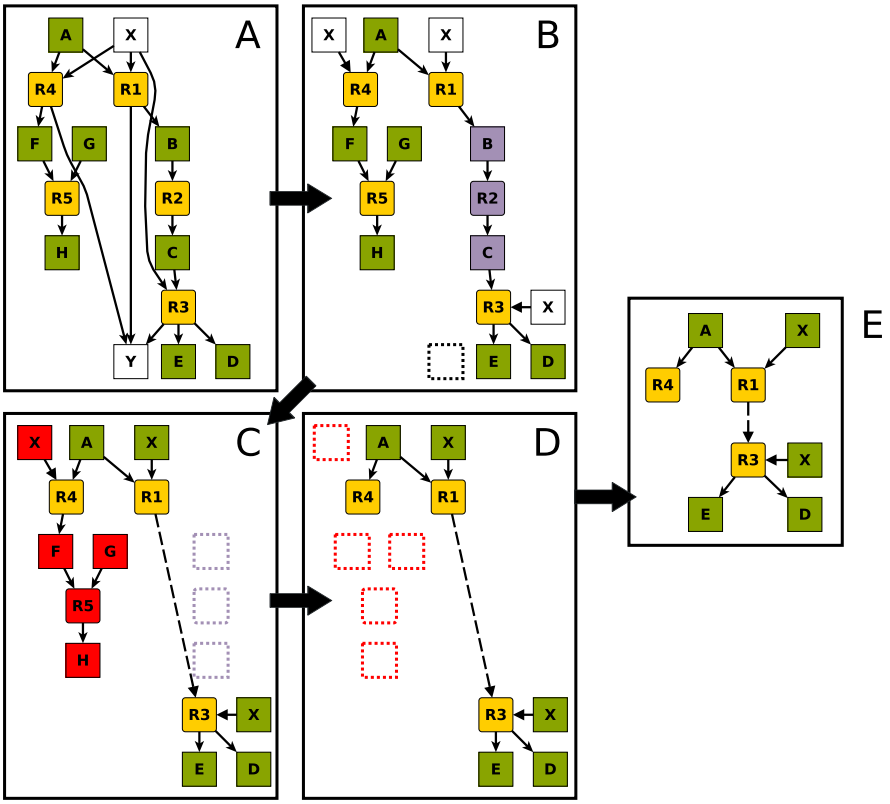

Figure 3.2: Illustration of the steps carried out by AMEBA for an example network. Nodes which will be addressed in a step are also highlighted in the same color in the preceding step. A) Full graph; B) Metabolite Y was removed and metabolite X was disconnected; C) Intermediate nodes were bridged by a dashed edge; D) All nodes with a distance greater than two from the selected node (R1) were removed. E) Layout of the final graph

for calculating the layout of the final graph. The interactive mode has been created based up on the xdot module (http://code.google.com/p/jrfonseca/wiki/XDot). If not run interactively, the output format is either Graphviz dot or GML (Graph Modelling Language). A screenshot of the graphical user interface can bee seen in Figure 3.1.

3.3 Conclusion

Although based on rather simple rules, AMEBA is able to visualize complex metabolic networks by focusing on relevant context. Due to the very short runtime compared to other approaches, AMEBA can also be used interactively to carry out an exploratory analysis conveniently. Furthermore, by fine-tuning the parameters, AMEBA can be used to produce high-quality graphs suitable for publications or further editing. A popular strategy is to limit the analysis to compounds exchanging carbon atoms (Pey *et al.*, 2011; Heath *et al.*, 2011). This can easily be adopted in AMEBA by disconnecting the corresponding metabolites. An obvious and probably quite useful extension of the AMEBA implementation would be the integration of additional data stemming from wet-lab experiments.

4

LARGE-SCALE COMPUTATIONAL ANALYSIS OF THE METABOLISM OF *DINOROSEOBACTER SHIBAE*

> *The most elementary and valuable statement in science, the beginning of wisdom, is: I do not know.*
>
> — Lt. Commander Data, Star Trek: The Next Generation

4.1 Introduction

The *Roseobacter* clade is a versatile group of Gram-negative α-proteobacteria, which can be found in all oceans worldwide. Especially during phytoplankton blooms they account for a large fraction of the marine bacterial community (Brinkhoff *et al.*, 2008; Buchan *et al.*, 2005). Here, we focus on the aerobic anoxygenic phototroph *Dinoroseobacter shibae* DFL12^{T} (Biebl *et al.*, 2005). Although the bacterium has been isolated from the surface of the dinoflagellate *Prorocentrum lima*, it can also be motile by the means of a single polar flagellum. It harbors five plasmids and needs additional vitamins (biotin, nicotinate, and 4-aminobenzoate) to grow in minimal seawater medium. To obtain energy, *D. shibae* can use oxygen, nitrate or dimethyl sulfoxide (DMSO) as terminal electron acceptor. Additionally, energy

generation is possible via light dependent aerobic anoxygenic photosynthesis (Biebl *et al.*, 2005; Wagner-Döbler *et al.*, 2010).

Despite their common taxonomic classification, many members of the *Roseobacter* clade have adopted a unique life style and accordingly have developed a tailored metabolism (Brinkhoff *et al.*, 2008; Moran *et al.*, 2007). For instance, *D. shibae* is believed to live in symbiosis with its host and to provide the algae with vitamins in exchange for carbon sources originating from photosynthesis (Geng and Belas, 2010; Wagner-Döbler *et al.*, 2010). Some members of the *Roseobacter* clade produce storage compounds belonging to the group of polyhydroxyalkanoates, which are biopolymers with a potential industrial use (Yurkov and Beatty, 1998). Under optimal conditions, *Dinoroseobacter* sp. JL1447, a close relative of *D. shibae*, has been found to produce large quantities of polyhydroxyalkanoates (Xiao and Jiao, 2011). Moreover, *D. shibae* and other *Roseobacters* produce dimethyl sulfide (DMS) during DMSO respiration and when dimethylsulfoniopropionate (DMSP) is used as carbon source. This molecule contributes to the characteristic odor of the ocean and effects the climate by seeding cloud formation (Curson *et al.*, 2011). All these properties demonstrate that *D. shibae* notably differs from well-studied organisms.

Hence, the *Roseobacter* clade and its members were subject of intensive research in the past few years (Brinkhoff *et al.*, 2008; Buchan *et al.*, 2005). Since the initial description of *D. shibae* in 2005, further studies on the genome sequencing and transcriptome analyses under changing illumination conditions have been published (Biebl *et al.*, 2005; Wagner-Döbler *et al.*, 2010; Tomasch *et al.*, 2011). Furthermore, important parts of the metabolism of *D. shibae* were elucidated by ^{13}C labeling experiments, a study on DMSP catabolism, and a study targeting energy conservation (Fürch *et al.*, 2009; Dickschat *et al.*, 2010; Holert *et al.*, 2011). Remarkably, no phosphofructokinase activity has been observed in *D. shibae* during growth on glucose (Fürch *et al.*, 2009). Recently, a basic metabolic model of *Rhodobacter sphaeroides*, an other member of the *Roseobacter*

clade, has been created (Imam *et al.*, 2011). However, no systematic and detailed computational analysis of the metabolism of any member of this ubiquitous group of marine bacteria has been carried out to date.

In this chapter, a large-scale computational analysis of the metabolism of the marine bacterium *Dinoroseobacter shibae* is presented. Prior to the analysis, we created an elaborate genome-scale metabolic model (Kim *et al.*, 2011; Oberhardt *et al.*, 2009) of *D. shibae*, denoted *i*Dsh827. It has been validated against experimental data and covers 827 open reading frames. Moreover, *i*Dsh827 is the first genome-scale metabolic model which explicitly takes account of the energy demand of bacterial mobility. Additionally, our model is the first one which uses aerobic anoxygenic photosynthesis. In total, 268 546 distinct simulations featuring a large variety of different growth conditions, e.g. varying carbon and nitrogen sources, aerobic and anaerobic conditions, and the availability of light have been carried out. A large fraction of the scenarios is dedicated to plasmid and single gene knock-out mutants. In detail, the aim of this chapter is to

- analyze metabolic fluxes in *D. shibae* with focus on energy balance
- provide a possible explanation for aerobic denitrificion
- identify conditions enhancing the usage of the DMSP demethylation pathway
- explore the role of the phosphofructokinase in *D. shibae*
- study the effect of plasmid loss
- elucidate the behavior of single gene knock-out mutants
- find mutants producing significantly more DMS than the wild type

4.2 Methods

4.2.1 *Reconstruction process*

The starting point of the reconstruction process was the genome annotation of *D. shibae* provided by the EnzymeDetector (Quester and Schomburg, 2011). To obtain a consistent annotation, the query method described in Section 2.3.1 of the previous chapter was used with 9 for the low and 13 for the high threshold. Furthermore, manual additions were made to the annotation during the reconstruction to fill gaps in the metabolic network. The metabolic network was created using the semi-automated reconstruction method described in Section 2.3.2. Moreover, the non-growth-associated maintenance requirement (nGAM) and the growth-associated maintenance requirement (GAM) were assumed to be the same as in *E. coli* (3.15 $^{\text{mmol ATP}}/_{\text{g}_{\text{DW}}\ \text{h}}$ and 53.95 $^{\text{mmol ATP}}/_{\text{g}_{\text{DW}}\ \text{h}}$, Orth *et al.*, 2011). While the first value models the energy demand of processes not related to growth like DNA repair and preservation of turgor pressure, the second value accounts for the energy needed for reproduction. Most of this energy is needed for the synthesis of proteins, DNA, and RNA.

The number of protons in $^{\text{mmol}}/_{\text{g}_{\text{DW}}\ \text{h}}$ needed to drive the flagellar motor $P_{motility}$ has been estimated based on the number of protons needed for one rotation of the motor $N = 1200$ (Meister *et al.*, 1987), the average number of rotations per second $v = 10s^{-1}$ (Berg, 2003), and the average dry weight of one *Roseobacter* cell $m = 300fg$ (Vázquez *et al.*, 2004):

$$P_{motility} = \frac{N \cdot v \cdot 60 \cdot 60 \cdot 10^3}{m \cdot 6.022 \cdot 10^{23}} \approx 240\,{}^{\text{mmol}}/_{\text{g}_{\text{DW}}\ \text{h}}$$

However, only about 10% of the organisms in a culture of marine bacteria are motile during the early exponential growth phase modeled here (Mitchell *et al.*, 1995). Hence, we constrained the motility proton flux to 24 $^{\text{mmol}}/_{\text{g}_{\text{DW}}\ \text{h}}$.

4.2.2 *Flux balance analysis*

Flux balance analysis (FBA) is a method to calculate a flux distribution in a metabolic model, which optimizes a given objective function – usually growth of the organism (Fell and Small, 1986; Kauffman *et al.*, 2003). The reaction information from the metabolic model is gathered in the $m \times n$ *stoichiometric matrix* S, where m is the number of metabolites and n is the number of reactions in the model. Each entry S_{ij} holds the stoichiometric coefficient of metabolite i in reaction j. The flux through each reaction is given by the flux vector v. Imposing a steady-state condition we obtain a system of linear equalities:

$$S \cdot v = 0. \tag{4.1}$$

Additionally, the fluxes can be constrained by upper and lower bounds α and β:

$$\alpha_i \leq v_i \leq \beta_i \quad \forall_i. \tag{4.2}$$

If no further information on the bounds of a reaction is available, a widely-used approach is to set α_i and β_i to arbitrary large values (Thiele and Palsson, 2010; Schellenberger *et al.*, 2011). In contrast, we chose to omit the constraints in such cases. This prevents the occurrence of high flux loops in the solution. A more elaborate description of the reasoning, which lead us to this decision can be found in Section 6.1 of the Appendix.

Together, the Equations 4.1 and 4.2 describe a convex polytope, which has been named *flux cone* in the field of metabolic modeling. Usually, the resulting equation system is underdetermined and linear programming is applied to optimize a certain objective function f. The most common choice for an objective is growth – i. e. biomass production (Feist and Palsson, 2010). Now, the linear optimization problem is to maximize $f(v)$ under the constraints of the Equations 4.1 and 4.2. Moreover, if the original objective function is to be maximized, it must be negated. If the problem is feasible, the simplex algorithm or

any of its successors find a value for each flux variable v_i. However, the solution of the FBA is not unique in most cases and depends on the basic feasible solution chosen in the first step of the algorithm. This phenomenon is due to naturally occurring redundancies in metabolic networks (Mahadevan and Schilling, 2003).

4.2.3 *Flux variability analysis*

Although FBA assigns a value to each flux in the metabolic network, it does not indicate whether this specific value is necessary to maximize the objective function. If alternate optima exist, a flux can be variable in a certain range or can even be unbounded. To reveal this uncertainty, flux variability analysis (FVA) determines the maximal value v_i^{max} and minimal value v_i^{min} for each flux in the network while maintaining the optimal objective value Z determined by FBA (Mahadevan and Schilling, 2003). Thus, the linear optimization problem is to subsequently maximize and minimize each flux v_i under the additional constraint $f(v) = Z$ and the constraints of the Equations 4.1 and 4.2. As this method requires two optimization runs for each flux, it is quite time-consuming for genome-scale metabolic models. Hence, a variant called fast FVA has been proposed (Gudmundsson and Thiele, 2010). This approach first determines all maximal values and initializes each optimization run with the result of the previous run. The same is done accordingly for all minimal values. Often, this results in a significantly reduced run time of the optimization algorithm because in most cases the wanted optima lie close to each other.

4.2.4 *Large-scale computational analysis*

In metabolic modeling the traditional approach is to limit the simulations to a few physiological states, for which experimental support exits (Kim *et al.*, 2011). In contrast, this work ex-

plores several different scenarios based on the experimental data gathered for a subset of these scenarios. This is achieved by running a simulation for all possible combinations of the corresponding parameters. All scenarios were simulated using flux balance analysis and each flux was tested for variability under the additional constraint of optimal biomass production by fast flux variability analysis as described above. The computational analyses were carried out on a computer equipped with a 2.67 GHz Intel Core i7 CPU and 4 GB of RAM. The software in use was the metano toolbox (Riemer *et al.*, manuscript in preparation, http://metano.tu-bs.de). In order to shorten the total run time and to make use of the multi-core architecture of modern processors, a script automatically generated parameter combinations and started up to eight simulations in parallel. For further evaluation, the resulting flux values v_i, v_i^{max}, and v_i^{min} were stored in a relational database. Single gene knockouts were simulated by constraining the flux through all reactions associated with that particular gene to zero.

4.3 Results

4.3.1 *Biomass composition*

A fundamental assumption made in most constrained-based simulations is that the organism tries to maximize its growth rate as much as possible under the given environmental conditions. Therefore, the model *i*Dsh827 contains a biomass reaction, which consumes appropriate quantities of 113 different metabolites needed for the reproduction of *D. shibae*. The flux through this reaction corresponds to the growth rate and is the objective function of all simulations presented here. Hence, the contribution of each metabolite to the biomass composition was quantified by experiments and based on literature values of related organisms. While the protein and DNA content of

D. shibae was determined experimentally[1], the other fractions were estimated or taken from literature (see Table 4.1). The fractions of peptidoglycan and the soluble pool were presumed to be approximately equal to the values determined for *E. coli* (Feist *et al.*, 2007). Moreover, those compounds whose proportion of the biomass are still unknown were estimated to make up 0.1% of the total dry weight all together. Furthermore, the RNA and lipid content were supposed to be equal to the values of *Rhodobacter sphaeroides* (Imam *et al.*, 2011). Finally, polyhydroxybutyrate was assumed to account for the remaining biomass fraction, which seems plausible in light of the values measured for other *Roseobacters* (Xiao and Jiao, 2011).

The relative portions of the nucleotides and amino acids were estimated from the genome sequence as suggested by the reconstruction protocol (Thiele and Palsson, 2010). The predominant respiratory lipoquinone (ubiquinone-10) and the predominant cellular fatty acid (18:1ω7*c*) were chosen to represent their corresponding compound group (Biebl *et al.*, 2005). Furthermore, the ratio of Kdo2-lipid A to the O-antigen in the lipopolysaccharide was calculated from values measured for *Roseobacter denitrificans* (Jarosławski *et al.*, 2009). Under anaerobic conditions, the oxygen atoms in the singlet oxygen quencher spheroidenone neither originate from water nor from CO_2 but probably from other cell components (Yeliseev and Kaplan, 1997). Hence, we included its precursor methoxyneurosporene in the biomass reaction. A detailed measurement of the content of the soluble pool is only available for *E. coli* (Bennett *et al.*, 2009). Nevertheless, we used these values to constitute the soluble pool content in *i*Dsh827. Therefore, we removed compounds which were either specific for the growth conditions used in the study or which were not part of our model. As the genome did not contain any hints for spermidine production in *D. shibae*, we did not include this compound into the biomass reaction. Due to the fact that aerobic anoxygenic phototrophs produce bacte-

1 At this point, I gratefully acknowledge the work of Nelli Bill, who carried out the experiments.

riochlorophyll *a* exclusively in the dark under aerobic conditions (Harashima *et al.*, 1980), we included two biomass reactions in the model: one with and one without bacteriochlorophyll *a*. The former reaction contains a term corresponding to $4\,\mathrm{nmol}/\mathrm{mg}_{\mathrm{protein}}$ as determined for *D. shibae* (Biebl *et al.*, 2005). Before running a simulation, the appropriate biomass reaction is enabled automatically based on the preset conditions. Both biomass reactions are normalized to one gram dry weight.

Table 4.1: Cellular content of *D. shibae*

Component	Percentage	Reference
Protein	47.0%	experimentally det.
DNA	2.5%	experimentally det.
RNA	7.1%	Imam *et al.*, 2011
Lipids	12.8%	Imam *et al.*, 2011
Peptidoglycan	2.5%	Feist *et al.*, 2007
Lipopolysaccharides	4.0%	Jarosławski *et al.*, 2009
Bacteriochlorophyll *a*	0.08%	Biebl *et al.*, 2005
Soluble pool	2.9%	Feist *et al.*, 2007
Polyhydroxybutyrate	21.0%	estimated
Components with unknown fraction	0.1%	estimated

4.3.2 *iDsh827: A genome-scale metabolic model of D. shibae*

The reconstructed metabolic network of *D. shibae* gives insight into the metabolism of this representative of the cosmopolitan *Roseobacter* clade. In detail, the metabolic model *i*Dsh827 consists of 1 488 reactions covering 827 open reading frames (Table 4.2) and is based upon an aggregated genome annotation. A graphical representation of the distribution of evidence scores can bee seen in Figure 4.1 and the complete list of all genes covered in *i*Dsh827 is given in Table 6.2. To reproduce the observed phenotype as accurately as possible, multiple manual refinements guided by experimental results found in the literature were made. The design choices during the refinement

process are highlighted in the next sections. A complete list of all reactions, which can potentially be active in the model, is shown in Table 6.3.

Table 4.2: Properties of the genome-scale metabolic model *i*Dsh827

Property	Value	
Total number of genes in *D. shibae*	4 245	
Genes covered	827	(19.4%)
Enzymes	622	
Reactions	1 488	
Non-blocked reactions	778	
Distinct biomass compounds	113	

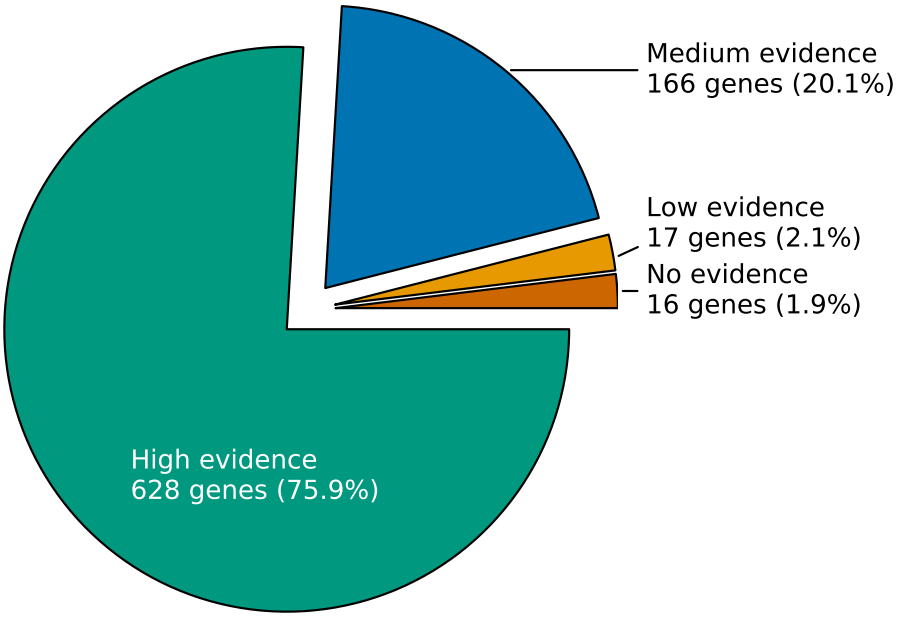

Figure 4.1: Distribution of EnzymeDetector evidence scores for the 827 genes covered in the genome-scale metabolic model. High scores: 13-21; Medium scores: 9-12; Low scores: 1-8; No score: zero or not annotated in the genome

Transport and boundary reactions

Tripartite ATP-independent periplasmic transporters predominate in the genome of *D. shibae* (Wagner-Döbler *et al.*, 2010). Hence, we included sodium symporters for each carbon source

in the model. As a notable exception, we allowed glycerol and glyoxylate to diffuse freely through the membrane using channel proteins. Otherwise, growth on these carbon source could not be reproduced by the model. In order to achieve comparable results, we normalized the uptake of the carbon sources to the number of carbon atoms. Hence, for a given uptake rate, the number of carbon atoms taken up is the same for all carbon sources. The medium (12 carbon atoms $^{\text{mmol}}/_{g_{DW}\ h}$) and the high (39.2 carbon atoms $^{\text{mmol}}/_{g_{DW}\ h}$) uptake rates correspond to the experimentally determined uptake rate of glucose and succinate, respectively. Additionally, we simulated nutrient-poor conditions by limiting the uptake rate to only one carbon atom. Furthermore, we included a sodium/proton antiporter, which exchanges two protons for one sodium ion (Taglicht *et al.*, 1993; Arkin *et al.*, 2007). Thus, the sodium ions imported together with the carbon source are able to leave the cell. The number of protons transported over the membrane in the reactions of the oxidative phosphorylation correspond to the values determined for *E. coli* (Feist *et al.*, 2007; Orth *et al.*, 2011). A list of all proton-translocating reactions is given in Table 4.3.

Besides the transporters and boundary reactions for the different nutrients, we included reactions which supply the model with the vitamins biotin, nicotinate, and 4-aminobenzoate essential for growth of *D. shibae* (Biebl *et al.*, 2005). Moreover, we incorporated the usage of light as an energy source by introducing a photon boundary reaction fixed to an uptake rate of 34.6 photons $^{\text{mmol}}/_{g_{DW}\ h}$. We fitted this value to reproduce the decrease of the oxygen uptake of *D. shibae* when exposed to light (Holert *et al.*, 2011). Another uncommon boundary reaction exclusively supplies oxygen for the production of the vitamin B12 precursor α-ribazole. This is necessary because no anaerobic alternative for the reaction catalyzed by the 5,6-dimethylbenzimidazole synthase is currently known. Aside from boundary reactions for the volatile products usually excreted by microorganisms (including DMS and methanethiol in the case of *Roseobacters*), we added additional sink reactions

to allow compounds which cannot be degraded to leave the system. For instance, the 5,6-dimethylbenzimidazole synthase already mentioned above produces an unknown compound, which is disposed by a boundary reaction. Furthermore, 5'-deoxyadenosine is created during the synthesis of thiamin. In our model, the adenine is salvaged (Choi-Rhee and Cronan, 2005) and the remaining 5-deoxy-D-ribose is excreted. Another side product of the thiamin synthesis is 4-methylphenol, which may accumulate in the cell (Kriek *et al.*, 2007). Moreover, glycolaldehyde is created by the dihydroneopterin aldolase eventually leading to tetrahydrofolate. Although glycolaldehyde is predicted to be degraded by a low-specificity L-threonine aldolase, in some scenarios a sink reaction was necessary. The total fraction of carbon lost through these additional sink reactions is four orders of magnitude smaller than the carbon input flux and thus has little impact on our results. Finally, secretion reactions for lactate, acetate, urea, urate, and L-glutamine were included. However, our simulations revealed that none of these boundary reactions have to be active in any of the wild type scenarios considered here.

Energy demand of motility

The bacterial flagellar motor in *D. shibae* is homologous to the machinery in *E. coli* and hence it is likely driven by the proton-motive force (Sowa and Berry, 2008). Remarkably, the energy spent on mobility is negligible in enteric bacteria but marine bacteria are much more mobile (Johansen *et al.*, 2002). Hence, we incorporated this energy demand using a reaction, which transfers a certain amount of protons from the periplasmic space to the cytosol. The actual value depends on the fraction of motile bacteria chosen for the specific simulation run (see Table 4.4).

Table 4.3: Proton-translocating reactions in *i*Dsh827

Reaction or Enzyme name	Reaction equation
cytochrome-c oxidase	8 H+ + 1 oxygen + 4 |Cytochromes-C-Reduced| $\rightarrow$ 2 H2O + 4 |Cytochromes-C-Oxidized| + 4 $H+_{ex}$
NADH:ubiquinone reductase (H+-translocating)	1 NADH + 5 H+ + 1 |Ubiquinones| $\leftrightarrow$ 1 NAD+ + 1 |Ubiquinols| + 4 $H+_{ex}$
ubiquinol oxidase	1 oxygen + 4 H+ + 2 |Ubiquinols| $\rightarrow$ 4 $H+_{ex}$ + 2 H2O + 2 |Ubiquinones|
H+-transporting two-sector ATPase	1 ATP + 3 H+ + 1 H2O $\leftrightarrow$ 1 ADP + 1 phosphate + 4 $H+_{ex}$
ubiquinol-cytochrome-c reductase	1 |Ubiquinols| + 2 |Cytochromes-C2-Oxidized| + 2 H+ $\rightarrow$ 1 |Ubiquinones| + 2 |Cytochromes-C2-Reduced| + 4 $H+_{ex}$
Na+/proton antiporter	1 Na+ + 2 $H+_{ex}$ $\rightarrow$ 1 $Na+_{ex}$ + 2 H+
flagellar motor proton flux	1 $H+_{ex}$ $\rightarrow$ 1 H+

Manually added or modified reactions

Some reactions required for production of biomass components have either no EC number assigned, contain generic metabolites or are stoichiometrically unbalanced. Such reactions were added manually and corrected, if applicable. For instance, some enzymes of the thiamin synthesis pathway lack EC numbers (Jurgenson *et al.*, 2009). Furthermore, the phosphatidylglycerol synthesis was constructed to use fatty acids with correct lengths. In some cases, generic cofactors had to be replaced by actual metabolites as found in the BRENDA (Scheer *et al.*, 2011). To allow the anaerobic synthesis of ubiquinol, we added hydroxylation reactions in which the molecular oxygen is replaced by water (Alexander and Young, 1978). The aerobic anoxygenic photosynthesis was modeled by two reactions: One reaction consumes the photons at the reaction center and the other one translocates two protons via cytochrome bc1 (Klamt *et al.*, 2008). As the phosphofructokinase is known to be inactive in *D. shibae*, we constrained the flux trough the corresponding reactions to zero (Fürch *et al.*, 2009).

4.3.3 *Large-scale computational analysis*

In total, we carried out 268 546 simulations to study the metabolic network of *D. shibae* under various environmental conditions and the effect of genetic perturbations in terms of single gene and plasmid knock-outs. The number of simulations per genotype can be calculated from the number of possible values for each parameter (Table 4.4):

$$27 \times 3 \times 5 \times 3 \times 2 \times 3 = 7290 \text{ scenarios.}$$

Growth of the wild type under various conditions

The first set of simulations, consisting of 7 290 scenarios, was carried out to study the behavior of the wild type strain un-

der different environmental conditions. Therefore, we varied one condition at a time and ran a simulation for each possible combination of scenario parameters (see Table 4.4). Besides different nutrient sources, we also varied the uptake rate of the carbon source, the availability of terminal electron acceptors, the illumination, and the fraction of motile bacteria. As *D. shibae* is able to grow aerobically and anaerobically, we included scenarios with oxygen, DMSO or nitrate as terminal electron acceptor or a combination of each of the anaerobic electron acceptors with oxygen. A condensed overview of the wild type scenarios can be seen in Figure 4.2. While the x-axis represents the growth rate observed in the scenario, the y-axis depicts the flux through the citrate synthase (positive values correspond to the formation of citrate). The lines, which resemble error bars, indicate the minimal and maximal flux through the reaction in the given scenario as determined by flux variability analysis. Hence, we term them *variance bars*. For the sake of clarity, this figure is limited to five carbon sources, the medium uptake rate, and ammonia as nitrogen source. For each carbon source, eight scenarios with different terminal electron acceptors (oxygen/DMSO), illumination conditions (dark/light), and motility fractions (no or 20% motility) are shown. The nitrate scenarios are not shown in this figure because they coincide with the DMSO scenarios.

In general, we observe that oxygen supports faster growth than DMSO and that light significantly enhances the growth on all carbon sources. In all dark scenarios, except for the glycolate scenarios, the citrate synthase runs in forward direction. Under light conditions, the activity of the citrate synthase is considerably reduced or even reversed. Notably, the anaerobic glycolate scenario in light is the only one which produces visible variance bars.

The analysis of the metabolic branch point oxaloacetate with AMEBA, which was introduced in the previous chapter, reveals strong flux changes in response to light. Details for the carbon sources glucose and DMSP can be seen in Figures 4.3 and 4.4,

respectively. On both carbon sources the relative contribution of the anapleurotic synthesis of oxaloacetate by the pyruvate carboxylase increases in light. However, the effect is much more pronounced on glucose because on DMSP oxaloacetate is also created by the citrate synthase operating backwards. As consequence, the total flux through oxaloacetate in light decreases on glucose but increases on DMSP. As already indicated by our results above, the flux through the TCA cycle is reduced or even reversed in light. Hence, an increased amount of oxaloacetate is routed to anabolic pathways.

Aerobic denitrification in light

When applying a scenario where oxygen and nitrate are available, our simulations predict that parallel usage of both electron acceptors is possible under certain conditions. The aerobic denitrification appeared as a non-zero variability of the molecular nitrogen export flux. We observed this variability independent from the nitrogen source but only in light and on the carbon sources 2-oxoglutarate, acetate, (R)-3-hydroxybutanoate, L-glutamate, polyhydroxybutyrate, DMSP, myo-inositol, and ethanol. The effect is restricted to the lowest carbon uptake rate for most carbon sources. However, L-glutamate and myo-inositol seem to support aerobic denitrification also with the medium uptake rate and ethanol displays the described behavior for all uptake rates covered in the simulations.

Usage of DMSP degradation pathways

In the genome of *D. shibae*, three genes coding for different DMSP-degrading enzymes are present. One gene product (DmdA) catalyzes the demethylation of DMSP while the other two (DddL and DddD) cleave DMSP. All three DMSP degradation pathways produce volatiles, which are excreted to the environment. The demethylation pathway produces methanethiol whereas the cleavage pathways produce DMS. From a stoichiometric point of view, the cleavage pathways are equivalent.

Table 4.4: Conditions whose combinations were covered in the simulations. The uptake rate of the carbon source is given in *mmol* carbon atoms per *gram* dry weight and *hour*.

Parameter	Cardinality	Possible values
Carbon source	27	(R)-3-hydroxybutanoate, (R)-lactate, (S)-lactate, 2-oxoglutarate, acetate, alpha-D-glucose, alpha-D-xylopyranose, alpha-L-rhamnose, alpha-maltose, beta-D-fructofuranose, β-D-glucose, beta-D-ribofuranose, citrate, D-ribitol, D-xylitol, DMSP, ethanol, fumarate, glycerol, glycolate, glyoxylate, L-glutamate, myo-inositol, polyhydroxybutyrate, propionate, pyruvate, succinate
Nitrogen source	3	ammonia, urea, nitrate
Sulfur source	1	sulfate
Phosphorus source	1	phosphate
Terminal electron acceptor	5	oxygen, nitrate, dimethyl sulfoxide, oxygen and nitrate, oxygen and dimethyl sulfoxide
Carbon uptake rate	3	1 (low), 12 (medium), 39.2 (high)
Illumination	2	light (34.6 photons $^{\text{mmol}}/_{g_{DW}\ h}$), dark (0 photons $^{\text{mmol}}/_{g_{DW}\ h}$)
Fraction of motile bacteria	3	0%, 10%, 20%

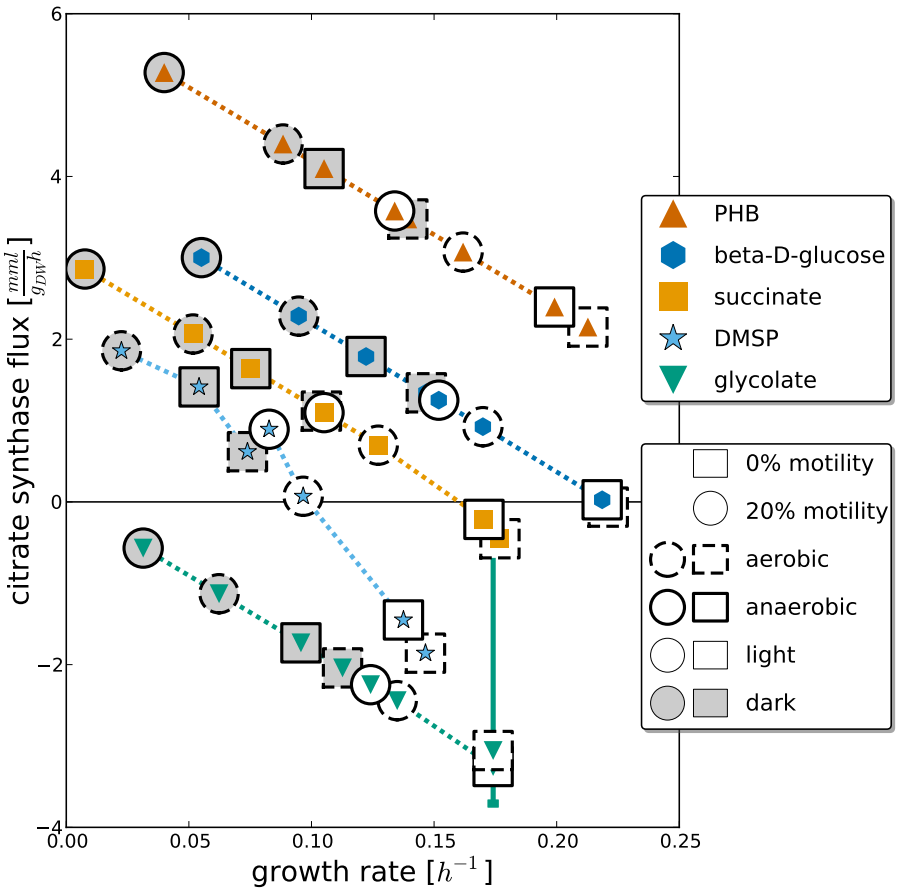

Figure 4.2: Overview of the wild type scenarios. In this figure the growth rate is charted against the flux through the citrate synthase. The carbon source is given by the color and shape of the inner marker. Moreover, the outer marker indicates motility (shape), aerobic/anaerobic conditions (line style), and illumination (background color). No growth was predicted in any high motility scenario for dark and anaerobic conditions if DMSP was used as carbon source. Hence, this entry is missing in the figure. PHB: polyhydroxybutyrate; DMSP: dimethylsulfoniopropionate

Hence, we focused our analysis on the relative contribution of the demethylation pathway compared to the cleavage pathways. In Table 4.5 the contribution of the demethylation pathway under diverse conditions in dependence of the carbon uptake rate is shown. These values represent the maximal fraction of DMSP degraded by the gene product of DmdA, as determined by flux variability analysis. If the carbon uptake rate is low, DMSP sup-

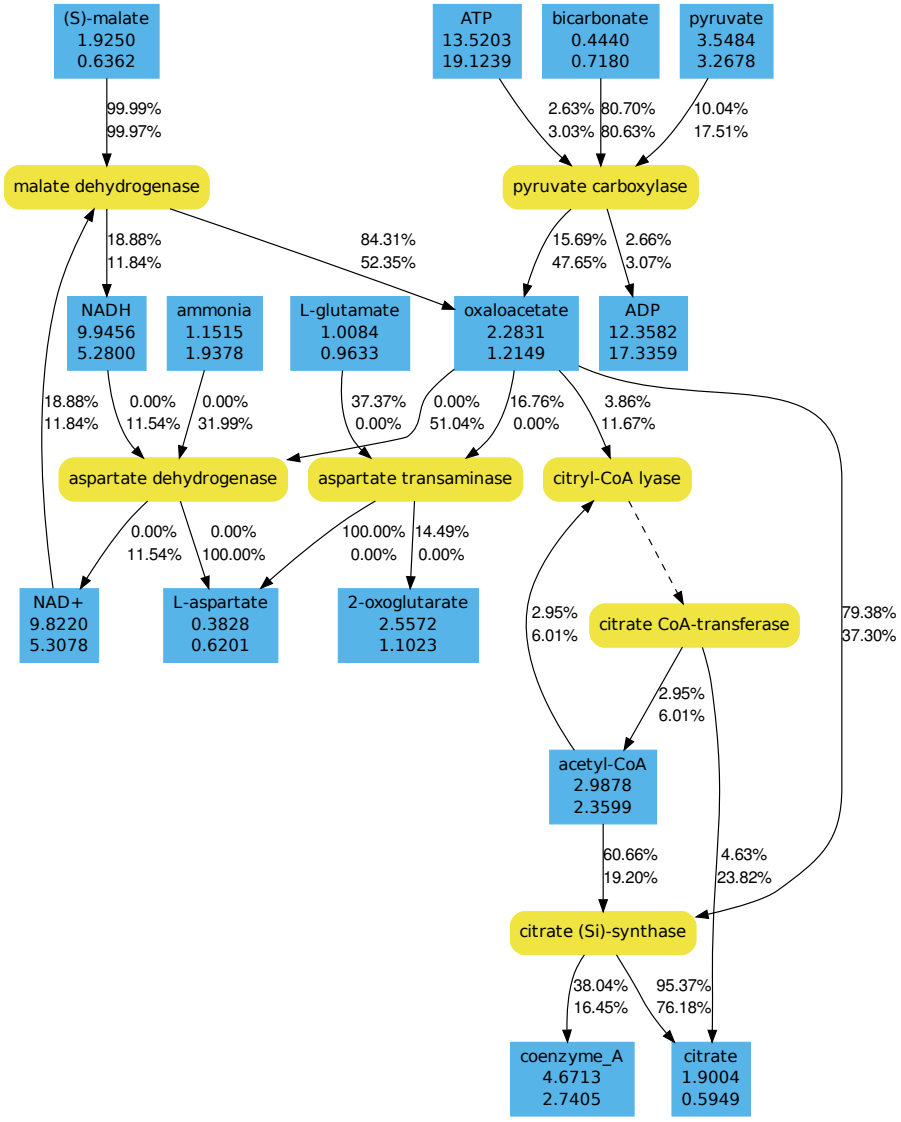

Figure 4.3: Metabolic context of oxaloacetate. Reactions are shown in yellow (round boxes) while metabolites are shown in blue (angular boxes). The total flux through a metabolite is given in $^{\text{mmol}}/_{g_{\text{DW}}\ \text{h}}$. Outgoing and incoming fluxes are given in percentages of the total flux. The upper numbers correspond to a dark scenario and the lower numbers to a light scenario. In both cases growth on glucose was simulated under aerobic conditions.

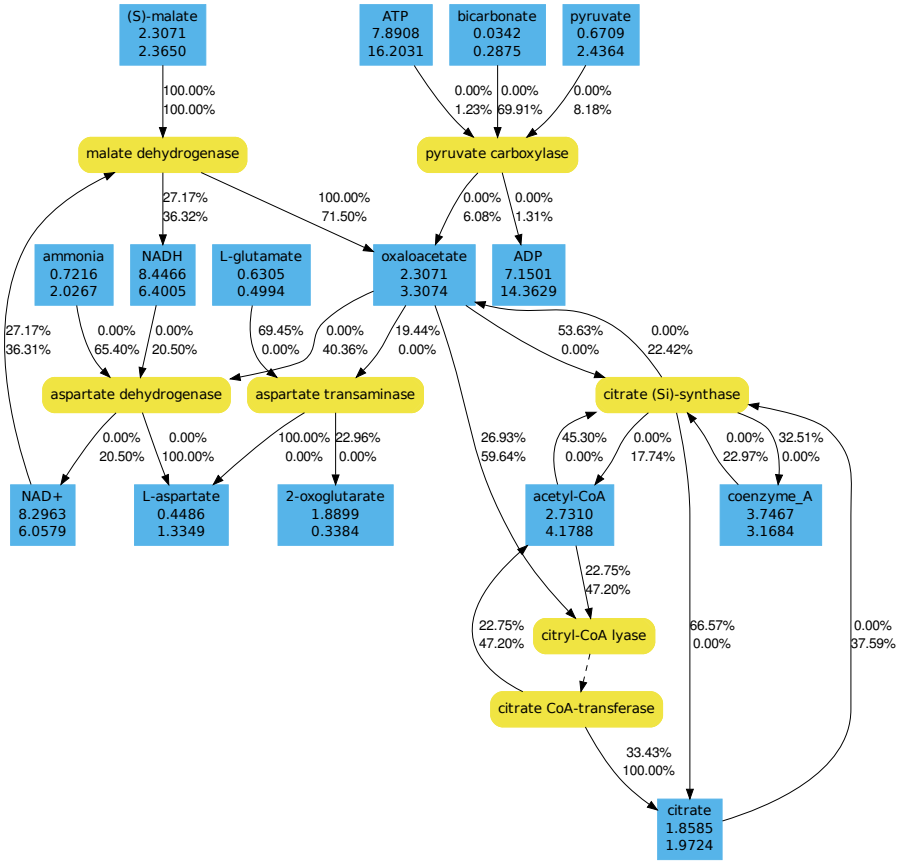

Figure 4.4: Same setup as in Figure 4.3 but with DMSP as carbon source.

Table 4.5: Relative contribution of the DMSP demethylation pathway in dependence of varying scenario parameters

			Carbon uptake rate		
			low	medium	high
dark	DMSO	ammonia	no growth	0.4%	1.1%
		nitrate	no growth	0.4%	1.0%
	oxygen	ammonia	no growth	12.1%	18.9%
		nitrate	no growth	10.2%	16.0%
light	DMSO	ammonia	100.0%	27.4%	1.6%
		nitrate	100.0%	13.8%	1.4%
	oxygen	ammonia	100.0%	39.0%	24.6%
		nitrate	100.0%	26.0%	20.8%

The percentage and the background color indicate the maximal fraction of demethylated DMSP determined by FVA while the remainder represents the DMSP degraded by the cleavage pathway. The maximal difference to the minimal contribution is 1.2%.

ports growth only in presence of light by using the demethylation pathway exclusively. In darkness, the available carbon is not sufficient to cover the basic energy demand of the cell – namely the non-growth-associated maintenance requirement and the proton flux for motility. Furthermore, we observed an increased usage of the demethylation pathway for the medium uptake rate in light compared to the dark. Interestingly, the values of the high uptake rate do not follow the same pattern. In these cases, more DMSP is demethylated under aerobic than under anaerobic conditions. To a lesser extend this is also true for the medium uptake rate. Moreover, the usage of nitrate as a nitrogen source correlates with a decreased usage of the demethylation pathway compared to ammonium.

Enabling the phosphofructokinase gene

To study the effect of a functional phosphofructokinase we carried out the same set of simulations for a phosphofructokinase enabled mutant as described above for the wild type. In agreement with established biochemical knowledge, only scenarios

with glucose as carbon source were affected by this modification. The maximal increase of the growth rate is about 0.035 h^{-1} (Figure 4.5). However, not all glucose scenarios displayed enhanced growth (leftmost bar). More specifically, none of the illuminated scenarios with a low carbon uptake rate has an increased growth rate (dark blue bar).

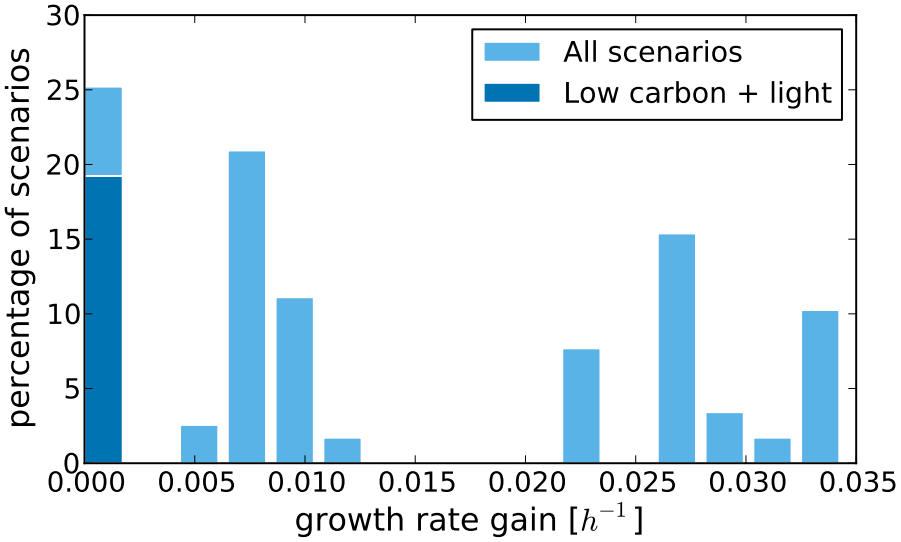

Figure 4.5: Histogram of the growth rate gain observed if phosphofructokinase is enabled in all glucose scenarios. The scenarios representing oligotrophic scenarios in light are shown in dark blue. Scenarios where both strains do not display growth are not considered.

Effect of plasmid loss

Another set of 43 740 scenarios explored the effect of a loss of all or a single plasmid using the same simulation parameters as mentioned above. These simulations revealed that the loss of all plasmids or the single loss of the 86 kb plasmid is lethal in all scenarios. The single loss of each other plasmid is predicted to be not lethal. However, closer inspection revealed that if the 153 kb plasmid is removed, the growth rate is slightly reduced compared to the wild type in a subset of the scenarios. All of those are illuminated aerobic scenarios. However, the phenomenon is restricted to the carbon sources propionate and glycerol for the low uptake rate and to

alpha-maltose, D-ribitol, beta-D-glucose, alpha-D-glucose, beta-D-fructofuranose, glycerol, alpha-L-rhamnose, succinate, fumarate, beta-D-ribofuranose, alpha-D-xylopyranose, D-xylitol, L-glutamate, and 2-oxoglutarate for the medium uptake rate. Moreover, the effect also occurs with the high uptake rate on the two carbon sources mentioned last.

Single gene knock-out mutants

We studied the effect of single gene knock-outs in 210 225 simulations. As only a loss of all copies of a gene would alter the topology of the metabolic network, we restricted the analyses to genes without paralogous genes. Furthermore, we only simulated scenarios with a medium uptake rate and 10% motile bacteria. All other parameters were varied as shown in Table 4.4. In most cases (72.6%, see Figure 4.6) the knock-out did not affect growth in any scenario. This number includes all genes with paralogous genes. Moreover, 25.3% of all knock-outs were lethal in every scenario considered here.

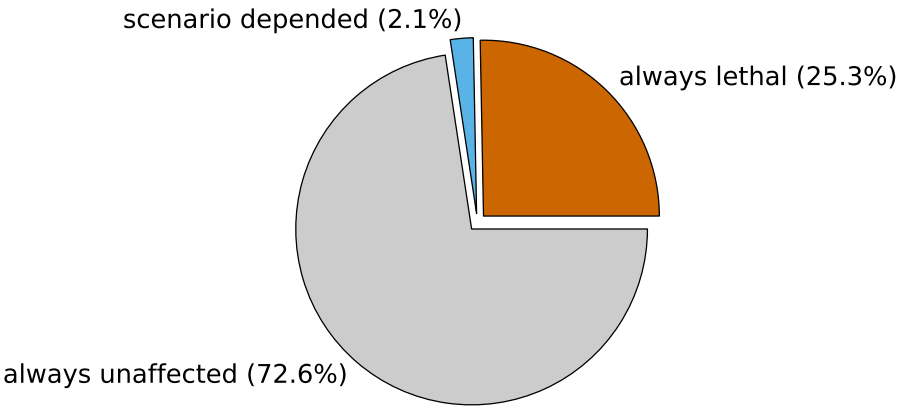

Figure 4.6: Distribution of the growth phenotype of the single gene knock-out mutants.

Only 47 knock-out mutants (2.1%) displayed a more multifaceted behavior (Figure 4.7). A detailed analysis of each mutant is beyond the scope of this work and certainly requires experimental validation. However, we note that most mutants show pronounced patterns, which correspond to similar scenario conditions. For instance, the Cobalt-precorrin-5B

(C(1))-methyltransferase encoded on Dshi_1691 is needed for the anaerobic synthesis of vitamin B_{12}. Hence, the deletion of this gene is lethal in all anaerobic scenarios. The only gene in this set, which lies on a plasmid is Dshi_3801 from the 153 kb plasmid (Figure 4.7, third row). As mentioned above, this gene codes for a catalase. If it is knocked out, the aerobic 2-oxoglutarate and the L-glutamate scenarios in light showed decreased growth. This is consistent with our observations of the plasmid knock-outs simulations. The reason is that the hydrogen peroxide created during the production of pyridoxal 5'-phosphate and the operation of the glycine oxidase must now be degraded by a cytochrome-c peroxidase. The reaction catalyzed by this enzyme depends on reducing equivalents and hence is metabolically more expensive.

Screening for elevated DMS production

A recent simulation studying the effect on climate of doubling DMS emissions (Thomas *et al.*, 2011) inspired us to screen the single knock-out mutants for elevated DMS production. The DMS created from DMSO by the dimethylsulfoxide reductase was not considered in this screening because only an overall increase of cloud-seeding volatiles would affect climate. Thus, we assured that all DMS originates from DMSP. As one might expect, the mutants with a blocked demethylation pathway showed the maximal increase of DMS production compared to the wild type (Table 4.6). In aerobic illuminated scenarios their production rate was increased by 63.8% while the growth rate was reduced to 71.6%. Unexpectedly, an additional mutant showed considerable values. The DMS production of the L-serine ammonia-lyase mutant (Dshi_5008) was increased by 27.9% and the growth rate decreased to 73.2%. On all other tested carbon sources, growth was not affected.

Enzyme missing in the mutant	Locus tag	Percent wild type growth rate	Percent additional DMS production
3-methylmercaptopropionyl-CoA ligase	Dshi_0833	71.6%	63.8%
3-methylmercaptopropionyl-CoA dehydrogenase	Dshi_0839	71.6%	63.8%
methylthioacryloyl-CoA hydrolase	Dshi_1107	71.6%	63.8%
L-serine ammonia-lyase	Dshi_5008	73.2%	27.9%

Table 4.6: Single gene knock-out mutants displaying a significantly increased DMS production rate while growing on DMSP. All values correspond to an aerobic illuminated scenario with a medium uptake rate.

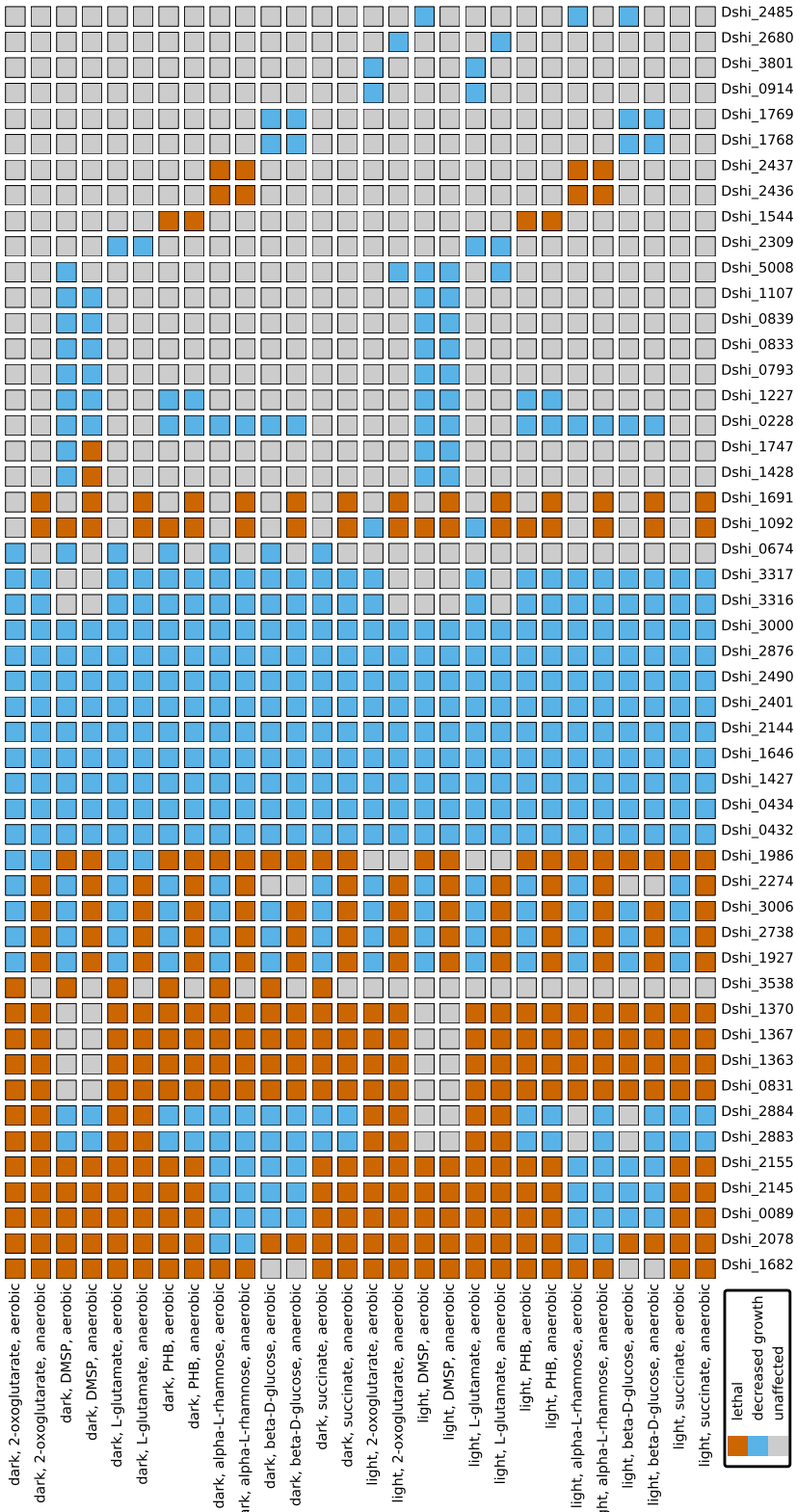

Figure 4.7: Growth of single gene knock-out mutants in different scenarios. Mutants are identified by the locus tag of the disabled gene and scenarios are given by their conditions (illumination, carbon source, and electron acceptor).

4.4 Discussion

4.4.1 *Need for efficient transporters*

Our simulations showed that the phenotype of *D. shibae* growing on glycerol or glyoxylate can only be reproduced if these compounds are allowed to pass the membrane without active transport. Otherwise, the total energy requirement of the cell, including the energy needed for the active transport, cannot be covered by the degradation of these compounds. Hence, we suppose that other transporters requiring less energy exist in *D. shibae*. However, no channel proteins for facilitated diffusion of carbon sources are annotated in the genome.

4.4.2 *Energy metabolism*

In most scenarios shown in Figure 4.2, the TCA cycle operates in forward direction and thus is used to obtain energy. However, in the simulations with glycolate as sole carbon source the isocitrate lyase converts the glycolate to D-threo-isocitrate. At this point the flux splits: 80% follow the TCA cycle in forward direction and 20% are routed to citrate. Hence, the citrate synthase runs backwards in the glycolate scenarios.

According to our simulations, the activity of the TCA cycle is significantly reduced or even reversed in light, because the aerobic anoxygenic photosynthesis satisfies the energy demand of the organism in large parts. This is in agreement with experimental results, which showed a reduced carbon dioxide excretion in light (Tomasch *et al.*, 2011). Under these conditions, the main producer of citrate in the simulation is the citrate CoA-transferase, which salvages acetate. Nevertheless, the production of oxaloacetate is increased to supply anabolic reactions. Another effect of the reduced TCA cycle activity is a decreased production of NADPH by the isocitrate dehydrogenase. Hence, the organism must increase the flux through other reactions for

compensation under illuminated conditions. For instance, our results showed an increased usage of the pentose phosphate pathway in comparison to dark conditions if glucose is used as carbon source. In general, a flexible energy metabolism is probably very important for *D. shibae* because the amount of energy generated by the aerobic anoxygenic photosynthesis can vary greatly. This can be due to changing illumination conditions but also due to the degradation of the light harvesting complex in the course of time (Biebl and Wagner-Döbler, 2006).

Furthermore, our simulations confirmed that formation of phosphoenolpyruvate from pyruvate neither needs to be active in the glucose scenarios (Fürch *et al.*, 2009) nor in any other scenario studied here. However, we found that the reverse reaction is active in all scenarios.

As we pointed out in the results section, the anaerobic glycolate scenario in light is the only one displaying variance bars. This is probably due to an energy overflow, which occurs if more energy (external protons) than needed for growth is generated by the aerobic anoxygenic photosynthesis. Thus, energy-wasting futile reactions can take place in any part of the metabolic network. Futile reactions waste energy and produce heat and thus are usually disadvantageous for the organism. Hence, they are probably tightly regulated. However, the uncertainty stems form the fact that the simulations cannot predict which set of futile reactions take place. A possibility we did not test in our simulations is a leakage of protons through the membrane. Another uncertainty in energy balance is the precise number of periplasmic protons used for motility. This number may vary greatly depending on environmental conditions and the average speed of the motile bacteria (Johansen *et al.*, 2002).

4.4.3 *Light and oxygen enhance the demethylation of DMSP*

According to our results, light and the presence of oxygen stimulate the usage of the DMSP demethylation pathway. Interest-

ingly, the effect is depended on the carbon uptake rate. While oxygen always enhances the activity of the demethylation pathway, the effect of light is much more pronounced in scenarios with a medium uptake rate. On average, the cleavage pathway is used to a greater extend but the fraction of demethylation decreases as the uptake rate increases. This is consistent with measurements made using fifteen different *Roseobacter* strains (González *et al.*, 1999). Although DMSP may have become an abundant compound only recently (Curson *et al.*, 2011), *D. shibae* and other *Roseobacters* seem to be well-suited to use it efficiently under various conditions. Whether the regulation of these pathways is really as sophisticated as predicted by our model remains an open question.

4.4.4 *Excess of reducing equivalents can cause aerobic denitrification*

Our results support the hypothesis proposed in a recent review stating that under certain conditions, nitrate respiration is not being used for energy generation but has some other function, which may be redox balancing (Shapleigh, 2011). As described above, the energy demand of the organism is more than covered by the anaerobic anoxygenic photosynthesis under low nutrient conditions. Nevertheless, our simulations showed that a terminal electron acceptor is still required for optimal growth to be retained in the light. This is due to an excess of reducing equivalents produced by different metabolic processes. These reducing equivalents need to be reoxidized to retain redox homeostasis. Again, flux balance analysis is not able to exactly determine which terminal electron acceptor is preferably used to achieve this goal. However, we used flux variability analysis to identify alternate optimal solutions. Indeed, some solutions involve denitrification under aerobic illuminated conditions. Intriguingly, this behavior has been reported for *Roseobacter denitrificans* (Doi and Shioi, 1991). We speculate that aerobic denitrification might be the preferred way to dispose electrons *in*

vivo because it does not waste carbon and produces multiple oxidized redox equivalents.

4.4.5 *Phosphofructokinase is probably of little use for D. shibae*

D. shibae is very likely adapted to an oligotrophic marine environment and a regular day/night cycle (Wagner-Döbler and Biebl, 2006). Hence, the organism may benefit only moderately from phosphofructokinase activity. This is especially true during the day when the energy demand is covered by the aerobic anoxygenic photosynthesis in large parts. On the one hand, this suggests a permanent shutdown of the phosphofructokinase. On the other hand, another possible explanation is that light induces a down regulation of the phosphofructokinase in *D. shibae* because the energy generated in lower glycolysis is not needed. This would also explain the inactivity of the enzyme observed by Fürch *et al.* as their cultures were grown in constant light (Fürch *et al.*, 2009).

4.4.6 *Plasmid and single gene knock-out mutants*

In general, we remark that it can be enlightening to simulate a great variety of scenarios for each knock-out mutant. Since some effects do not occur in all scenarios, more subtle differences between the mutants can be revealed this way. This would not be possible with the commonly used method, which relies on one or two minimal media scenarios (Puchałka *et al.*, 2008; Orth *et al.*, 2011).

The simulated loss of plasmids brought up two interesting aspects regarding the 153 kb and the 86 kb plasmid. The 153 kb plasmid harbors the only copy of a catalase (Dshi_3801), which decomposes hydrogen peroxide to oxygen and water. Albeit hydrogen peroxide is created by other metabolic reactions in our simulations, singlet oxygen is also created during aerobic

anoxygenic photosynthesis, which imposes an elevated oxidative stress level on the organism (Berghoff *et al.*, 2011). Hence, the catalase gene might be a beneficial acquisition for *D. shibae*. Furthermore, this hypothesis is supported by the fact that the catalase gene is upregulated in response to light (Tomasch *et al.*, 2011).

The 86 kb plasmid contains the complete synthesis pathway leading to dTDP-α-L-rhamnose, which is an important compound of the outer membrane. Hence, our simulations predicted no growth in case of a loss of this plasmid. However, pseudogenes and transposases located on the plasmid may indicate it is no longer needed by the organism (Wagner-Döbler *et al.*, 2010). An explanation might be that *D. shibae* is about to change its surface structure or biofilm formation capabilities and thus the genes of the dTDP-α-L-rhamnose pathway are no longer needed.

4.4.7 *Shutdown of DMSP demethylation stimulates DMS production*

For the first time, we demonstrated that in theory a single gene knock-out is sufficient to significantly enhance the production of the cloud-seeding molecule DMS. In case of the mutants with a blocked demethylation pathway, the DMSP must be degraded inevitable by the cleavage pathway to retain growth. Hence, the more than 60% increase of the DMS production can explained by the fact that 39.0% of the DMSP degraded by the demethylation pathway (Table 4.5) is now redirected to the DMS-producing cleavage pathway. A similar effect occurred when the gene coding for the L-serine ammonia-lyase was removed. Although the demethylation pathway was kept intact, its activity was greatly reduced. The reason is that the carbon atom bound to tetrahydrofolate during the demethylation of DMSP, can no longer be routed to the central carbon metabolism. This is due to the fact that the glycine hydrox-

ymethyltransferase binds this carbon atom to glycine producing L-serine whose degradation to pyruvate and ammonia is now inoperative. Alternatively, a salvage via the methionine synthase would be possible but we found no methionine degradation pathway in *D. shibae*. As the growth on the other carbon sources is not affected, the mutants could be grown on succinate for example and transferred to DMSP for DMS production afterward.

5

CONCLUSION

> *Everything that living things do can be understood in terms of the jigglings and wigglings of atoms.*
>
> — Richard Feynman

Besides a detailed computational analysis of the metabolism of *Dinoroseobacter shibae*, this thesis introduced several methods to facilitate the creation and analysis of metabolic models (Figure 5.1). All of these methods have been implemented and are available as free software.

The first step was to automate large parts of the laborious reconstruction process of the metabolic network. For this purpose, we outlined a method to query an integrated annotation database and proposed a detailed workflow for a semi-automated reconstruction process. The approach covers the mapping from enzyme or genes to reactions, application of thermodynamic rules of thumb, reactions balancing, and addition of spontaneous reactions. The main difference between the traditional reconstruction process and the automated approach presented in this work is that we use an aggregated genome annotation and an existing reaction database to rapidly create a preliminary model. Hence, more time can be spent on refinements of the model and on the elaborate interpretation of the results generated by the simulations.

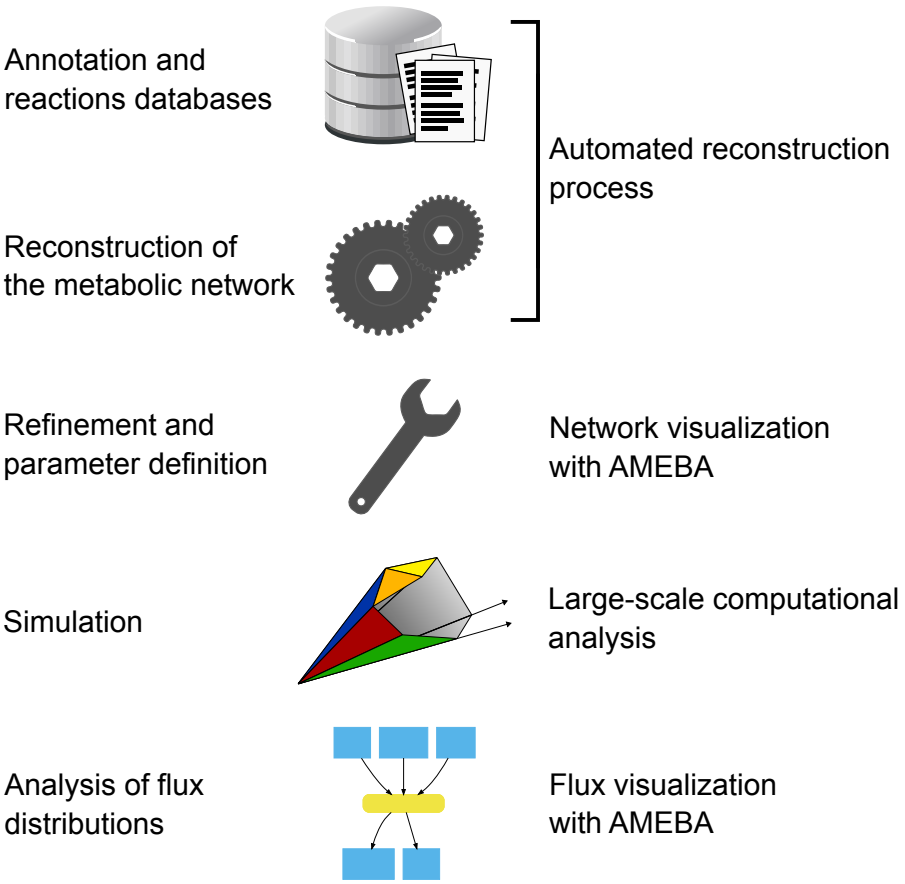

Figure 5.1: Overview of the general steps of metabolic modeling and the methods (and software) contributed by this work.

In addition, we introduced a novel visualization method for metabolic networks, which uses a generalized definition of branch points to focus on relevant metabolic context. The short processing time of the algorithm allows an interactive usage and thus an exploratory analysis of fluxes in a metabolic network.

Ultimately, these new methods have been used to enable a rapid creation of a metabolic model of *D. shibae* and a large-scale computational analysis of the metabolic capabilities of this marine bacterium, which would not have been possible with the traditional metabolic modeling approach.

In addition to a large variety of environmental conditions, we also studied plasmid and single gene knock-out mutants in our simulations. We analyzed our results with regard to en-

ergy metabolism and revealed among others a pronounced metabolic answer to the availability of light. In light, the activity of the TCA cycle is reduced or even reversed. Moreover, our results gave insight into the changing split-up of the DMSP flux to the cleavage and the demethylation pathway under the different conditions simulated. More specific, the cleavage pathway is preferred most of the time but light and oxygen stimulate the activity of the demethylation pathway. Furthermore, we found an excess of reducing equivalents to be a possible explanation for aerobic denitrification. The addition of an active phosphofructokinase to the metabolic network revealed that the enzyme is probably of little use under the conditions usually encountered by *D. shibae*. From the plasmid knock-out mutants, two showed interesting behavior. On the one hand, the 153 kb plasmid mutant showed a decreased growth in some scenarios in the light due to a missing catalase, which has been confirmed by a single gene knock-out. On the other hand, the loss of the 86 kb plasmid is predicted to be lethal because a complete synthesis pathway of an important compound of the outer membrane is encoded there. While the great majority of single gene knock-outs did not affect growth, some showed a multifaceted behavior and are lethal or growth-limiting only in a subset of scenarios. Additionally, we screened our single gene knock-out mutants for an elevated production of the cloud-seeding molecule DMS from DMSP. It turned out that four mutants showed a significantly increased production while maintaining more than 70% of the growth rate of the wild type. All of these mutants block or hamper the DMSP demethylation pathway.

Altogether, this thesis provided a new view on metabolic networks by employing new approaches in the fields of metabolic reconstruction, computational analysis, and interpretation of flux distributions.

6

APPENDIX

6.1 Arbitrary bounds cause high-flux cycles

Flux balance analysis uses a linear problem solver to find a solution, which assigns a value to each flux variable in a metabolic network. In the geometric interpretation, this solution corresponds to a vertex of the flux cone where the value of the objective function is maximal. Often, this vertex lies at an edge of a hyperplane describing an unlimited number of equivalent solutions. However, the inclusion of "arbitrarily large bounds" (Schellenberger *et al.*, 2011) for otherwise unconstrained reactions creates several additional vertices in this hyperplane and thus additional solutions the simplex algorithm may find. In these solutions, at least one reaction carries the maximal flux specified by the arbitrary constraints. Due to the steady-state condition, other reactions must also increase their flux to compensate this. If none of these reactions is a boundary reaction, they form a stoichiometrically balanced cycle. In conclusion, arbitrary bounds induce high fluxes through reactions forming stoichiometrically balanced cycles. Without those additional constraints the corresponding vertices of such solutions would not exist and the solver would instead find a solution where all unnecessary cycles are inactive.

6.2 List of genes covered in the model *i*Dsh827

Locus tag	GI	Plasmid	EC	Gene name	Score
Dshi_0001	159042557	chromosome	1.4.1.13	gltD	21
Dshi_0006	159042562	chromosome	2.3.1.117	dapD	21
Dshi_0012	159042568	chromosome	3.5.1.18	dapE1	21
Dshi_0028	159042584	chromosome	3.2.2.-	mutY	13
Dshi_0031	159042587	chromosome	2.7.1.130	lpxK	21
Dshi_0032	159042588	chromosome	2.-.-.-	kdtA	13
Dshi_0039	159042595	chromosome	3.5.4.25	ribA	19
Dshi_0054	159042610	chromosome	2.5.1.18	gst2	16
Dshi_0057	159042613	chromosome	6.1.1.4	leuS	15
Dshi_0060	159042616	chromosome	2.6.1.17		4
Dshi_0062	159042618	chromosome	1.14.13.-	ubiH	13
Dshi_0063	159042619	chromosome	3.1.3.25	suhB2	18
Dshi_0067	159042623	chromosome	4.2.1.17	caiD	9
Dshi_0071	159042627	chromosome	2.3.2.2	ggt1	17
Dshi_0074	159042630	chromosome	2.3.1.9	thlA	17
Dshi_0079	159042635	chromosome	2.3.1.-		13
Dshi_0081	159042637	chromosome	1.1.1.85	imdh	21
Dshi_0083	159042639	chromosome	4.2.1.33	leuD	19
Dshi_0085	159042641	chromosome	4.2.1.33	ipmi1	21
Dshi_0089	159042645	chromosome	5.4.2.1	ipgm	21
Dshi_0092	159042648	chromosome	3.6.1.-		13
Dshi_0125	159042681	chromosome	1.3.1.34	fadH	17
Dshi_0129	159042685	chromosome	4.2.1.9	ilvD1	21
Dshi_0131	159042687	chromosome	6.4.1.2	accD	21
Dshi_0132	159042688	chromosome	6.3.2.17	folC	17
Dshi_0134	159042690	chromosome	4.2.1.96	pcd	17
Dshi_0142	159042698	chromosome	2.4.1.129	mrcB	10
Dshi_0145	159042701	chromosome	2.6.1.57		13
Dshi_0146	159042702	chromosome	2.8.1.2	sseA	17
Dshi_0149	159042705	chromosome	4.2.1.52	dapA	21
Dshi_0150	159042706	chromosome	3.2.1.-		13
Dshi_0157	159042713	chromosome	2.5.1.17	cobA2	18
Dshi_0158	159042714	chromosome	6.6.1.2	cobN	21
Dshi_0165	159042721	chromosome	6.3.1.10	cobD	17
Dshi_0166	159042722	chromosome	4.1.1.81	cobC	12
Dshi_0171	159042727	chromosome	4.99.1.3	cbiX2	18
Dshi_0172	159042728	chromosome	5.4.1.2	cobH	19
Dshi_0173	159042729	chromosome	2.1.1.132	cobL	20
Dshi_0174	159042730	chromosome	2.1.1.130	cobI	10
Dshi_0175	159042731	chromosome	2.1.1.131	cbiG	11
Dshi_0175	159042731	chromosome	1.14.13.83	cbiG	6
Dshi_0176	159042732	chromosome	2.1.1.133	cobM	19
Dshi_0178	159042734	chromosome	4.4.1.8		13
Dshi_0181	159042737	chromosome	2.1.2.9	fmt	21
Dshi_0185	159042741	chromosome	2.7.7.41	cdsA2	17
Dshi_0188	159042744	chromosome	1.17.1.2	ispH	21
Dshi_0192	159042748	chromosome	2.7.6.3	hppk	17
Dshi_0194	159042750	chromosome	2.7.6.5	relA	21
Dshi_0196	159042752	chromosome	2.6.99.2	pdxJ	20
Dshi_0198	159042754	chromosome	2.7.8.7	acpS	17
Dshi_0213	159042769	chromosome	4.1.1.49	pckA	21
Dshi_0214	159042770	chromosome	1.1.1.157	hbdA	20
Dshi_0228	159042784	chromosome	2.7.1.40	pykA	21
Dshi_0235	159042791	chromosome	6.1.1.20	pheS	21
Dshi_0237	159042793	chromosome	6.1.1.20	pheT	21
Dshi_0239	159042795	chromosome	1.4.1.21	nadX	17
Dshi_0240	159042796	chromosome	2.5.1.18	gst3	16
Dshi_0244	159042800	chromosome	1.4.1.1	adh	17
Dshi_0253	159042809	chromosome	6.2.1.12		13
Dshi_0273	159042829	chromosome	3.6.5.3	fusA	10
Dshi_0274	159042830	chromosome	3.6.5.3	tufA1	10
Dshi_0306	159042862	chromosome	2.7.4.3	adk	19

Locus tag	GI	Plasmid	EC	Gene name	Score
Dshi_0315	159042871	chromosome	5.4.99.12	rluC	10
Dshi_0316	159042872	chromosome	3.1.3.18	gph	16
Dshi_0324	159042880	chromosome	2.7.2.8	argB	21
Dshi_0325	159042881	chromosome	1.1.1.100	fabG3	10
Dshi_0332	159042888	chromosome	3.1.26.5	rnpA	16
Dshi_0335	159042891	chromosome	1.16.1.1	merA	17
Dshi_0347	159042903	chromosome	1.16.8.1	bluB	10
Dshi_0349	159042905	chromosome	5.4.99.5	pheA1	15
Dshi_0358	159042914	chromosome	3.5.4.10	purH	13
Dshi_0358	159042914	chromosome	2.1.2.3	purH	21
Dshi_0373	159042929	chromosome	6.2.1.3	fadD3	17
Dshi_0382	159042938	chromosome	6.2.1.30	paaK	17
Dshi_0386	159042942	chromosome	3.5.3.8	hutG	10
Dshi_0428	159042983	chromosome	2.3.1.-	phaC	13
Dshi_0432	159042987	chromosome	3.5.3.6	arcA	21
Dshi_0433	159042988	chromosome	2.1.3.3	arcB	21
Dshi_0434	159042989	chromosome	2.7.2.2	arcC	19
Dshi_0435	159042990	chromosome	3.6.3.14	atpD1	21
Dshi_0436	159042991	chromosome	3.6.3.14	atpC2	14
Dshi_0439	159042994	chromosome	3.6.3.14	atpB2	15
Dshi_0440	159042995	chromosome	3.6.3.14	atpE1	15
Dshi_0441	159042996	chromosome	3.6.3.14	atpF1	14
Dshi_0442	159042997	chromosome	3.6.3.14	atpA2	21
Dshi_0443	159042998	chromosome	3.6.3.14	atpG1	17
Dshi_0452	159043007	chromosome	1.3.3.11	pqqC	20
Dshi_0473	159043028	chromosome	1.1.1.284		14
Dshi_0474	159043029	chromosome	3.1.2.12		20
Dshi_0504	159043059	chromosome	1.2.1.2	fdnG	17
Dshi_0505	159043060	chromosome	1.2.1.2	fdnH	16
Dshi_0506	159043061	chromosome	1.2.1.2	fdnI	17
Dshi_0520	159043073	chromosome	2.7.1.100	mtnK	19
Dshi_0521	159043074	chromosome	5.3.1.23	mtnA	21
Dshi_0523	159043076	chromosome	4.1.2.17	fucA	19
Dshi_0534	159043087	chromosome	1.2.4.1	pdhA2	17
Dshi_0535	159043088	chromosome	1.2.4.1	pdhB1	17
Dshi_0536	159043089	chromosome	2.3.1.12	pdhC2	18
Dshi_0541	159043094	chromosome	1.3.99.22	hemN1	20
Dshi_0546	159043099	chromosome	3.6.3.20	ugpC2	13
Dshi_0551	159043104	chromosome	1.1.1.9	xylD	21
Dshi_0552	159043105	chromosome	5.3.1.27		9
Dshi_0554	159043107	chromosome	1.1.1.56	rbtD	20
Dshi_0555	159043108	chromosome	2.7.1.16	araB	10
Dshi_0555	159043108	chromosome	2.7.1.47	araB	4
Dshi_0577	159043130	chromosome	1.2.1.3	aldH2	17
Dshi_0583	159043136	chromosome	2.5.1.55	kdsA	20
Dshi_0590	159043143	chromosome	1.1.1.79		10
Dshi_0592	159043145	chromosome	2.4.1.129	ftsI1	10
Dshi_0596	159043149	chromosome	2.3.3.13	leuA	21
Dshi_0601	159043154	chromosome	6.3.1.5	nadE	11
Dshi_0601	159043154	chromosome	6.3.5.1	nadE	14
Dshi_0615	159043168	chromosome	4.1.1.23	pyrF	18
Dshi_0620	159043173	chromosome	1.1.1.100	fabG2	10
Dshi_0628	159043181	chromosome	6.3.2.12		2
Dshi_0630	159043183	chromosome	1.1.5.3	glpD	17
Dshi_0632	159043185	chromosome	2.7.2.1	ackA	20
Dshi_0633	159043186	chromosome	2.3.1.8	pta2	12
Dshi_0651	159043204	chromosome	3.6.1.22		12
Dshi_0653	159043206	chromosome	4.2.1.51	pheA2	17
Dshi_0659	159043212	chromosome	1.3.99.22	hemN2	21
Dshi_0661	159043214	chromosome	1.9.3.1	fixN	21
Dshi_0662	159043215	chromosome	1.9.3.1	fixO	17
Dshi_0663	159043216	chromosome	1.9.3.1	fixQ	14
Dshi_0664	159043217	chromosome	1.9.3.1	fixP	17
Dshi_0667	159043220	chromosome	3.6.3.4	fixI	11
Dshi_0669	159043222	chromosome	3.4.16.4	dacC2	17
Dshi_0674	159043227	chromosome	1.3.3.3	hemF	19
Dshi_0675	159043228	chromosome	2.3.2.2	ggt2	17

Locus tag	GI	Plasmid	EC	Gene name	Score
Dshi_0680	159043233	chromosome	4.1.1.21	purK	10
Dshi_0688	159043241	chromosome	1.3.99.1		12
Dshi_0689	159043242	chromosome	4.1.3.30	prpB	12
Dshi_0690	159043243	chromosome	3.3.2.1	entB	9
Dshi_0695	159043248	chromosome	4.2.1.33	leuC	21
Dshi_0696	159043249	chromosome	4.2.1.33	leuD_2	17
Dshi_0713	159043265	chromosome	3.1.1.75		10
Dshi_0718	159043270	chromosome	6.4.1.3	pccB	17
Dshi_0723	159043275	chromosome	6.4.1.3	pccA	21
Dshi_0726	159043278	chromosome	5.4.99.2	bhbA	21
Dshi_0728	159043280	chromosome	1.6.99.5	mnhA	10
Dshi_0731	159043283	chromosome	1.6.99.5	mnhD	10
Dshi_0739	159043291	chromosome	3.6.1.40	ppx	13
Dshi_0744	159043296	chromosome	6.1.1.15	proS	21
Dshi_0748	159043300	chromosome	3.6.3.-	lolD	13
Dshi_0762	159043314	chromosome	2.6.1.1	aspC	21
Dshi_0762	159043314	chromosome	2.6.1.-	aspC	
Dshi_0767	159043319	chromosome	4.4.1.5		15
Dshi_0768	159043320	chromosome	2.1.1.148	thyX	21
Dshi_0775	159043327	chromosome	1.1.1.93	ttuC	17
Dshi_0775	159043327	chromosome	1.1.1.83	ttuC	15
Dshi_0775	159043327	chromosome	4.1.1.73	ttuC	17
Dshi_0777	159043329	chromosome	6.1.1.3	thrS	21
Dshi_0787	159043339	chromosome	2.7.8.26	cobS1	14
Dshi_0788	159043340	chromosome	2.4.2.21	cobT	20
Dshi_0793	159043345	chromosome	2.5.1.49	metB2	17
Dshi_0794	159043346	chromosome	4.2.1.19	hisB	19
Dshi_0795	159043347	chromosome	2.4.2.-	hisH	13
Dshi_0796	159043348	chromosome	2.1.3.3	argF	14
Dshi_0798	159043350	chromosome	2.6.1.11	argD	21
Dshi_0805	159043357	chromosome	2.3.3.15		21
Dshi_0815	159043367	chromosome	4.4.1.5		9
Dshi_0821	159043373	chromosome	2.1.2.1	glyA	21
Dshi_0822	159043374	chromosome	2.7.1.23	ppnK	20
Dshi_0825	159043377	chromosome	6.2.1.17		11
Dshi_0827	159043379	chromosome	3.5.4.5	cdd	16
Dshi_0828	159043380	chromosome	2.4.2.4	deoA	20
Dshi_0829	159043381	chromosome	5.4.2.7	deoB	20
Dshi_0830	159043382	chromosome	3.5.4.4	add	18
Dshi_0831	159043383	chromosome	2.4.2.9	upp	19
Dshi_0833	159043385	chromosome	6.2.1.-	DmdB	6
Dshi_0835	159043387	chromosome	5.1.2.3	fadJ	17
Dshi_0837	159043389	chromosome	2.5.1.18		9
Dshi_0839	159043391	chromosome	1.3.8.-	DmdC	
Dshi_0849	159043401	chromosome	3.1.3.5		20
Dshi_0850	159043402	chromosome	3.6.4.13	deaD	11
Dshi_0853	159043405	chromosome	6.2.1.3	fadD2	10
Dshi_0877	159043429	chromosome	3.1.3.26		10
Dshi_0887	159043439	chromosome	2.6.1.45	sgaA2	20
Dshi_0888	159043440	chromosome	4.3.1.19		17
Dshi_0890	159043442	chromosome	4.3.1.12		19
Dshi_0891	159043443	chromosome	2.5.1.47	cysK	19
Dshi_0908	159043460	chromosome	3.5.99.2		9
Dshi_0911	159043463	chromosome	2.5.1.3	thiE	18
Dshi_0914	159043466	chromosome	1.4.3.19	thiO	17
Dshi_0915	159043467	chromosome	2.7.4.7	thiD	16
Dshi_0922	159043474	chromosome	2.7.4.9	tmk	19
Dshi_0923	159043475	chromosome	3.4.16.4	dacC1	17
Dshi_0931	159043483	chromosome	1.1.1.1	adhA	20
Dshi_0947	159043499	chromosome	3.1.1.29	pthA	19
Dshi_0948	159043500	chromosome	1.1.2.3	lldD2	17
Dshi_0952	159043504	chromosome	4.2.1.20	trpA	20
Dshi_0961	159043513	chromosome	1.13.11.1		9
Dshi_0969	159043518	chromosome	1.1.1.67	mtlK	21
Dshi_0977	159043526	chromosome	2.5.1.7	murA	21
Dshi_0979	159043528	chromosome	1.1.1.23	hisD	21
Dshi_0996	159043545	chromosome	1.6.99.5		10

Locus tag	GI	Plasmid	EC	Gene name	Score
Dshi_0998	159043547	chromosome	3.5.4.2	ade	21
Dshi_1000	159043549	chromosome	6.2.1.3	fadD4	21
Dshi_1001	159043550	chromosome	1.1.1.95	serA2	17
Dshi_1002	159043551	chromosome	2.5.1.48	metB1	19
Dshi_1007	159043556	chromosome	3.1.1.24	catD	10
Dshi_1008	159043557	chromosome	1.3.1.9	fabI1	19
Dshi_1009	159043558	chromosome	2.3.1.41	fabB	17
Dshi_1010	159043559	chromosome	4.2.1.58	fabA	
Dshi_1010	159043559	chromosome	4.2.1.61	fabA	
Dshi_1010	159043559	chromosome	4.2.1.60	fabA	18
Dshi_1012	159043561	chromosome	2.5.1.6	metK	21
Dshi_1021	159043570	chromosome	2.1.1.33	trmB	20
Dshi_1022	159043571	chromosome	2.5.1.19	aroA	21
Dshi_1023	159043572	chromosome	2.7.4.14	cmk	19
Dshi_1029	159043578	chromosome	5.3.1.24	trpF	18
Dshi_1031	159043580	chromosome	4.2.1.20	trpB	21
Dshi_1048	159043597	chromosome	4.2.1.17		9
Dshi_1051	159043600	chromosome	4.2.1.79		10
Dshi_1067	159043616	chromosome	1.15.1.1	sod	19
Dshi_1073	159043622	chromosome	2.1.1.13		17
Dshi_1074	159043623	chromosome	2.1.1.13		11
Dshi_1076	159043625	chromosome	6.3.2.6	purC	21
Dshi_1078	159043627	chromosome	1.1.1.1		17
Dshi_1079	159043628	chromosome	6.3.5.3	purQ	20
Dshi_1082	159043631	chromosome	2.3.2.8	ate	21
Dshi_1092	159043641	chromosome	4.1.3.1		0
Dshi_1095	159043644	chromosome	1.2.1.3		21
Dshi_1099	159043648	chromosome	1.8.4.11	msrA2	18
Dshi_1100	159043649	chromosome	2.1.1.-	prmA	13
Dshi_1107	159043656	chromosome	3.1.2.-		13
Dshi_1114	159043663	chromosome	6.3.4.-	tilS	13
Dshi_1134	159043683	chromosome	2.8.3.5		18
Dshi_1136	159043685	chromosome	2.8.3.5		20
Dshi_1140	159043689	chromosome	1.9.3.1	ctaC	13
Dshi_1141	159043690	chromosome	2.5.1.-	ctaB	13
Dshi_1144	159043693	chromosome	1.9.3.1	ctaE	20
Dshi_1146	159043695	chromosome	4.2.3.1	thrC	21
Dshi_1150	159043699	chromosome	1.18.1.2		17
Dshi_1152	159043701	chromosome	1.8.4.8	cysH	19
Dshi_1153	159043702	chromosome	1.8.1.2	cysI	11
Dshi_1155	159043704	chromosome	1.3.1.76		17
Dshi_1158	159043707	chromosome	3.2.2.1	rih	11
Dshi_1161	159043710	chromosome	3.5.1.32		17
Dshi_1169	159043718	chromosome	3.5.1.28	amiC	17
Dshi_1171	159043720	chromosome	2.4.1.129		10
Dshi_1180	159043729	chromosome	5.-.-.-	queA	13
Dshi_1182	159043731	chromosome	2.3.1.37	hemA2	21
Dshi_1184	159043733	chromosome	1.17.7.1	ispG	21
Dshi_1186	159043735	chromosome	1.1.1.262	pdxA	20
Dshi_1199	159043748	chromosome	3.1.3.25	suhB1	19
Dshi_1207	159043756	chromosome	6.3.5.6	gatB	11
Dshi_1210	159043759	chromosome	1.2.99.2	coxM	19
Dshi_1211	159043760	chromosome	1.2.99.2	coxS	18
Dshi_1212	159043761	chromosome	1.2.99.2	coxL2	21
Dshi_1216	159043765	chromosome	1.1.1.169	panE	20
Dshi_1223	159043772	chromosome	3.4.11.2	pepN	21
Dshi_1227	159043776	chromosome	2.3.3.9	glcB	21
Dshi_1230	159043779	chromosome	3.7.1.3		20
Dshi_1233	159043782	chromosome	1.6.1.2	pntA	17
Dshi_1234	159043783	chromosome	1.6.1.2	pntB	17
Dshi_1235	159043784	chromosome	2.7.1.17	xylB1	19
Dshi_1236	159043785	chromosome	1.8.5.3	dmsC	
Dshi_1237	159043786	chromosome	1.8.5.3	dmsB	
Dshi_1238	159043787	chromosome	1.8.5.3	dmsA	
Dshi_1239	159043788	chromosome	3.2.1.23	lacZ	21
Dshi_1241	159043790	chromosome	4.1.2.21	dgoA	16
Dshi_1242	159043791	chromosome	2.7.1.58	dgoK	17

Locus tag	GI	Plasmid	EC	Gene name	Score
Dshi_1244	159043793	chromosome	4.2.1.9	ilvD2	17
Dshi_1245	159043794	chromosome	3.2.1.22	melA	21
Dshi_1254	159043803	chromosome	1.2.1.12		20
Dshi_1259	159043808	chromosome	3.6.3.4		15
Dshi_1265	159043814	chromosome	1.1.1.18	idhA	19
Dshi_1266	159043815	chromosome	4.1.2.13	fbaA	18
Dshi_1268	159043817	chromosome	2.7.1.92	iolC	13
Dshi_1269	159043818	chromosome	3.7.1.-	iolD	7
Dshi_1271	159043820	chromosome	4.2.1.44		12
Dshi_1273	159043822	chromosome	5.1.1.1		10
Dshi_1282	159043831	chromosome	1.2.1.2	fdhA	17
Dshi_1283	159043832	chromosome	6.3.4.3	fhs	21
Dshi_1285	159043834	chromosome	1.5.1.5	folD	21
Dshi_1288	159043837	chromosome	3.5.1.32		17
Dshi_1289	159043838	chromosome	6.3.5.2		18
Dshi_1293	159043842	chromosome	2.6.1.16	glmS	21
Dshi_1294	159043843	chromosome	2.7.7.23	glmU	21
Dshi_1295	159043844	chromosome	3.1.3.18		17
Dshi_1300	159043849	chromosome	6.4.1.4	mccB	17
Dshi_1301	159043850	chromosome	6.4.1.4	mccA	17
Dshi_1302	159043851	chromosome	2.5.1.18		10
Dshi_1303	159043852	chromosome	4.1.3.4	mvaB	18
Dshi_1304	159043853	chromosome	4.2.1.18	mvaA	16
Dshi_1307	159043856	chromosome	1.6.5.3	nuoA	16
Dshi_1309	159043858	chromosome	1.6.99.5	nuoC	14
Dshi_1313	159043862	chromosome	1.6.5.3	nuoE	19
Dshi_1320	159043869	chromosome	1.6.99.5	nuoG	14
Dshi_1321	159043870	chromosome	1.6.99.5	nuoH	14
Dshi_1329	159043878	chromosome	1.6.99.5	nuoN	14
Dshi_1331	159043880	chromosome	2.7.1.33		15
Dshi_1339	159043888	chromosome	1.1.1.100		10
Dshi_1341	159043890	chromosome	3.6.3.30		11
Dshi_1350	159043899	chromosome	2.7.4.6	ndk	17
Dshi_1361	159043910	chromosome	1.1.2.4	dld1	17
Dshi_1362	159043911	chromosome	1.4.1.13		11
Dshi_1363	159043912	chromosome	1.3.1.2	pyrD1	10
Dshi_1366	159043915	chromosome	2.6.1.18		17
Dshi_1367	159043916	chromosome	3.5.1.6	amaB	4
Dshi_1370	159043919	chromosome	3.5.2.2	dht	21
Dshi_1375	159043924	chromosome	4.1.1.17		17
Dshi_1376	159043925	chromosome	3.5.2.10		17
Dshi_1378	159043927	chromosome	1.6.5.2		10
Dshi_1379	159043928	chromosome	1.6.5.2		10
Dshi_1381	159043930	chromosome	3.5.4.1		10
Dshi_1394	159043943	chromosome	2.3.2.6	aat	21
Dshi_1399	159043948	chromosome	6.2.1.1	acsA	21
Dshi_1426	159043975	chromosome	4.2.1.2		17
Dshi_1427	159043976	chromosome	2.8.3.10	citF	17
Dshi_1428	159043977	chromosome	1.1.1.59	DddA	
Dshi_1429	159043978	chromosome	1.1.1.100	fabG	10
Dshi_1430	159043979	chromosome	1.2.1.3		14
Dshi_1439	159043988	chromosome	4.4.1.15		13
Dshi_1467	159044016	chromosome	2.7.2.11	proB	21
Dshi_1469	159044018	chromosome	1.2.1.41	proA	21
Dshi_1473	159044022	chromosome	2.3.1.51		9
Dshi_1474	159044023	chromosome	6.1.1.-		13
Dshi_1492	159044041	chromosome	2.5.1.75	miaA	21
Dshi_1493	159044042	chromosome	2.7.4.22	pyrH	14
Dshi_1495	159044044	chromosome	2.5.1.31	uppS	19
Dshi_1496	159044045	chromosome	2.7.7.41	cdsA1	16
Dshi_1497	159044046	chromosome	1.1.1.267	dxr	21
Dshi_1501	159044050	chromosome	4.2.1.-	fabZ	13
Dshi_1501	159044050	chromosome	4.2.1.59	fabZ	
Dshi_1502	159044051	chromosome	2.3.1.129	lpxA	20
Dshi_1504	159044053	chromosome	2.4.1.182	lpxB	20
Dshi_1506	159044055	chromosome	2.1.1.61	mnmA	10
Dshi_1510	159044059	chromosome	3.6.4.12	recG	11

Locus tag	GI	Plasmid	EC	Gene name	Score
Dshi_1514	159044063	chromosome	2.5.1.3		10
Dshi_1515	159044064	chromosome	3.5.4.19	hisI	17
Dshi_1526	159044075	chromosome	2.5.1.54	aroH	17
Dshi_1529	159044078	chromosome	2.7.4.8	gmk	20
Dshi_1536	159044085	chromosome	3.6.3.27	pstB	21
Dshi_1544	159044093	chromosome	1.1.1.30		13
Dshi_1551	159044100	chromosome	4.2.1.10		19
Dshi_1554	159044103	chromosome	5.3.1.22		11
Dshi_1563	159044112	chromosome	4.2.1.24	hemB1	20
Dshi_1577	159044126	chromosome	4.6.1.12	ispDF	13
Dshi_1577	159044126	chromosome	2.7.7.60	ispDF	21
Dshi_1578	159044127	chromosome	3.1.3.27		10
Dshi_1581	159044130	chromosome	2.4.2.8	hpt	18
Dshi_1586	159044135	chromosome	2.1.1.-	mttb	13
Dshi_1587	159044136	chromosome	6.3.5.2	guaA	21
Dshi_1593	159044142	chromosome	2.3.1.46	metA	21
Dshi_1604	159044153	chromosome	4.2.1.17		10
Dshi_1608	159044157	chromosome	4.2.3.4	aroB	21
Dshi_1609	159044158	chromosome	2.7.1.71	aroK	18
Dshi_1618	159044167	chromosome	2.3.1.-	lpxD	13
Dshi_1618	159044167	chromosome	2.3.1.191	lpxD	
Dshi_1621	159044170	chromosome	2.7.1.11		17
Dshi_1642	159044191	chromosome	6.1.1.7	alaS	21
Dshi_1646	159044195	chromosome	1.1.1.205	guaB	17
Dshi_1647	159044196	chromosome	4.1.2.-	hpcH	13
Dshi_1648	159044197	chromosome	3.6.3.19	malK	13
Dshi_1649	159044198	chromosome	3.2.1.20		15
Dshi_1654	159044203	chromosome	3.2.1.21	bglA	20
Dshi_1655	159044204	chromosome	2.7.1.2	glk	18
Dshi_1667	159044216	chromosome	1.7.1.4	nasD	21
Dshi_1668	159044217	chromosome	1.7.1.4	nasE	15
Dshi_1669	159044218	chromosome	1.7.99.4	nasA	17
Dshi_1671	159044220	chromosome	1.3.1.76	cysG	17
Dshi_1671	159044220	chromosome	4.99.1.4	cysG	7
Dshi_1675	159044224	chromosome	1.5.1.20		10
Dshi_1677	159044226	chromosome	2.1.1.13		11
Dshi_1682	159044231	chromosome	5.3.1.9	pgi	21
Dshi_1683	159044232	chromosome	3.1.1.31		17
Dshi_1684	159044233	chromosome	1.1.1.49	zwf	21
Dshi_1690	159044239	chromosome	1.3.1.54	cobK	19
Dshi_1691	159044240	chromosome	2.1.1.195	cbiD	
Dshi_1692	159044241	chromosome	2.1.1.107	cobA1	20
Dshi_1693	159044242	chromosome	6.3.5.9	cobB	10
Dshi_1696	159044245	chromosome	2.3.3.13		11
Dshi_1698	159044247	chromosome	6.1.1.16	cysS	21
Dshi_1702	159044251	chromosome	3.6.3.-	znuC	13
Dshi_1713	159044262	chromosome	6.3.5.3	purL	21
Dshi_1720	159044269	chromosome	2.3.1.180	fabH	15
Dshi_1723	159044272	chromosome	3.5.4.13		18
Dshi_1725	159044274	chromosome	1.5.1.3		1
Dshi_1726	159044275	chromosome	3.2.1.52	nagZ	17
Dshi_1728	159044277	chromosome	6.1.1.19	argS	21
Dshi_1729	159044278	chromosome	3.1.5.1		11
Dshi_1732	159044281	chromosome	2.1.1.-	hemK	13
Dshi_1735	159044284	chromosome	3.5.3.11	speB	20
Dshi_1738	159044287	chromosome	2.2.1.1	tktA	21
Dshi_1740	159044289	chromosome	1.2.1.12	gap2	21
Dshi_1742	159044291	chromosome	1.2.1.12	gap1	21
Dshi_1744	159044293	chromosome	2.7.7.3	coaD	19
Dshi_1747	159044296	chromosome	1.2.1.18	DddC	0
Dshi_1747	159044296	chromosome	1.2.1.27	mmsA	17
Dshi_1749	159044298	chromosome	6.3.-.-		13
Dshi_1751	159044300	chromosome	4.2.1.17		10
Dshi_1752	159044301	chromosome	1.1.1.31	mmsB	17
Dshi_1753	159044302	chromosome	4.2.1.17		19
Dshi_1759	159044308	chromosome	1.2.1.38	argC	21
Dshi_1760	159044309	chromosome	5.1.1.3	murI	21

Locus tag	GI	Plasmid	EC	Gene name	Score
Dshi_1762	159044311	chromosome	1.2.7.8		17
Dshi_1768	159044317	chromosome	4.1.3.16	eda	15
Dshi_1768	159044317	chromosome	4.1.2.14	eda	16
Dshi_1769	159044318	chromosome	4.2.1.12	edd	21
Dshi_1779	159044328	chromosome	2.2.1.6	ilvI	17
Dshi_1781	159044330	chromosome	2.2.1.6	ilvH	10
Dshi_1785	159044334	chromosome	1.17.4.1	nrdJ	21
Dshi_1789	159044338	chromosome	1.4.3.5	pdxH	19
Dshi_1790	159044339	chromosome	1.3.1.9	fabI2	20
Dshi_1793	159044342	chromosome	2.4.2.22	gpt	18
Dshi_1796	159044345	chromosome	4.1.3.27	trpE	21
Dshi_1798	159044347	chromosome	4.1.3.27	trpG	18
Dshi_1799	159044348	chromosome	2.4.2.18	trpD	21
Dshi_1800	159044349	chromosome	4.1.1.48	trpC	20
Dshi_1805	159044354	chromosome	6.1.1.17	gltX	21
Dshi_1806	159044355	chromosome	2.3.3.1	gltA2	21
Dshi_1811	159044360	chromosome	1.8.1.4	lpdV	21
Dshi_1820	159044369	chromosome	3.1.3.70		17
Dshi_1824	159044373	chromosome	2.4.1.7		14
Dshi_1825	159044374	chromosome	2.3.1.8	pta1	19
Dshi_1828	159044377	chromosome	2.3.3.15	xcs	21
Dshi_1839	159044388	chromosome	6.3.1.2	glnA	21
Dshi_1842	159044391	chromosome	4.3.2.2	purB	17
Dshi_1849	159044398	chromosome	4.2.1.84	nthA	18
Dshi_1851	159044400	chromosome	4.2.1.3	acnA	21
Dshi_1855	159044404	chromosome	3.6.3.41	ccmA	18
Dshi_1863	159044412	chromosome	6.1.1.11	serS	21
Dshi_1867	159044416	chromosome	6.3.1.2	glnT	21
Dshi_1885	159044434	chromosome	1.14.13.1		10
Dshi_1887	159044436	chromosome	3.1.13.5		15
Dshi_1888	159044437	chromosome	2.1.2.2	purN	16
Dshi_1889	159044438	chromosome	6.3.3.1	purM	21
Dshi_1896	159044445	chromosome	1.1.1.132	algD	20
Dshi_1897	159044446	chromosome	5.3.1.8	algA	13
Dshi_1897	159044446	chromosome	2.7.7.22	algA	17
Dshi_1900	159044449	chromosome	5.4.2.8	algC	21
Dshi_1927	159044476	chromosome	2.2.1.2	tal	19
Dshi_1933	159044481	chromosome	6.1.1.5	ileS	15
Dshi_1935	159044483	chromosome	1.8.1.9		11
Dshi_1938	159044486	chromosome	5.4.99.12	truA	21
Dshi_1943	159044491	chromosome	3.5.4.1	codA	17
Dshi_1966	159044513	chromosome	1.8.1.4	lpdA	17
Dshi_1967	159044514	chromosome	2.3.1.12	aceF	17
Dshi_1968	159044515	chromosome	1.2.4.1	aceE	21
Dshi_1976	159044522	chromosome	2.7.1.15		9
Dshi_1986	159044532	chromosome	1.1.1.42	icd	17
Dshi_1996	159044542	chromosome	5.3.1.5	xylA	21
Dshi_1997	159044543	chromosome	2.7.1.17	xylB2	17
Dshi_2005	159044551	chromosome	1.11.1.5		12
Dshi_2010	159044556	chromosome	3.6.3.28	phnC1	13
Dshi_2017	159044563	chromosome	3.6.3.20	ugpC4	20
Dshi_2020	159044566	chromosome	5.4.2.2	pgm	21
Dshi_2034	159044580	chromosome	1.1.1.23	hisD2	21
Dshi_2038	159044584	chromosome	4.2.1.7		11
Dshi_2042	159044587	chromosome	2.6.1.77	tpa	21
Dshi_2045	159044590	chromosome	2.3.3.15	xsc	14
Dshi_2055	159044599	chromosome	1.11.1.9		9
Dshi_2060	159044604	chromosome	4.2.1.3	acnB	20
Dshi_2061	159044605	chromosome	2.7.2.4	lysC	17
Dshi_2068	159044612	chromosome	2.4.2.28		13
Dshi_2070	159044614	chromosome	4.4.1.5		9
Dshi_2074	159044618	chromosome	2.4.2.7	apt	19
Dshi_2078	159044622	chromosome	5.3.1.1	tpiA	21
Dshi_2080	159044624	chromosome	1.5.1.20	metF	19
Dshi_2086	159044630	chromosome	1.2.99.2	coxL3	17
Dshi_2087	159044631	chromosome	6.1.1.9	valS	21
Dshi_2088	159044632	chromosome	2.6.1.9		12

Locus tag	GI	Plasmid	EC	Gene name	Score
Dshi_2090	159044634	chromosome	2.6.1.45		13
Dshi_2096	159044640	chromosome	6.3.5.10	cobQ	10
Dshi_2111	159044655	chromosome	3.5.1.10	purU	17
Dshi_2113	159044656	chromosome	2.1.2.1	glyA_2	21
Dshi_2114	159044657	chromosome	1.5.3.1		9
Dshi_2115	159044658	chromosome	1.5.3.1	soxA2	21
Dshi_2116	159044659	chromosome	1.5.3.1		10
Dshi_2117	159044660	chromosome	1.5.3.1	soxB	21
Dshi_2124	159044667	chromosome	3.5.2.10		13
Dshi_2126	159044669	chromosome	3.5.3.3		21
Dshi_2132	159044675	chromosome	2.4.2.14	purF	21
Dshi_2136	159044679	chromosome	3.1.3.5	surE	21
Dshi_2144	159044687	chromosome	4.1.2.5		19
Dshi_2145	159044688	chromosome	4.2.1.11	eno	21
Dshi_2150	159044693	chromosome	2.7.1.-	anmK	13
Dshi_2151	159044694	chromosome	6.1.1.1	tyrS	21
Dshi_2155	159044698	chromosome	2.7.2.3	pgk	21
Dshi_2156	159044699	chromosome	4.1.2.13	fda	20
Dshi_2158	159044701	chromosome	1.2.4.1	pdhA1	21
Dshi_2159	159044702	chromosome	1.2.4.1	pdhB2	21
Dshi_2160	159044703	chromosome	2.3.1.12	pdhC1	20
Dshi_2161	159044704	chromosome	2.3.1.30	cysE	17
Dshi_2180	159044723	chromosome	2.3.1.179	fabF	15
Dshi_2182	159044725	chromosome	1.1.1.100		10
Dshi_2183	159044726	chromosome	2.3.1.39	fabD	17
Dshi_2203	159044746	chromosome	2.7.7.18	nadD	11
Dshi_2206	159044749	chromosome	6.1.1.6	lysK	21
Dshi_2208	159044751	chromosome	3.4.16.4		11
Dshi_2226	159044769	chromosome	6.3.1.2		11
Dshi_2233	159044776	chromosome	2.3.1.-	phbC	13
Dshi_2234	159044777	chromosome	3.1.1.75		11
Dshi_2235	159044778	chromosome	2.1.1.14		11
Dshi_2242	159044785	chromosome	1.1.1.23	hisD3	21
Dshi_2250	159044793	chromosome	2.5.1.9	ribH	11
Dshi_2251	159044794	chromosome	4.1.99.12	ribB	7
Dshi_2251	159044794	chromosome	3.5.4.25	ribB	11
Dshi_2252	159044795	chromosome	2.5.1.9	ribC	16
Dshi_2256	159044799	chromosome	3.5.4.26	ribD	7
Dshi_2256	159044799	chromosome	1.1.1.193	ribD	17
Dshi_2262	159044805	chromosome	2.7.7.-	dnaG	13
Dshi_2264	159044807	chromosome	1.5.3.1		15
Dshi_2265	159044808	chromosome	1.5.3.1		9
Dshi_2266	159044809	chromosome	1.5.3.1		15
Dshi_2273	159044816	chromosome	1.1.1.3		17
Dshi_2274	159044817	chromosome	3.1.3.11	glpX	17
Dshi_2275	159044818	chromosome	3.1.-.-	recJ	13
Dshi_2278	159044821	chromosome	1.7.2.3	dmsA1	15
Dshi_2283	159044826	chromosome	1.14.13.92	pamO	14
Dshi_2309	159044852	chromosome	3.5.3.1		20
Dshi_2310	159044853	chromosome	4.3.1.12		21
Dshi_2311	159044854	chromosome	1.5.1.12	putA	17
Dshi_2314	159044857	chromosome	2.5.1.47		11
Dshi_2317	159044860	chromosome	2.1.1.79	cfa	17
Dshi_2320	159044863	chromosome	2.1.2.10	dmdA	18
Dshi_2332	159044875	chromosome	1.3.3.4		3
Dshi_2334	159044877	chromosome	4.2.1.2	fumC	21
Dshi_2346	159044889	chromosome	2.4.2.29	tgt	21
Dshi_2350	159044893	chromosome	2.3.1.157		2
Dshi_2365	159044908	chromosome	3.5.1.5	ureC	21
Dshi_2368	159044911	chromosome	3.5.1.5	ureB	17
Dshi_2369	159044912	chromosome	3.5.1.5	ureA	17
Dshi_2371	159044914	chromosome	3.5.2.3	pyrC2	21
Dshi_2372	159044915	chromosome	2.4.2.10	pyrE	21
Dshi_2373	159044916	chromosome	3.6.4.12	dnaB	15
Dshi_2378	159044921	chromosome	5.1.1.1	alr	21
Dshi_2381	159044924	chromosome	2.3.1.181	lipB	15
Dshi_2383	159044926	chromosome	1.9.3.1	ctaD	21

Locus tag	GI	Plasmid	EC	Gene name	Score
Dshi_2387	159044930	chromosome	6.3.5.5	carA	21
Dshi_2396	159044939	chromosome	1.1.1.86	ilvC	21
Dshi_2397	159044940	chromosome	5.4.2.10	glmM	21
Dshi_2398	159044941	chromosome	2.5.1.15	folP	17
Dshi_2399	159044942	chromosome	4.1.2.25		9
Dshi_2401	159044944	chromosome	2.7.9.1		21
Dshi_2402	159044945	chromosome	6.1.1.14	glyS	21
Dshi_2404	159044947	chromosome	6.1.1.14	glyQ	21
Dshi_2407	159044950	chromosome	2.5.1.18		10
Dshi_2411	159044952	chromosome	3.5.4.16		8
Dshi_2415	159044956	chromosome	3.5.1.108	lpxC	
Dshi_2415	159044956	chromosome	3.5.1.-	lpxC	13
Dshi_2419	159044960	chromosome	6.3.2.4	ddl	21
Dshi_2420	159044961	chromosome	1.1.1.158	murB	21
Dshi_2422	159044963	chromosome	6.3.2.8	murC	21
Dshi_2423	159044964	chromosome	2.4.1.227	murG	21
Dshi_2436	159044977	chromosome	4.1.2.19		4
Dshi_2437	159044978	chromosome	2.7.1.5	rhaA	8
Dshi_2437	159044978	chromosome	5.3.1.14	rhaA	21
Dshi_2442	159044983	chromosome	1.2.1.4	aldH1	17
Dshi_2444	159044985	chromosome	1.1.1.262	pdxA_2	20
Dshi_2446	159044987	chromosome	4.2.1.52		11
Dshi_2451	159044992	chromosome	6.3.2.9	murD	21
Dshi_2469	159045010	chromosome	2.7.8.13	mraY	21
Dshi_2470	159045011	chromosome	6.3.2.10	murF	19
Dshi_2471	159045012	chromosome	6.3.2.13	murE	20
Dshi_2472	159045013	chromosome	2.4.1.129	ftsI2	17
Dshi_2474	159045015	chromosome	2.1.1.-	mraW	13
Dshi_2483	159045024	chromosome	3.6.4.12	uvrD	11
Dshi_2484	159045025	chromosome	1.1.2.3	lldD1	19
Dshi_2485	159045026	chromosome	6.4.1.1		21
Dshi_2489	159045030	chromosome	2.6.1.45		21
Dshi_2490	159045031	chromosome	4.1.3.34	citE1	17
Dshi_2491	159045032	chromosome	6.2.1.5	sucC2	13
Dshi_2492	159045033	chromosome	6.2.1.5	sucD2	12
Dshi_2512	159045052	chromosome	1.-.-.-	dusA	13
Dshi_2537	159045077	chromosome	4.1.1.55		11
Dshi_2566	159045106	chromosome	1.2.4.4		11
Dshi_2575	159045115	chromosome	3.6.1.31	hisE	15
Dshi_2576	159045116	chromosome	4.1.3.-	hisF	13
Dshi_2578	159045118	chromosome	5.3.1.16	hisA	19
Dshi_2612	159045152	chromosome	3.5.1.-	npdA	13
Dshi_2630	159045170	chromosome	5.1.99.1		16
Dshi_2633	159045173	chromosome	6.1.1.12	aspS	21
Dshi_2637	159045177	chromosome	1.14.13.81		10
Dshi_2639	159045179	chromosome	6.3.5.5	carB	21
Dshi_2641	159045181	chromosome	2.7.1.21	tdk	19
Dshi_2645	159045185	chromosome	1.5.1.2	proC	17
Dshi_2654	159045194	chromosome	1.8.1.9	trxB	20
Dshi_2655	159045195	chromosome	1.11.1.5	ccpA	20
Dshi_2656	159045196	chromosome	2.7.1.25		6
Dshi_2656	159045196	chromosome	2.7.7.4		15
Dshi_2658	159045198	chromosome	1.2.99.2		10
Dshi_2659	159045199	chromosome	1.2.99.2	coxL1	10
Dshi_2660	159045200	chromosome	1.2.99.2		11
Dshi_2680	159045220	chromosome	1.4.4.2	gcvP	21
Dshi_2682	159045222	chromosome	2.1.2.10	gcvT2	17
Dshi_2683	159045223	chromosome	5.1.3.3	mro	18
Dshi_2684	159045224	chromosome	3.5.2.17		10
Dshi_2685	159045225	chromosome	1.2.1.12	gap3	19
Dshi_2688	159045228	chromosome	1.10.3.-	appC	13
Dshi_2689	159045229	chromosome	1.10.3.-	cydB	13
Dshi_2691	159045231	chromosome	3.1.2.6		19
Dshi_2700	159045240	chromosome	3.8.1.2	dhlB	18
Dshi_2702	159045242	chromosome	4.3.1.19		9
Dshi_2704	159045244	chromosome	2.5.1.61	hemC	20
Dshi_2705	159045245	chromosome	4.1.1.37	hemE	21

Locus tag	GI	Plasmid	EC	Gene name	Score
Dshi_2707	159045247	chromosome	6.1.1.10	metG	21
Dshi_2711	159045251	chromosome	6.6.1.2	cobS2	21
Dshi_2714	159045254	chromosome	4.1.1.65	psd	19
Dshi_2719	159045259	chromosome	6.6.1.2	cobT1	21
Dshi_2728	159045268	chromosome	6.3.4.13	purD	20
Dshi_2737	159045277	chromosome	1.8.1.7	gor	20
Dshi_2738	159045278	chromosome	5.3.1.6	rpiA	21
Dshi_2739	159045279	chromosome	2.7.6.2		9
Dshi_2742	159045282	chromosome	6.3.4.4	purA	21
Dshi_2744	159045284	chromosome	6.3.4.2	pyrG	21
Dshi_2748	159045288	chromosome	6.1.1.17	gltX_2	21
Dshi_2749	159045289	chromosome	1.11.1.5		11
Dshi_2760	159045300	chromosome	3.1.3.18		10
Dshi_2771	159045311	chromosome	3.5.4.3	guaD	17
Dshi_2773	159045313	chromosome	3.5.99.3		11
Dshi_2774	159045314	chromosome	3.1.3.15		0
Dshi_2783	159045323	chromosome	3.5.1.28		9
Dshi_2785	159045325	chromosome	6.3.5.6	gatA	11
Dshi_2790	159045330	chromosome	5.4.99.12		10
Dshi_2797	159045337	chromosome	2.7.1.4		11
Dshi_2798	159045338	chromosome	3.1.-.-	dtd	13
Dshi_2829	159045369	chromosome	6.3.2.3	gshB	20
Dshi_2836	159045376	chromosome	6.1.1.2	trpS	20
Dshi_2837	159045377	chromosome	2.6.1.42		12
Dshi_2851	159045391	chromosome	2.3.1.184		3
Dshi_2854	159045394	chromosome	2.3.1.15		11
Dshi_2855	159045395	chromosome	5.4.99.2	mutB	10
Dshi_2858	159045398	chromosome	2.4.2.1	deoD	21
Dshi_2861	159045401	chromosome	1.3.99.1	sdhB	21
Dshi_2865	159045405	chromosome	1.3.99.1	sdhA	21
Dshi_2865	159045405	chromosome	1.3.5.1	sdhA	4
Dshi_2876	159045416	chromosome	1.1.1.37	mdh	21
Dshi_2878	159045418	chromosome	6.2.1.5	sucC	21
Dshi_2882	159045422	chromosome	6.2.1.5	sucD1	20
Dshi_2883	159045423	chromosome	1.2.4.2	sucA	21
Dshi_2884	159045424	chromosome	2.3.1.61	sucB	21
Dshi_2886	159045426	chromosome	1.8.1.4	lpd	21
Dshi_2887	159045427	chromosome	1.2.1.16	gabD	17
Dshi_2891	159045431	chromosome	1.1.1.100	fabG_2	10
Dshi_2896	159045436	chromosome	1.1.3.15		11
Dshi_2924	159045464	chromosome	3.6.1.1	ppaC	19
Dshi_2927	159045467	chromosome	2.7.7.2	ribF	10
Dshi_2927	159045467	chromosome	2.7.1.26	ribF	11
Dshi_2931	159045471	chromosome	2.7.6.1	prs	21
Dshi_2933	159045473	chromosome	3.6.3.14	atpC1	14
Dshi_2934	159045474	chromosome	3.6.3.14	atpD2	21
Dshi_2935	159045475	chromosome	3.6.3.14	atpG2	16
Dshi_2936	159045476	chromosome	3.6.3.14	atpA1	21
Dshi_2937	159045477	chromosome	3.6.3.14	atpH	15
Dshi_2945	159045485	chromosome	1.3.1.12	tyrC	17
Dshi_2946	159045486	chromosome	2.6.1.9	hisC	21
Dshi_2947	159045487	chromosome	2.5.1.44	hss	21
Dshi_2949	159045489	chromosome	1.17.4.1		11
Dshi_2951	159045491	chromosome	2.5.1.47		11
Dshi_2952	159045492	chromosome	6.3.2.1	panC	21
Dshi_2953	159045493	chromosome	2.4.2.17	hisG	12
Dshi_2955	159045495	chromosome	6.1.1.21	hisS	21
Dshi_2958	159045498	chromosome	1.17.1.4	xghB	17
Dshi_2959	159045499	chromosome	1.17.1.4	xdhA	17
Dshi_2960	159045500	chromosome	1.17.1.4	xdhC	9
Dshi_2966	159045506	chromosome	2.1.2.11	panB	20
Dshi_2970	159045510	chromosome	1.1.1.26	gyaR	19
Dshi_2975	159045515	chromosome	3.6.1.23	dut	17
Dshi_2976	159045516	chromosome	4.1.1.36	coaBC	17
Dshi_2976	159045516	chromosome	6.3.2.5	coaBC	13
Dshi_2979	159045519	chromosome	2.7.7.62	cobU	9
Dshi_2980	159045520	chromosome	3.1.3.73		2

Locus tag	GI	Plasmid	EC	Gene name	Score
Dshi_2992	159045532	chromosome	3.8.1.3	dehH	19
Dshi_2999	159045539	chromosome	6.2.1.3	fadD1	10
Dshi_3000	159045540	chromosome	4.1.1.9	mcd	18
Dshi_3006	159045546	chromosome	5.1.3.1	rpe	19
Dshi_3014	159045554	chromosome	1.14.11.18		11
Dshi_3016	159045556	chromosome	4.1.2.4	deoC	20
Dshi_3017	159045557	chromosome	1.2.1.3	ald	20
Dshi_3020	159045560	chromosome	3.5.1.18	dapE2	18
Dshi_3021	159045561	chromosome	1.2.1.3	puuC	11
Dshi_3027	159045567	chromosome	3.6.3.14	atpF2	14
Dshi_3028	159045568	chromosome	3.6.3.14	atpX	14
Dshi_3029	159045569	chromosome	3.6.3.14	atpE2	14
Dshi_3030	159045570	chromosome	3.6.3.14	atpB1	15
Dshi_3033	159045573	chromosome	2.1.1.-	rsmB1	13
Dshi_3040	159045580	chromosome	1.3.1.26	dapB	21
Dshi_3042	159045582	chromosome	5.4.99.12	truB	13
Dshi_3046	159045586	chromosome	1.1.1.81	ttuD	19
Dshi_3047	159045587	chromosome	1.1.1.60	glxR	10
Dshi_3050	159045590	chromosome	4.1.3.6	citE2	10
Dshi_3054	159045594	chromosome	2.3.1.51		9
Dshi_3059	159045599	chromosome	4.1.1.20	lysA	17
Dshi_3062	159045602	chromosome	4.3.2.1	argH	21
Dshi_3066	159045606	chromosome	2.3.1.9	atoB	21
Dshi_3067	159045607	chromosome	1.1.1.36	fabG1	20
Dshi_3072	159045612	chromosome	2.5.1.1	ispB	4
Dshi_3073	159045613	chromosome	2.7.1.148	ispE	21
Dshi_3091	159045631	chromosome	2.1.3.2	pyrB	21
Dshi_3094	159045634	chromosome	3.5.2.3	pyrC1	19
Dshi_3097	159045637	chromosome	6.3.2.2	gsh	21
Dshi_3100	159045640	chromosome	2.5.1.39	ubiA	4
Dshi_3100	159045640	chromosome	2.5.1.-	ubiA	13
Dshi_3105	159045645	chromosome	2.7.8.5	pgsA	18
Dshi_3106	159045646	chromosome	5.4.99.12	rluA	13
Dshi_3119	159045659	chromosome	2.3.3.1	gltA1	18
Dshi_3120	159045660	chromosome	2.8.3.16	yfdW2	10
Dshi_3128	159045668	chromosome	3.6.3.20	ugpC5	12
Dshi_3129	159045669	chromosome	3.6.3.20	ugpC1	10
Dshi_3141	159045681	chromosome	3.6.3.20	ugpC3	10
Dshi_3145	159045685	chromosome	4.1.2.20	garL	11
Dshi_3146	159045686	chromosome	6.4.1.2	accA	21
Dshi_3149	159045689	chromosome	3.4.13.22	ddpX	11
Dshi_3150	159045690	chromosome	2.6.1.21	dat	17
Dshi_3165	159045705	chromosome	1.7.99.4	napA	15
Dshi_3171	159045711	chromosome	4.99.1.3	cbiX1	10
Dshi_3172	159045712	chromosome	1.7.2.1	nirN	11
Dshi_3177	159045717	chromosome	1.7.2.1	nirF	10
Dshi_3179	159045719	chromosome	2.1.1.107	nirE	19
Dshi_3190	159045730	chromosome	2.3.1.37	hemA3	21
Dshi_3203	159045743	chromosome	3.5.3.19	allA	17
Dshi_3205	159045745	chromosome	3.5.2.17		9
Dshi_3212	159045752	chromosome	1.7.1.1	NULL	4
Dshi_3228	159045768	chromosome	5.1.1.7	dapF	19
Dshi_3236	159045776	chromosome	4.2.1.1	cynT	17
Dshi_3240	159045780	chromosome	1.2.1.11	asd	17
Dshi_3246	159045786	chromosome	3.6.3.14	fliI	13
Dshi_3268	159045808	chromosome	1.12.98.1		12
Dshi_3275	159045815	chromosome	4.2.3.5	aroC	21
Dshi_3276	159045816	chromosome	1.10.2.2	petC	17
Dshi_3277	159045817	chromosome	1.10.2.2	petB	17
Dshi_3278	159045818	chromosome	1.10.2.2	petA	18
Dshi_3279	159045819	chromosome	2.5.1.18		9
Dshi_3282	159045822	chromosome	1.2.1.2	fdhD	10
Dshi_3289	159045829	chromosome	3.2.2.4	amn	17
Dshi_3294	159045834	chromosome	2.2.1.7	dxs1	21
Dshi_3295	159045835	chromosome	2.5.1.10	ispA	16
Dshi_3301	159045841	chromosome	2.6.1.42	ilvE	19
Dshi_3308	159045848	chromosome	2.5.1.18	gst1	17

Locus tag	GI	Plasmid	EC	Gene name	Score
Dshi_3313	159045853	chromosome	4.4.1.3	dddL	2
Dshi_3316	159045856	chromosome	3.1.3.3	serB	17
Dshi_3317	159045857	chromosome	2.6.1.52	serC	21
Dshi_3318	159045858	chromosome	1.1.1.95	serA1	17
Dshi_3324	159045864	chromosome	1.1.2.4	dld2	10
Dshi_3325	159045865	chromosome	2.6.1.45	sgaA1	20
Dshi_3329	159045869	chromosome	4.2.1.17		16
Dshi_3330	159045870	chromosome	2.8.3.16	yfdW1	10
Dshi_3331	159045871	chromosome	2.3.1.9	bktB	17
Dshi_3344	159045884	chromosome	2.7.1.39		3
Dshi_3345	159045885	chromosome	2.4.2.11	pncB	21
Dshi_3347	159045887	chromosome	3.5.1.19	pncA	16
Dshi_3350	159045890	chromosome	2.7.9.3	selD	18
Dshi_3368	159045908	chromosome	2.1.1.163	ubiE	15
Dshi_3370	159045910	chromosome	4.2.1.17		19
Dshi_3386	159045926	chromosome	2.7.8.6	wcaJ	10
Dshi_3393	159045933	chromosome	1.1.1.85	leuB	19
Dshi_3400	159045940	chromosome	2.1.1.64	ubiG2	17
Dshi_3414	159045954	chromosome	1.1.1.94	gpsA	19
Dshi_3416	159045956	chromosome	4.2.1.75	hemD	16
Dshi_3420	159045960	chromosome	2.7.1.30	glpK	21
Dshi_3426	159045966	chromosome	3.3.1.1	ahcY	21
Dshi_3427	159045967	chromosome	2.4.1.44	rafI	10
Dshi_3444	159045984	chromosome	3.2.1.-	mltA	13
Dshi_3449	159045989	chromosome	2.7.1.24	coaE	18
Dshi_3450	159045990	chromosome	1.1.1.25	aroE	21
Dshi_3460	159046000	chromosome	1.3.99.22	hemN3	17
Dshi_3462	159046002	chromosome	3.6.1.15	ham1	13
Dshi_3463	159046003	chromosome	2.7.7.56	rph	21
Dshi_3467	159046007	chromosome	1.1.1.40	maeB	21
Dshi_3468	159046008	chromosome	1.8.4.11	msrA1	17
Dshi_3472	159046012	chromosome	6.3.4.5	argG	21
Dshi_3473	159046013	chromosome	4.3.1.19	ilvA	20
Dshi_3474	159046014	chromosome	5.5.1.2	pcaB	18
Dshi_3476	159046016	chromosome	1.13.11.3	pcaG	18
Dshi_3477	159046017	chromosome	1.13.11.3	pcaH	19
Dshi_3478	159046018	chromosome	4.1.1.44	pcaC	16
Dshi_3479	159046019	chromosome	1.14.13.2	pobA	21
Dshi_3483	159046023	chromosome	3.6.3.29	modC	20
Dshi_3492	159046032	chromosome	2.1.1.-	rumA	13
Dshi_3498	159046038	chromosome	4.99.1.1	hemH	21
Dshi_3502	159046042	chromosome	6.6.1.1	bchI	21
Dshi_3503	159046043	chromosome	6.6.1.1	bchD	19
Dshi_3504	159046044	chromosome	6.6.1.1	bchO	12
Dshi_3508	159046048	chromosome	1.14.99.-	crtI	13
Dshi_3509	159046049	chromosome	2.5.1.32	crtB	20
Dshi_3512	159046052	chromosome	4.2.1.131	crtC	
Dshi_3513	159046053	chromosome	1.14.99.-	crtD	13
Dshi_3514	159046054	chromosome	2.5.1.29	crtE	20
Dshi_3515	159046055	chromosome	2.1.1.-	crtF	13
Dshi_3516	159046056	chromosome	1.-.-.-	bchC	13
Dshi_3517	159046057	chromosome	1.3.1.33	bchX	6
Dshi_3518	159046058	chromosome	1.3.1.33	bchY	10
Dshi_3519	159046059	chromosome	1.3.1.33	bchZ	10
Dshi_3526	159046066	chromosome	2.2.1.7	dxs2	21
Dshi_3527	159046067	chromosome	5.3.3.2	idi	19
Dshi_3528	159046068	chromosome	1.3.1.83	bchP	15
Dshi_3530	159046070	chromosome	2.5.1.62	bchG	18
Dshi_3533	159046073	chromosome	4.2.1.-	bchF	13
Dshi_3534	159046074	chromosome	1.3.7.7	bchN	
Dshi_3535	159046075	chromosome	1.3.7.7	bchB	
Dshi_3536	159046076	chromosome	6.6.1.1	bchH	15
Dshi_3537	159046077	chromosome	1.3.7.7	bchL	
Dshi_3538	159046078	chromosome	2.1.1.11	bchM	19
Dshi_3544	159046084	chromosome	1.14.13.81	acsF	20
Dshi_3546	159046086	chromosome	2.3.1.37	hemA1	21
Dshi_3550	159046090	chromosome	2.1.1.64	ubiG1	21

Locus tag	GI	Plasmid	EC	Gene name	Score
Dshi_3553	159046093	chromosome	6.2.1.1	acs	21
Dshi_3554	159046094	chromosome	2.7.4.3	adk1	19
Dshi_3564	159046104	chromosome	3.6.1.-	mutT	13
Dshi_3565	159046105	chromosome	2.3.1.35	argJ	21
Dshi_3565	159046105	chromosome	2.3.1.1	argJ	17
Dshi_3574	159046114	chromosome	3.1.3.7	cysQ	10
Dshi_3575	159046115	chromosome	2.7.7.38	kdsB	18
Dshi_3577	159046117	chromosome	2.7.7.9	galU	20
Dshi_3588	159046128	chromosome	5.3.1.13	yrbH	17
Dshi_3590	159046130	chromosome	1.6.5.3		17
Dshi_3593	159046133	chromosome	3.6.1.27	uppP	19
Dshi_3603	159046145	plasmid1	3.6.3.4		15
Dshi_3609	159046151	plasmid1	3.6.3.3		14
Dshi_3632	159046174	plasmid1	4.4.1.-	DddD	
Dshi_3681	159046223	plasmid1	4.1.99.17	ThiC	
Dshi_3719	159046259	plasmid1	1.2.99.2		11
Dshi_3720	159046260	plasmid1	1.2.99.2		12
Dshi_3721	159046261	plasmid1	1.2.99.2		11
Dshi_3789	159046328	plasmid1	3.6.3.4		15
Dshi_3801	159046341	plasmid2	1.11.1.6		11
Dshi_3811	159046351	plasmid2	3.7.1.2		14
Dshi_3812	159046352	plasmid2	1.13.11.5		15
Dshi_3817	159046357	plasmid2	2.3.1.16		11
Dshi_3824	159046364	plasmid2	6.2.1.30		11
Dshi_3826	159046366	plasmid2	1.1.1.35		11
Dshi_3830	159046370	plasmid2	1.1.1.94		13
Dshi_3832	159046372	plasmid2	2.4.1.213		15
Dshi_3840	159046380	plasmid2	2.2.1.6		11
Dshi_3841	159046381	plasmid2	1.4.1.4		14
Dshi_3861	159046399	plasmid2	1.1.1.22		15
Dshi_3868	159046406	plasmid2	5.1.3.2		14
Dshi_3877	159046415	plasmid2	4.1.99.17	ThiC	
Dshi_3891	159046429	plasmid2	1.9.3.1		14
Dshi_3892	159046430	plasmid2	1.9.3.1		12
Dshi_3898	159046436	plasmid2	3.2.1.20		13
Dshi_3941	159046480	plasmid3	3.6.3.4		15
Dshi_4065	159046603	plasmid3	3.6.3.4		15
Dshi_4080	159046614	plasmid4	4.1.99.17	ThiC	
Dshi_4114	159046643	plasmid4	5.1.3.13		12
Dshi_4115	159046644	plasmid4	4.2.1.46		11
Dshi_4117	159046646	plasmid4	1.1.1.133		13
Dshi_4118	159046647	plasmid4	2.7.7.24		14
Dshi_4139	159046662	plasmid4	4.2.1.47		15
Dshi_4142	159046665	plasmid4	1.1.1.271		14
Dshi_4146	159046669	plasmid4	5.3.1.8		14
Dshi_4160	159046683	plasmid5	1.3.1.33		14
Dshi_4194	159046717	plasmid5	2.3.2.2		11
Dshi_4200	159046723	plasmid5	1.2.99.2		12
Dshi_4201	159046724	plasmid5	1.2.99.2		11
Dshi_4202	159046725	plasmid5	1.2.99.2		11
Dshi_4206	159046729	plasmid5	2.6.1.42		12
Dshi_4221	159046744	plasmid5	1.1.1.60		10
Dshi_5004	284928597	chromosome	1.1.1.28		14
Dshi_5008	284928600	chromosome	4.3.1.17		10

6.3 List of non-blocked reactions in the model *i*Dsh827

Reaction name and equation
(R)-3-hydroxybutanoate_Na+_symport 1 (R)-3-hydroxybutanoate$_{ex}$ + 1 Na+$_{ex}$ → 1 Na+ + 1 (R)-3-hydroxybutanoate

Reaction name and equation
(R)-lactate_Na+_symport
1 (R)-lactate$_{ex}$ + 1 Na+$_{ex}$ → 1 Na+ + 1 (R)-lactate
(S)-lactate_Na+_symport
1 (S)-lactate$_{ex}$ + 1 Na+$_{ex}$ → 1 Na+ + 1 (S)-lactate
-boundary-(R)-3-hydroxybutanoate_flux
↔ 1 (R)-3-hydroxybutanoate$_{ex}$
-boundary-(R)-lactate_flux
↔ 1 (R)-lactate$_{ex}$
-boundary-(R)-lactate_trans
1 (R)-lactate$_{ex}$ ← 1 (R)-lactate
-boundary-(S)-lactate_flux
↔ 1 (S)-lactate$_{ex}$
-boundary-(S)-lactate_trans
1 (S)-lactate$_{ex}$ ← 1 (S)-lactate
-boundary-2-oxoglutarate_flux
↔ 1 2-oxoglutarate$_{ex}$
-boundary-4-aminobenzoate_flux
↔ 1 4-aminobenzoate$_{ex}$
-boundary-4-aminobenzoate_trans
1 4-aminobenzoate$_{ex}$ → 1 4-aminobenzoate
-boundary-4-methylphenol_flux
1 4-methylphenol →
-boundary-5-deoxy-D-ribose_flux
1 5-deoxy-D-ribose →
-boundary-Biomass_flux
53.95 ATP + 53.95 H2O + 1 Biomass_Dshibae → 53.95 ADP + 53.95 phosphate + 53.95 H+
-boundary-CO2_flux
↔ 1 CO2$_{ex}$
-boundary-CO2_trans
1 CO2$_{ex}$ ↔ 1 CO2
-boundary-Co2+_flux
↔ 1 Co2+$_{ex}$
-boundary-Co2+_trans
1 Co2+$_{ex}$ → 1 Co2+
-boundary-D-ribitol_flux
↔ 1 D-ribitol$_{ex}$
-boundary-D-xylitol_flux
↔ 1 D-xylitol$_{ex}$
-boundary-Fe2+_flux
↔ 1 Fe2+$_{ex}$
-boundary-Fe2+_trans
1 Fe2+$_{ex}$ → 1 Fe2+
-boundary-H2O_flux
↔ 1 H2O$_{ex}$
-boundary-H2O_trans
1 H2O$_{ex}$ ↔ 1 H2O
-boundary-L-alanine_flux
↔ 1 L-alanine$_{ex}$
-boundary-L-aspartate_flux
↔ 1 L-aspartate$_{ex}$
-boundary-L-glutamate_flux
↔ 1 L-glutamate$_{ex}$
-boundary-L-glutamine_flux
↔ 1 L-glutamine$_{ex}$
-boundary-L-glutamine_trans
1 L-glutamine$_{ex}$ ← 1 L-glutamine
-boundary-Mg2+_flux
↔ 1 Mg2+$_{ex}$
-boundary-Mg2+_trans
1 Mg2+$_{ex}$ → 1 Mg2+
-boundary-N2_flux
↔ 1 N2$_{ex}$
-boundary-N2_trans
1 N2$_{ex}$ ← 1 N2
-boundary-PHB_flux
↔ 1 PHB$_{ex}$
-boundary-PHB_trans

Reaction name and equation
1 PHB_{ex} ← 1 PHB
-boundary-UNKNOWN_flux
1 UNKNOWN →
-boundary-acetate_flux
↔ 1 $acetate_{ex}$
-boundary-acetate_trans
1 $acetate_{ex}$ ← 1 acetate
-boundary-adenine_flux
↔ 1 $adenine_{ex}$
-boundary-alpha-D-glucose_flux
↔ 1 $alpha\text{-}D\text{-}glucose_{ex}$
-boundary-alpha-D-xylopyranose_flux
↔ 1 $alpha\text{-}D\text{-}xylopyranose_{ex}$
-boundary-alpha-L-rhamnose_flux
↔ 1 $alpha\text{-}L\text{-}rhamnose_{ex}$
-boundary-alpha-maltose_flux
↔ 1 $alpha\text{-}maltose_{ex}$
-boundary-ammonia_flux
↔ 1 $ammonia_{ex}$
-boundary-beta-D-fructofuranose_flux
↔ 1 $beta\text{-}D\text{-}fructofuranose_{ex}$
-boundary-beta-D-glucose_flux
↔ 1 $beta\text{-}D\text{-}glucose_{ex}$
-boundary-beta-D-ribofuranose_flux
↔ 1 $beta\text{-}D\text{-}ribofuranose_{ex}$
-boundary-biotin_flux
↔ 1 $biotin_{ex}$
-boundary-biotin_trans
1 $biotin_{ex}$ → 1 biotin
-boundary-citrate_flux
↔ 1 $citrate_{ex}$
-boundary-cytosine_flux
↔ 1 $cytosine_{ex}$
-boundary-dimethyl_sulfide_flux
↔ 1 $dimethyl\_sulfide_{ex}$
-boundary-dimethyl_sulfide_trans
1 $dimethyl\_sulfide_{ex}$ ← 1 dimethyl_sulfide
-boundary-dimethyl_sulfoxide_flux
↔ 1 $dimethyl\_sulfoxide_{ex}$
-boundary-dimethyl_sulfoxide_trans
1 $dimethyl\_sulfoxide_{ex}$ ↔ 1 dimethyl_sulfoxide
-boundary-dimethylsulfoniopropionate_flux
↔ 1 $dimethylsulfoniopropionate_{ex}$
-boundary-ethanol_flux
↔ 1 $ethanol_{ex}$
-boundary-fumarate_flux
↔ 1 $fumarate_{ex}$
-boundary-glycerol_flux
↔ 1 $glycerol_{ex}$
-boundary-glycolaldehyde_flux
1 glycolaldehyde →
-boundary-glycolate_flux
↔ 1 $glycolate_{ex}$
-boundary-glyoxylate_flux
↔ 1 $glyoxylate_{ex}$
-boundary-guanosine_flux
↔ 1 $guanosine_{ex}$
-boundary-inosine_flux
↔ 1 $inosine_{ex}$
-boundary-methanethiol_flux
↔ 1 $methanethiol_{ex}$
-boundary-methanethiol_trans
1 $methanethiol_{ex}$ ← 1 methanethiol
-boundary-myo-inositol_flux
↔ 1 $myo\text{-}inositol_{ex}$
-boundary-nicotinate_flux
↔ 1 $nicotinate_{ex}$

Reaction name and equation
-boundary-nicotinate_trans
1 nicotinate$_{ex}$ → 1 nicotinate
-boundary-nitrate_flux
↔ 1 nitrate$_{ex}$
-boundary-oxygen_alpha-ribazole_flux
→ 1 oxygen_alpha-ribazole
-boundary-oxygen_flux
↔ 1 oxygen$_{ex}$
-boundary-oxygen_trans
1 oxygen$_{ex}$ ↔ 1 oxygen
-boundary-phosphate_flux
↔ 1 phosphate$_{ex}$
-boundary-photons_flux
→ 1 photons
-boundary-propionate_flux
↔ 1 propionate$_{ex}$
-boundary-proton_flux
↔ 1 H+
-boundary-pyruvate_flux
↔ 1 pyruvate$_{ex}$
-boundary-succinate_flux
↔ 1 succinate$_{ex}$
-boundary-sulfate_flux
↔ 1 sulfate$_{ex}$
-boundary-sulfate_trans
1 sulfate$_{ex}$ → 1 sulfate
-boundary-uracil_flux
↔ 1 uracil$_{ex}$
-boundary-urate_flux
1 urate →
-boundary-urea_flux
↔ 1 urea$_{ex}$
-boundary-urea_trans
1 urea$_{ex}$ ← 1 urea
-boundary-xanthine_flux
↔ 1 xanthine$_{ex}$
-multiple_pathways-1.1.1.35-RXN-11662
1 NAD+ + 1 (S)-3-hydroxybutanoyl-CoA ↔ 1 acetoacetyl-CoA + 1 NADH + 1 H+
-multiple_pathways-1.1.1.36-RXN-5901
1 (R)-3-hydroxybutanoyl-CoA + 1 NADP+ ← 1 acetoacetyl-CoA + 1 NADPH + 1 H+
-multiple_pathways-1.1.1.37-MALATE-DEH-RXN
1 (S)-malate + 1 NAD+ ↔ 1 NADH + 1 oxaloacetate + 1 H+
-multiple_pathways-1.1.1.40-MALIC-NADP-RXN
1 (S)-malate + 1 NADP+ → 1 CO2 + 1 NADPH + 1 pyruvate
-multiple_pathways-1.1.1.94-GLYC3PDEHYDROGBIOSYN-RXN_NAD
1 sn-glycerol-3-phosphate + 1 NAD+ ← 1 dihydroxyacetone_phosphate + 1 H+ + 1 NADH
-multiple_pathways-1.1.1.94-GLYC3PDEHYDROGBIOSYN-RXN_NADP
1 sn-glycerol-3-phosphate + 1 NADP+ ← 1 dihydroxyacetone_phosphate + 1 H+ + 1 NADPH
-multiple_pathways-1.14.99.40-RXN-8771
1 FMNH2 + 1 NADH + 1 oxygen_alpha-ribazole + 1 H+ → 1 5,6-dimethylbenzimidazole + 1 D-erythrose-4-phosphate + 1 NAD+ + 1 UNKNOWN
-multiple_pathways-1.2.1.3-RXN66-3
1 acetaldehyde + 1 NAD+ + 1 H2O → 1 acetate + 1 NADH + 2 H+
-multiple_pathways-1.3.3.3-RXN0-1461
1 coproporphyrinogen_III + 1 oxygen + 2 H+ → 2 CO2 + 1 protoporphyrinogen_IX + 2 H2O
-multiple_pathways-1.5.1.20-1.5.1.20-RXN
1 5-methyl-tetrahydrofolate + 1 NAD+ ↔ 1 5,10-methylenetetrahydrofolate + 1 NADH + 1 H+
-multiple_pathways-1.6.5.3-NADH-DEHYDROG-A-RXN
1 NADH + 5 H+ + 1 |Ubiquinones| ↔ 1 NAD+ + 1 |Ubiquinols| + 4 H+$_{ex}$
-multiple_pathways-1.7.1.4-RXN0-6377_NAD
1 nitrite + 5 H+ + 3 NADH → 1 ammonium + 2 H2O + 3 NAD+
-multiple_pathways-1.7.1.4-RXN0-6377_NADP
1 nitrite + 5 H+ + 3 NADPH → 1 ammonium + 2 H2O + 3 NADP+
-multiple_pathways-1.7.2.1-NITRITE-REDUCTASE-CYTOCHROME-RXN
1 nitric_oxide + 1 H2O + 1 |Cytochromes-C-Oxidized| ↔ 1 nitrite + 2 H+ + 1 |Cytochromes-C-Reduced|
-multiple_pathways-2.1.2.1-GLYOHMETRANS-RXN

Reaction name and equation
1 L-serine + 1 tetrahydrofolate ↔ 1 glycine + 1 5,10-methylenetetrahydrofolate + 1 H2O
-multiple_pathways-2.2.1.1-1TRANSKETO-RXN
1 D-sedoheptulose-7-phosphate + 1 D-glyceraldehyde-3-phosphate ↔ 1 D-ribose-5-phosphate + 1 D-xylulose-5-phosphate
-multiple_pathways-2.2.1.7-DXS-RXN
1 D-glyceraldehyde-3-phosphate + 1 H+ + 1 pyruvate → 1 CO2 + 1 1-deoxy-D-xylulose_5-phosphate
-multiple_pathways-2.3.1.–LAUROYLACYLTRAN-RXN
1 alpha-Kdo-(2→4)-alpha-Kdo-(2→6)-lipid_IVA + 1 |Dodecanoyl-ACPs| ↔ 1 ACP + 1 (KDO)2-(lauroyl)-lipid_IVA
-multiple_pathways-2.3.1.–MYRISTOYLACYLTRAN-RXN
1 (KDO)2-(lauroyl)-lipid_IVA + 1 |Myristoyl-ACPs| ↔ 1 ACP + 1 Kdo2-lipid_A
-multiple_pathways-2.3.1.8-PHOSACETYLTRANS-RXN
1 acetyl-CoA + 1 phosphate ↔ 1 acetylphosphate + 1 coenzyme_A
-multiple_pathways-2.3.1.9-ACETYL-COA-ACETYLTRANSFER-RXN
2 acetyl-CoA ↔ 1 acetoacetyl-CoA + 1 coenzyme_A
-multiple_pathways-2.6.1.1-ASPAMINOTRANS-RXN
1 2-oxoglutarate + 1 L-aspartate ↔ 1 L-glutamate + 1 oxaloacetate
-multiple_pathways-2.6.1.16-L-GLN-FRUCT-6-P-AMINOTRANS-RXN
1 D-fructose-6-phosphate + 1 L-glutamine → 1 alpha-D-glucosamine-6-phosphate + 1 L-glutamate
-multiple_pathways-2.6.1.42-BRANCHED-CHAINAMINOTRANSFERVAL-RXN
1 2-oxoglutarate + 1 L-valine ↔ 1 2-oxoisovalerate + 1 L-glutamate
-multiple_pathways-2.7.1.40-PEPDEPHOS-RXN
1 ATP + 1 pyruvate ↔ 1 ADP + 1 phosphoenolpyruvate + 1 H+
-multiple_pathways-2.7.2.1-ACETATEKIN-RXN
1 acetate + 1 ATP → 1 acetylphosphate + 1 ADP
-multiple_pathways-2.7.2.3-PHOSGLYPHOS-RXN
1 ATP + 1 3-phospho-D-glycerate ↔ 1 ADP + 1 1,3-bisphospho-D-glycerate
-multiple_pathways-2.7.7.23-NAG1P-URIDYLTRANS-RXN
1 N-acetyl-alpha-D-glucosamine_1-phosphate + 1 H+ + 1 UTP → 1 diphosphate + 1 UDP-alpha-N-acetyl-D-glucosamine
-multiple_pathways-2.7.7.9-GLUC1PURIDYLTRANS-RXN
1 alpha-D-glucose_1-phosphate + 1 H+ + 1 UTP ↔ 1 diphosphate + 1 UDP-alpha-D-glucose
-multiple_pathways-3.1.3.11-F16BDEPHOS-RXN
1 fructose-1,6-bisphosphate + 1 H2O → 1 D-fructose-6-phosphate + 1 phosphate
-multiple_pathways-3.1.3.73-RXN-8770
1 adenosylcobalamin_5′-phosphate + 1 H2O → 1 coenzyme_B12 + 1 phosphate
-multiple_pathways-3.5.3.1-ARGINASE-RXN
1 L-arginine + 1 H2O → 1 L-ornithine + 1 urea
-multiple_pathways-4.1.1.49-PEPCARBOXYKIN-RXN
1 ATP + 1 oxaloacetate → 1 ADP + 1 CO2 + 1 phosphoenolpyruvate
-multiple_pathways-4.1.2.13-F16ALDOLASE-RXN
1 fructose-1,6-bisphosphate ↔ 1 dihydroxyacetone_phosphate + 1 D-glyceraldehyde-3-phosphate
-multiple_pathways-4.1.2.4-DEOXYRIBOSE-P-ALD-RXN
1 2-deoxy-alpha-D-ribose_5-phosphate ↔ 1 acetaldehyde + 1 D-glyceraldehyde-3-phosphate
-multiple_pathways-4.3.1.17-4.3.1.17-RXN
1 L-serine → 1 ammonia + 1 H+ + 1 pyruvate
-multiple_pathways-4.3.2.1-ARGSUCCINLYA-RXN
1 L-arginino-succinate ↔ 1 L-arginine + 1 fumarate
-multiple_pathways-5.1.3.1-RIBULP3EPIM-RXN
1 D-ribulose-5-phosphate ↔ 1 D-xylulose-5-phosphate
-multiple_pathways-5.1.99.1-METHYLMALONYL-COA-EPIM-RXN
1 (R)-methylmalonyl-CoA ↔ 1 (S)-methylmalonyl-CoA
-multiple_pathways-5.3.1.1-TRIOSEPISOMERIZATION-RXN
1 D-glyceraldehyde-3-phosphate ↔ 1 dihydroxyacetone_phosphate
-multiple_pathways-5.3.1.6-RIB5PISOM-RXN
1 D-ribose-5-phosphate ↔ 1 D-ribulose-5-phosphate
-multiple_pathways-5.4.2.7-D-PPENTOMUT-RXN
1 2-deoxy-alpha-D-ribose_1-phosphate ↔ 1 2-deoxy-alpha-D-ribose_5-phosphate
-multiple_pathways-5.4.99.2-METHYLMALONYL-COA-MUT-RXN
1 (R)-methylmalonyl-CoA ↔ 1 succinyl-CoA
-multiple_pathways-6.2.1.17-PROPIONATE–COA-LIGASE-RXN
1 ATP + 1 coenzyme_A + 1 propionate → 1 AMP + 1 diphosphate + 1 propanoyl-CoA
-multiple_pathways-6.4.1.2-ACETYL-COA-CARBOXYLTRANSFER-RXN
1 acetyl-CoA + 1 ATP + 1 bicarbonate → 1 ADP + 1 malonyl-CoA + 1 phosphate + 1 H+

Reaction name and equation
-multiple_pathways-RXN-2881-spontaneous
1 formaldehyde + 1 tetrahydrofolate → 1 5,10-methylenetetrahydrofolate + 1 H2O
-no_pathway-1.-.-.–FCLREDUCT-RXN
1 GDP-4-dehydro-6-L-deoxygalactose + 1 NADPH + 1 H+ ↔ 1 GDP-L-fucose + 1 NADP+
-no_pathway-1.-.-.–RXN0-276
1 NAD+ + 1 S-hydroxymethylglutathione ↔ 1 S-formylglutathione + 1 NADH + 1 H+
-no_pathway-1.1.1.100-RXN-9514
1 NADPH + 1 H+ + 1 |Acetoacetyl-ACPs| → 1 NADP+ + 1 |Beta-3-hydroxybutyryl-ACPs|
-no_pathway-1.1.1.100-RXN-9518
1 NADP+ + 1 |R-3-hydroxyhexanoyl-ACPs| ← 1 NADPH + 1 H+ + 1 |3-oxo-hexanoyl-ACPs|
-no_pathway-1.1.1.100-RXN-9524
1 NADP+ + 1 |3-Hydroxy-octanoyl-ACPs| ← 1 NADPH + 1 H+ + 1 |3-Oxo-octanoyl-ACPs|
-no_pathway-1.1.1.100-RXN-9528
1 NADP+ + 1 |Beta-hydroxydecanoyl-ACPs| ← 1 NADPH + 1 H+ + 1 |3-oxo-decanoyl-ACPs|
-no_pathway-1.1.1.100-RXN-9532
1 NADP+ + 1 |R-3-hydroxydodecanoyl-ACPs| ← 1 NADPH + 1 H+ + 1 |3-oxo-dodecanoyl-ACPs|
-no_pathway-1.1.1.100-RXN-9536
1 NADP+ + 1 |R-3-hydroxymyristoyl-ACPs| ← 1 NADPH + 1 H+ + 1 |3-oxo-myristoyl-ACPs|
-no_pathway-1.1.1.100-RXN-9540
1 NADP+ + 1 |R-3-Hydroxypalmitoyl-ACPs| ← 1 NADPH + 1 H+ + 1 |3-oxo-palmitoyl-ACPs|
-no_pathway-1.1.1.100-RXN-9556
1 NADP+ + 1 |R-3-hydroxy-cis-vaccenoyl-ACPs| ← 1 NADPH + 1 H+ + 1 |3-oxo-cis-vaccenoyl-ACPs|
-no_pathway-1.1.1.157-3-HYDROXYBUTYRYL-COA-DEHYDROGENASE-RXN
1 NADP+ + 1 (S)-3-hydroxybutanoyl-CoA ← 1 acetoacetyl-CoA + 1 NADPH + 1 H+
-no_pathway-1.1.1.23-RXN-8001
1 histidinol + 2 NAD+ + 1 H2O → 1 L-histidine + 2 NADH + 3 H+
-no_pathway-1.1.1.30-3-HYDROXYBUTYRATE-DEHYDROGENASE-RXN
1 (R)-3-hydroxybutanoate + 1 NAD+ ↔ 1 acetoacetate + 1 NADH + 1 H+
-no_pathway-1.1.1.36-BHBDCLOS-RXN
1 (R)-3-hydroxybutanoyl-CoA + 1 NAD+ ↔ 1 acetoacetyl-CoA + 1 NADH + 1 H+
-no_pathway-1.1.1.79-GLYOXYLATE-REDUCTASE-NADP+-RXN
1 glycolate + 1 NADP+ ← 1 glyoxylate + 1 NADPH + 1 H+
-no_pathway-1.10.3.–RXN0-5266
1 oxygen + 4 H+ + 2 |Ubiquinols| → 4 $H+_{ex}$ + 2 H2O + 2 |Ubiquinones|
-no_pathway-1.11.1.5-CYTOCHROME-C-PEROXIDASE-RXN
2 H+ + 1 hydrogen_peroxide + 2 |Cytochromes-C-Reduced| → 2 H2O + 2 |Cytochromes-C-Oxidized|
-no_pathway-1.14.13.–RXN-12900
1 NADPH + 1 oxygen + 1 trimethylamine → 1 NADP+ + 1 trimethylamine_N-oxide + 1 H2O
-no_pathway-1.14.13.–RXN-9766
1 dimethyl_sulfide + 1 NADPH + 1 oxygen + 1 H+ → 1 dimethyl_sulfoxide + 1 NADP+ + 1 H2O
-no_pathway-1.14.13.92-1.14.13.92-RXN_NAD
1 phenylacetone + 1 oxygen + 1 H+ + 1 NADH ↔ 1 benzylacetate + 1 H2O + 1 NAD+
-no_pathway-1.14.13.92-1.14.13.92-RXN_NADP
1 phenylacetone + 1 oxygen + 1 H+ + 1 NADPH ↔ 1 benzylacetate + 1 H2O + 1 NADP+
-no_pathway-1.14.99.–RXN-7892
1 5,6-epoxy-3-hydroxy-12′-apo-beta-caroten-12′-al + 1 oxygen ↔ 1 4,9-dimethyldodeca-2,4,6,8,10-pentaene-1,12-dial + 1 5,6-epoxy-3-hydroxy-9-apo-beta-caroten-9-one
-no_pathway-1.14.99.–RXN-7893
1 9′-cis-neoxanthin + 1 oxygen ↔ 1 5,6-epoxy-3-hydroxy-12′-apo-beta-caroten-12′-al + 1 grasshopper_ketone
-no_pathway-1.14.99.–RXN-7894
1 9′-cis-neoxanthin + 1 oxygen ↔ 1 3,5-dihydroxy-6,7-didehydro-12′-apo-beta-caroten-12′-al + 1 5,6-epoxy-3-hydroxy-9-apo-beta-caroten-9-one
-no_pathway-1.14.99.–RXN-7895
1 3,5-dihydroxy-6,7-didehydro-12′-apo-beta-caroten-12′-al + 1 oxygen ↔ 1 grasshopper_ketone + 1 4,9-dimethyldodeca-2,4,6,8,10-pentaene-1,12-dial
-no_pathway-1.17.4.1-ADPREDUCT-RXN
1 dADP + 1 H2O + 1 |Ox-Thioredoxin| ← 2 H+ + 1 ADP + 1 |Red-Thioredoxin|

Reaction name and equation
-no_pathway-1.17.4.1-GDPREDUCT-RXN
1 dGDP + 1 H2O + 1 |Ox-Thioredoxin| ← 2 H+ + 1 GDP + 1 |Red-Thioredoxin|
-no_pathway-1.18.1.2-FLAVONADPREDUCT-RXN
1 NADP+ + 1 |Reduced-flavodoxins| ↔ 1 NADPH + 1 H+ + 1 |Oxidized-flavodoxins|
-no_pathway-1.2.1.18-1.2.1.18-RXN
1 coenzyme_A + 1 malonate_semialdehyde + 1 NADP+ → 1 acetyl-CoA + 1 CO2 + 1 NADPH
-no_pathway-1.2.1.18-RXN-9958_NAD
1 coenzyme_A + 1 malonate_semialdehyde + 1 NAD+ → 1 acetyl-CoA + 1 CO2 + 1 NADH
-no_pathway-1.2.1.18-RXN-9958_NADP
1 coenzyme_A + 1 malonate_semialdehyde + 1 NADP+ → 1 acetyl-CoA + 1 CO2 + 1 NADPH
-no_pathway-1.2.4.1-RXN-12508
1 2-(alpha-hydroxyethyl)thiamine_diphosphate + 1 lipoamide → 1 thiamin_diphosphate + 1 S-acetyldihydrolipoamide
-no_pathway-1.2.4.1-RXN-12583
1 H+ + 1 pyruvate + 1 thiamin_diphosphate → 1 2-(alpha-hydroxyethyl)thiamine_diphosphate + 1 CO2
-no_pathway-1.2.99.2-CARBON-MONOXIDE-DEHYDROGENASE-RXN
1 carbon_monoxide + 1 H2O + 1 FAD → 1 CO2 + 1 FADH2
-no_pathway-1.3.1.33-RXN-5285
1 divinyl_protochlorophyllide_a + 1 NADPH + 1 H+ ↔ 1 divinylchlorophyllide_a + 1 NADP+
-no_pathway-1.3.1.75-RXN-5286
1 chlorophyllide_a + 1 NADP+ ↔ 1 H+ + 1 divinylchlorophyllide_a + 1 NADPH
-no_pathway-1.3.1.9-RXN-9657
1 NADH + 1 H+ + 1 |Crotonyl-ACPs| → 1 NAD+ + 1 |Butanoyl-ACPs|
-no_pathway-1.3.1.9-RXN-9658
1 NAD+ + 1 |Hexanoyl-ACPs| ← 1 NADH + 1 H+ + 1 |Hex-2-enoyl-ACPs|
-no_pathway-1.3.1.9-RXN-9659
1 NAD+ + 1 |Octanoyl-ACPs| ← 1 NADH + 1 H+ + 1 |2-Octenoyl-ACPs|
-no_pathway-1.3.1.9-RXN-9660
1 NAD+ + 1 |Decanoyl-ACPs| ← 1 NADH + 1 H+ + 1 |Trans-D2-decenoyl-ACPs|
-no_pathway-1.3.1.9-RXN-9661
1 NAD+ + 1 |Dodecanoyl-ACPs| ← 1 NADH + 1 H+ + 1 |Dodec-2-enoyl-ACPs|
-no_pathway-1.3.1.9-RXN-9662
1 NAD+ + 1 |Myristoyl-ACPs| ← 1 NADH + 1 H+ + 1 |Tetradec-2-enoyl-ACPs|
-no_pathway-1.3.1.9-RXN-9663
1 NAD+ + 1 |Palmitoyl-ACPs| ← 1 NADH + 1 H+ + 1 |2-Hexadecenoyl-ACPs|
-no_pathway-1.3.8.–RXN-12572
1 3-methylmercaptopropionyl-CoA + 1 FAD → 1 methylthioacryloyl-CoA + 1 FADH2
-no_pathway-1.3.98.1-RXN-9929
1 (S)-dihydroorotate + 1 fumarate ↔ 1 orotate + 1 succinate
-no_pathway-1.4.1.21-1.4.1.21-RXN_NAD
1 L-aspartate + 1 H2O + 1 NAD+ ↔ 1 ammonia + 1 oxaloacetate + 2 H+ + 1 NADH
-no_pathway-1.4.1.21-1.4.1.21-RXN_NADP
1 L-aspartate + 1 H2O + 1 NADP+ ↔ 1 ammonia + 1 oxaloacetate + 2 H+ + 1 NADPH
-no_pathway-1.4.3.19-RXN-8672
1 D-alanine + 1 oxygen + 1 H2O → 1 ammonia + 1 hydrogen_peroxide + 1 H+ + 1 pyruvate
-no_pathway-1.5.1.12-RXN-11632_NAD
1 (S)-1-pyrroline-5-carboxylate + 2 H2O + 1 NAD+ → 1 L-glutamate + 1 H+ + 1 NADH
-no_pathway-1.5.1.12-RXN-11632_NADP
1 (S)-1-pyrroline-5-carboxylate + 2 H2O + 1 NADP+ → 1 L-glutamate + 1 H+ + 1 NADPH
-no_pathway-1.6.5.2-RXN-12303_NAD
1 plastoquinone-9 + 1 H+ + 1 NADH ↔ 1 plastoquinol-9 + 1 NAD+
-no_pathway-1.6.5.2-RXN-12303_NADP
1 plastoquinone-9 + 1 H+ + 1 NADPH ↔ 1 plastoquinol-9 + 1 NADP+
-no_pathway-1.7.2.3-1.7.2.3-RXN
1 trimethylamine + 1 H2O + 2 |Cytochromes-C-Oxidized| ↔ 3 H+ + 1 trimethylamine_N-oxide + 2 |Cytochromes-C-Reduced|
-no_pathway-1.7.99.4-RXN0-6369
1 nitrate + 1 |Ubiquinols| → 1 nitrite + 1 H2O + 1 |Ubiquinones|
-no_pathway-1.8.1.4-1.8.1.4-RXN
1 NAD+ + 1 dihydrolipoamide ↔ 1 NADH + 1 H+ + 1 lipoamide
-no_pathway-1.8.1.4-DIHYDLIPOXN-RXN
1 dihydrolipoamide + 1 NAD+ ↔ 1 lipoamide + 1 NADH + 1 H+
-no_pathway-1.8.5.3-DIMESULFREDUCT-RXN
1 dimethyl_sulfoxide$_{ex}$ + 1 |Ubiquinols| → 1 dimethyl_sulfide$_{ex}$ + 1 H2O$_{ex}$ + 1 |Ubiquinones|
-no_pathway-2.1.1.–RXN-10668

Reaction name and equation
1 1-hydroxyneurosporene + 1 S-adenosyl-L-methionine → 1 S-adenosyl-L-homocysteine + 1 methoxyneurosporene + 1 H+
-no_pathway-2.1.1.–RXN-9736
1 5-methyl-tetrahydrofolate + 1 3-S-methylmercaptopropionate + 1 H+ ← 1 dimethylsulfoniopropionate + 1 tetrahydrofolate
-no_pathway-2.1.1.148-RXN-8850
1 dUMP + 1 5,10-methylenetetrahydrofolate + 1 NADPH + 1 H+ → 1 NADP+ + 1 tetrahydrofolate + 1 dTMP
-no_pathway-2.1.1.201-RXN-9235
1 2-methoxy-6-all_trans-decaprenyl-2-methoxy-1,4-benzoquinol + 1 S-adenosyl-L-methionine → 1 S-adenosyl-L-homocysteine + 1 6-methoxy-3-methyl-2-all-trans-decaprenyl-1,4-benzoquinol + 1 H+
-no_pathway-2.1.1.222-RXN-9233
1 3-(all-trans-decaprenyl)benzene-1,2-diol + 1 S-adenosyl-L-methionine → 1 S-adenosyl-L-homocysteine + 1 2-methoxy-6-(all-trans-decaprenyl)phenol + 1 H+
-no_pathway-2.1.2.2-GART-RXN
1 10-formyl-tetrahydrofolate + 1 5-phospho-ribosyl-glycineamide ↔ 1 5′-phosphoribosyl-N-formylglycineamide + 1 H+ + 1 tetrahydrofolate
-no_pathway-2.3.1.–MALONYL-ACPDECARBOX-RXN
1 MALONYL-ACP → 1 ACETYL-ACP + 1 CO_2
-no_pathway-2.3.1.12-DIHYDLIPACETRANS-RXN
1 acetyl-CoA + 1 dihydrolipoamide ↔ 1 coenzyme_A + 1 S-acetyldihydrolipoamide
-no_pathway-2.3.1.179-2.3.1.179-RXN
1 MALONYL-ACP + 1 |Palmitoleoyl-ACPs| → 1 ACP + 1 CO_2 + 1 |3-oxo-cis-vaccenoyl-ACPs|
-no_pathway-2.3.1.41-RXN-9516
1 MALONYL-ACP + 1 |Butanoyl-ACPs| → 1 ACP + 1 CO_2 + 1 |3-oxo-hexanoyl-ACPs|
-no_pathway-2.3.1.41-RXN-9523
1 MALONYL-ACP + 1 |Hexanoyl-ACPs| → 1 ACP + 1 CO_2 + 1 |3-Oxo-octanoyl-ACPs|
-no_pathway-2.3.1.41-RXN-9527
1 MALONYL-ACP + 1 |Octanoyl-ACPs| → 1 ACP + 1 CO_2 + 1 |3-oxo-decanoyl-ACPs|
-no_pathway-2.3.1.41-RXN-9531
1 MALONYL-ACP + 1 |Decanoyl-ACPs| → 1 ACP + 1 CO_2 + 1 |3-oxo-dodecanoyl-ACPs|
-no_pathway-2.3.1.41-RXN-9535
1 MALONYL-ACP + 1 |Dodecanoyl-ACPs| → 1 ACP + 1 CO_2 + 1 |3-oxo-myristoyl-ACPs|
-no_pathway-2.3.1.41-RXN-9539
1 MALONYL-ACP + 1 |Myristoyl-ACPs| → 1 ACP + 1 CO_2 + 1 |3-oxo-palmitoyl-ACPs|
-no_pathway-2.4.1.129-RXN0-5405
2 N-acetylmuramoyl-L-alanyl-D-glutamyl-meso-2,6-diaminopimelyl-D-alanyl-D-alanine-diphosphoundecaprenyl-N-acetylglucosamine → 1 a_peptidoglycan_dimer_(meso-diaminopimelate_containing) + 1 H+ + 1 di-trans,octa-cis-undecaprenyl_diphosphate
-no_pathway-2.4.1.227-NACGLCTRANS-RXN
1 N-acetylmuramoyl-L-alanyl-D-glutamyl-meso-2,6-diaminopimelyl-D-alanyl-D-alanine-diphosphoundecaprenol + 1 UDP-alpha-N-acetyl-D-glucosamine ↔ 1 N-acetylmuramoyl-L-alanyl-D-glutamyl-meso-2,6-diaminopimelyl-D-alanyl-D-alanine-diphosphoundecaprenyl-N-acetylglucosamine + 1 H+ + 1 UDP
-no_pathway-2.5.1.31-RXN-8999
8 isopentenyl_diphosphate + 1 (2E,6E)-farnesyl_diphosphate → 8 diphosphate + 1 di-trans,octa-cis-undecaprenyl_diphosphate
-no_pathway-2.5.1.32-RXN-12245
1 prephytoene_diphosphate ↔ 1 all-trans-phytoene + 1 diphosphate
-no_pathway-2.5.1.32-RXN1F-144
2 all-trans-geranyl-geranyl_diphosphate ↔ 1 all-trans-phytoene + 2 diphosphate
-no_pathway-2.5.1.32-RXNARA-8002
1 prephytoene_diphosphate → 1 15-cis-phytoene + 1 diphosphate
-no_pathway-2.5.1.39-RXN-9230
1 4-hydroxybenzoate + 1 all-trans-decaprenyl_diphosphate → 1 3-decaprenyl-4-hydroxybenzoate + 1 diphosphate
-no_pathway-2.5.1.48-METBALT-RXN
1 2-oxobutanoate + 1 ammonia + 2 H+ + 1 succinate ↔ 1 O-succinyl-L-homoserine + 1 H_2O
-no_pathway-2.5.1.49-O-ACETYLHOMOSERINE-THIOL-LYASE-RXN
1 O-acetyl-L-homoserine + 1 methanethiol ↔ 1 acetate + 1 L-methionine + 1 H+
-no_pathway-2.5.1.91-RXN-9106
7 isopentenyl_diphosphate + 1 (2E,6E)-farnesyl_diphosphate → 1 all-trans-decaprenyl_diphosphate + 7 diphosphate

Reaction name and equation
-no_pathway-2.6.1.–ASPAROXO-RXN
1 L-asparagine + 1 glyoxylate → 1 2-oxosuccinamate + 1 glycine
-no_pathway-2.7.1.–ASCORBATE-PHOSPHORYLATION-IV-RXN
1 acetylphosphate + 1 L-ascorbate ↔ 1 2-phospho-L-ascorbate + 1 acetate + 1 H+
-no_pathway-2.7.1.–ASCORBATE-PHOSPHORYLATION-RXN
1 L-ascorbate + 1 ATP → 1 2-phospho-L-ascorbate + 1 ADP + 1 H+
-no_pathway-2.7.1.–RXN-11629
1 geranylgeraniol + 1 CTP ↔ 1 CDP + 1 all-trans-geranyl-geranyl_monophosphate + 1 H+
-no_pathway-2.7.1.–RXN-12325
1 ATP + 1 geranylgeraniol → 1 ADP + 1 all-trans-geranyl-geranyl_monophosphate + 1 H+
-no_pathway-2.7.1.–RXN0-6564
1 ATP + 1 4-hydroxy-L-threonine → 1 4-phospho-hydroxy-L-threonine + 1 ADP + 1 H+
-no_pathway-2.7.8.13-PHOSNACMURPENTATRANS-RXN
1 UDP-N-acetylmuramoyl-L-alanyl-D-glutamyl-meso-2,6-diaminopimelyl-D-alanyl-D-alanine + 1 ditrans,octacis-undecaprenyl_phosphate → 1 N-acetylmuramoyl-L-alanyl-D-glutamyl-meso-2,6-diaminopimelyl-D-alanyl-D-alanine-diphosphoundecaprenol + 1 uridine-5′-phosphate
-no_pathway-2.8.3.10-2.8.3.10-RXN
1 acetyl-CoA + 1 citrate ↔ 1 (3S)-citryl-CoA + 1 acetate
-no_pathway-3.1.1.29-RXN-12460
1 H2O + 1 |Charged-ASN-tRNAs| → 1 L-asparagine + 2 H+ + 1 |ASN-tRNAs|
-no_pathway-3.1.2.–RXN-12573
1 methylthioacryloyl-CoA + 2 H2O → 1 acetaldehyde + 1 CO2 + 1 coenzyme_A + 1 methanethiol
-no_pathway-3.1.3.7-325-BISPHOSPHATE-NUCLEOTIDASE-RXN
1 adenosine_3′,5′-bisphosphate + 1 H2O ↔ 1 AMP + 1 phosphate
-no_pathway-3.2.2.1-RXN0-366
1 guanosine + 1 H2O → 1 guanine + 1 alpha-D-ribofuranose
-no_pathway-3.4.13.22-3.4.13.22-RXN
1 D-alanyl-D-alanine + 1 H2O → 2 D-alanine
-no_pathway-3.4.16.4-RXN-11302
2 a_peptidoglycan_dimer_(meso-diaminopimelate_containing) + 4 H2O → 1 H+ + 1 a_peptidoglycan_with_D,D_cross-links_(meso-diaminopimelate_containing) + 4 D-alanine + 1 di-trans,octa-cis-undecaprenyl_diphosphate
-no_pathway-3.5.1.–ILEDEAMINE-RXN
1 L-isoleucine + 1 H2O → 1 2-keto-3-methyl-valerate + 1 ammonia + 3 H+
-no_pathway-3.5.1.–L-OXOACET-RXN
1 2-oxosuccinamate + 1 H2O ↔ 1 ammonium + 1 oxaloacetate
-no_pathway-3.5.1.–RXN0-5040
1 p-aminobenzoyl_glutamate + 1 H2O → 1 L-glutamate + 1 4-aminobenzoate
-no_pathway-3.6.1.–RXN0-383
1 CTP + 1 H2O → 1 CMP + 1 diphosphate + 1 H+
-no_pathway-3.6.1.–RXN0-384
1 dATP + 1 H2O → 1 dAMP + 1 diphosphate + 1 H+
-no_pathway-3.6.1.–RXN0-5107
1 dTTP + 1 H2O → 1 diphosphate + 1 H+ + 1 dTMP
-no_pathway-3.6.4.12-RXN-11135
1 ATP + 1 H2O → 1 ADP + 1 phosphate + 1 H+
-no_pathway-3.6.4.13-RXN-11109
1 ATP + 1 H2O → 1 ADP + 1 phosphate + 1 H+
-no_pathway-3.6.5.3-3.6.5.3-RXN
1 GTP + 1 H2O → 1 GDP + 1 phosphate + 1 H+
-no_pathway-4.1.1.–RXN-9231
1 3-decaprenyl-4-hydroxybenzoate + 1 H+ → 1 CO2 + 1 2-decaprenylphenol
-no_pathway-4.1.2.–RXN0-6563
1 4-hydroxy-L-threonine ↔ 1 glycine + 1 glycolaldehyde
-no_pathway-4.1.3.6-CITLY-RXN
1 citrate → 1 acetate + 1 oxaloacetate
-no_pathway-4.1.99.17-PYRIMSYN1-RXN
1 5-amino-1-(5-phospho-D-ribosyl)imidazole + 1 S-adenosyl-L-methionine → 1 4-amino-2-methyl-5-phosphomethylpyrimidine + 1 carbon_monoxide + 1 5′-deoxyadenosine + 1 formate + 1 L-methionine + 3 H+
-no_pathway-4.2.1.–CARNDETRU-RXN
1 L-carnitinyl-CoA ↔ 1 crotonobetainyl-CoA + 1 H2O
-no_pathway-4.2.1.–RXN0-6727
1 H+ + 1 ADP + 1 (S)-NADHX ↔ 1 AMP + 1 NADH + 1 phosphate
-no_pathway-4.2.1.131-RXN-10665

Reaction name and equation
1 1-hydroxyneurosporene ← 1 all-trans_neurosporene + 1 H2O
-no_pathway-4.2.1.20-TRYPSYN-RXN
1 (1S,2R)-1-C-(indol-3-yl)glycerol_3-phosphate + 1 L-serine → 1 D-glyceraldehyde-3-phosphate + 1 L-tryptophan + 1 H2O
-no_pathway-4.2.1.58-4.2.1.58-RXN
1 |Beta-3-hydroxybutyryl-ACPs| → 1 H2O + 1 |Crotonyl-ACPs|
-no_pathway-4.2.1.59-4.2.1.59-RXN
1 |3-Hydroxy-octanoyl-ACPs| → 1 H2O + 1 |2-Octenoyl-ACPs|
-no_pathway-4.2.1.59-RXN-9520
1 |R-3-hydroxyhexanoyl-ACPs| → 1 H2O + 1 |Hex-2-enoyl-ACPs|
-no_pathway-4.2.1.59-RXN-9533
1 |R-3-hydroxydodecanoyl-ACPs| → 1 H2O + 1 |Dodec-2-enoyl-ACPs|
-no_pathway-4.2.1.59-RXN-9537
1 |R-3-hydroxymyristoyl-ACPs| → 1 H2O + 1 |Tetradec-2-enoyl-ACPs|
-no_pathway-4.2.1.59-RXN-9655
1 |Beta-hydroxydecanoyl-ACPs| → 1 H2O + 1 |Trans-D2-decenoyl-ACPs|
-no_pathway-4.2.1.61-4.2.1.61-RXN
1 |R-3-Hydroxypalmitoyl-ACPs| → 1 H2O + 1 |2-Hexadecenoyl-ACPs|
-no_pathway-4.2.1.61-RXN-9557
1 |R-3-hydroxy-cis-vaccenoyl-ACPs| → 1 H2O + 1 |cis-vaccen-2-enoyl-ACPs|
-no_pathway-4.3.3.6-RXN-11322
1 D-glyceraldehyde-3-phosphate + 1 L-glutamine + 1 D-ribose-5-phosphate → 1 L-glutamate + 1 phosphate + 1 H+ + 1 pyridoxal_5′-phosphate + 3 H2O
-no_pathway-4.3.3.6-RXN-12590
1 ammonia + 1 D-glyceraldehyde-3-phosphate + 1 D-ribose-5-phosphate ↔ 1 phosphate + 1 pyridoxal_5′-phosphate + 4 H2O
-no_pathway-4.4.1.–RXN-10937
1 dimethylsulfoniopropionate + 1 H2O ↔ 1 3-hydroxypropionate + 1 dimethyl_sulfide + 1 H+
-no_pathway-4.4.1.3-DIMETHYLPROPIOTHETIN-DETHIOMETHYLASE-RXN
1 dimethylsulfoniopropionate → 1 acrylate + 1 dimethyl_sulfide + 1 H+
-no_pathway-5.-.-.–FCLEPIM-RXN
1 GDP-4-dehydro-6-deoxy-D-mannose ↔ 1 GDP-4-dehydro-6-L-deoxygalactose
-no_pathway-5.1.1.3-GLUTRACE-RXN
1 L-glutamate ↔ 1 D-glutamate
-no_pathway-5.1.2.3-5.1.2.3-RXN
1 (S)-3-hydroxybutanoyl-CoA ↔ 1 (R)-3-hydroxybutanoyl-CoA
-no_pathway-5.3.1.22-RXN0-305
1 hydroxypyruvate ↔ 1 tartronate_semialdehyde
-no_pathway-5.3.1.5-GLUCISOM-RXN
1 beta-D-glucose ↔ 1 beta-D-fructofuranose
-no_pathway-6.1.1.–RXN490-3616
1 ATP + 1 L-aspartate + 1 |ASN-tRNAs| → 1 AMP + 1 diphosphate + 1 |L-aspartyl-tRNAAsn|
-no_pathway-6.2.1.–RXN-12571
1 ATP + 1 coenzyme_A + 1 3-S-methylmercaptopropionate → 1 AMP + 1 3-methylmercaptopropionyl-CoA + 1 diphosphate
-no_pathway-6.3.-.–RXN-10884
1 ATP + 1 L-glutamate + 1 4-aminobenzoate → 1 AMP + 1 p-aminobenzoyl_glutamate + 1 diphosphate + 1 H+
-no_pathway-6.3.2.10-UDP-NACMURALGLDAPAALIG-RXN
1 ATP + 1 D-alanyl-D-alanine + 1 UDP-N-acetylmuramoyl-L-alanyl-D-glutamyl-meso-2,6-diaminopimelate → 1 ADP + 1 UDP-N-acetylmuramoyl-L-alanyl-D-glutamyl-meso-2,6-diaminopimelyl-D-alanyl-D-alanine + 1 phosphate + 1 H+
-no_pathway-6.3.5.6-6.3.5.6-RXN
1 ATP + 1 L-glutamine + 1 H2O + 1 |L-aspartyl-tRNAAsn| → 1 ADP + 1 L-glutamate + 1 phosphate + 2 H+ + 1 |Charged-ASN-tRNAs|
-no_pathway-GlpF-TRANS-RXN-131
1 glycerol$_{ex}$ ↔ 1 glycerol
-no_pathway-RXN-12753-spontaneous
1 NADH + 1 H2O → 2 H+ + 1 (S)-NADHX
-no_pathway-RXN0-5219-spontaneous
1 ammonia + 1 H+ ↔ 1 ammonium
-no_pathway-RXN0-6550
1 5′-deoxyadenosine + 1 H2O → 1 adenine + 1 5-deoxy-D-ribose
-no_pathway-acuK-RXN-10986
1 acrylyl-CoA + 2 H2O → 1 3-hydroxypropionate + 1 coenzyme_A + 1 H+

Reaction name and equation
-no_pathway-acuN-RXN-10985
1 acrylate + 1 coenzyme_A + 1 H+ → 1 acrylyl-CoA + 1 H2O
-no_pathway-crtI-RXN-8022
1 all-trans-zeta-carotene + 1 NAD+ → 1 H+ + 1 all-trans_neurosporene + 1 NADH
-no_pathway-crtI-RXN-8023
1 15-cis-phytoene + 1 NAD+ → 1 H+ + 1 all-trans_phytofluene + 1 NADH
-no_pathway-crtI-RXN-8024
1 all-trans_phytofluene + 1 NAD+ → 1 H+ + 1 all-trans-zeta-carotene + 1 NADH
-no_pathway-masA-3.1.3.77-RXN
1 5-(methylthio)-2,3-dioxopentyl_phosphate + 1 H2O ↔ 1 1,2-dihydroxy-5-(methylthio)pent-1-en-3-one + 1 phosphate + 1 H+
-no_pathway-masA-R82-RXN
1 5-(methylthio)-2,3-dioxopentyl_phosphate → 1 2-hydroxy-5-(methylthio)-3-oxopent-1-enyl_phosphate + 1 H+
-no_pathway-masA-R83-RXN
1 2-hydroxy-5-(methylthio)-3-oxopent-1-enyl_phosphate + 1 H2O → 1 1,2-dihydroxy-5-(methylthio)pent-1-en-3-one + 1 phosphate
2-ketoglutarate_dehydrogenase_complex-1.2.4.2-2OXOGLUTDECARB-RXN
1 2-oxoglutarate + 2 H+ + 1 lipoamide → 1 CO2 + 1 |Oxo-glutarate-dehydro-suc-DH-lipoyl|
2-ketoglutarate_dehydrogenase_complex-1.8.1.4-RXN-7716
1 NAD+ + 1 dihydrolipoamide ↔ 1 NADH + 1 H+ + 1 lipoamide
2-ketoglutarate_dehydrogenase_complex-2.3.1.61-RXN0-1147
1 H+ + 1 succinyl-CoA + 1 dihydrolipoamide ↔ 1 coenzyme_A + 1 |Oxo-glutarate-dehydro-suc-DH-lipoyl|
2-oxoglutarate_Na+_symport
1 2-oxoglutarate$_{ex}$ + 1 Na+$_{ex}$ → 1 Na+ + 1 2-oxoglutarate
5,6-dimethylbenzimidazole_biosynthesis-1.5.1.39-FMNREDUCT-RXN_NAD
1 FMNH2 + 1 NAD+ ↔ 1 FMN + 2 H+ + 1 NADH
5,6-dimethylbenzimidazole_biosynthesis-1.5.1.39-FMNREDUCT-RXN_NADP
1 FMNH2 + 1 NADP+ ↔ 1 FMN + 2 H+ + 1 NADPH
ATP_maintenance_requirement
1 ATP + 1 H2O → 1 ADP + 1 phosphate + 1 H+
Biomass-reaction_aerobic

Reaction name and equation
0.0309743 dTTP + 0.0542137 dGTP + 0.0285324 dATP + 0.0542319 dCTP + 0.0800166 ATP + 0.000294334 ADP + 0.144873 GTP + 0.0790352 UTP + 0.143393 CTP + 0.238003 L-proline + 0.26123 L-aspartate + 0.119589 L-lysine + 0.304207 L-glutamate + 0.380514 glycine + 0.449108 L-leucine + 0.322875 L-valine + 0.134497 L-glutamine + 0.0853216 L-histidine + 0.092345 L-tyrosine + 0.115801 L-methionine + 0.161522 L-phenylalanine + 0.21267 L-serine + 0.101462 L-asparagine + 0.0611165 L-tryptophan + 0.0385471 L-cysteine + 0.213971 L-isoleucine + 0.24623 L-threonine + 0.303138 L-arginine + 0.569435 L-alanine + 0.000358504 GDP + 0.000196223 L-homocysteine + 0.000715948 L-citrulline + 0.0015468 D-fructose-6-phosphate + 0.000233346 D-ribose-5-phosphate + 0.000233346 D-xylulose-5-phosphate + 0.000567455 acetylphosphate + 9.97023e-05 guanine + 2.59862e-05 sn-glycerol-3-phosphate + 6.78824e-06 histidinol + 0.000198344 dihydroxyacetone_phosphate + 0.000321381 acetyl-CoA + 1.15612e-05 acetoacetyl-CoA + 0.0015468 beta-D-glucose-6-phosphate + 7.47768e-06 shikimate + 0.000747768 D-glycerate + 5.35635e-06 L-ornithine + 1.87737e-05 malonyl-CoA + 6.09881e-05 fumarate + 4.68813e-06 dAMP + 2.82136e-06 propanoyl-CoA + 2.76833e-07 deoxyguanosine + 0.00016069 2-deoxy-alpha-D-ribose_5-phosphate + 8.53834e-06 cis-aconitate + 0.000190919 CMP + 0.00199935 6-phospho-D-gluconate + 0.000234937 2-oxoglutarate + 0.000149023 AMP + 0.000609881 alpha-D-glucosamine-6-phosphate + 1.49554e-06 deoxyadenosine + 0.000200465 dTDP + 0.0015468 alpha-D-glucose_1-phosphate + 4.34342e-05 N-acetyl-alpha-D-glucosamine_1-phosphate + 0.000301759 succinate + 0.00806104 fructose-1,6-bisphosphate + 4.41236e-05 NADH + 0.000890957 (S)-malate + 0.00132583 UDP-alpha-D-glucose + 3.5161e-06 adenosine_5′-phosphosulfate + 1.10309e-06 NADP+ + 0.000726554 coenzyme_A + 0.000312896 N-carbamoyl-L-aspartate + 1.84555e-06 anthranilate + 6.41701e-05 NADPH + 0.00014425 IMP + 6.31095e-06 (S)-dihydroorotate + 1.25689e-05 GMP + 0.00135235 NAD+ + 9.7581e-05 S-adenosyl-L-methionine + 6.94734e-08 adenosine + 0.00490026 UDP-alpha-N-acetyl-D-glucosamine + 0.000136826 5-phospho-alpha-D-ribose_1-diphosphate + 2.76833e-05 4-hydroxybenzoate + 4.76238e-05 keto-phenylpyruvate + 9.7581e-05 phosphoenolpyruvate + 2.68878e-05 dGMP + 0.000816711 3-phospho-D-glycerate + 9.17474e-05 FAD + 0.000123567 succinyl-CoA + 2.84788e-05 FMN + 0.000949294 UDP + 7.79587e-07 adenine + 2.29634e-05 N-acetyl-L-ornithine + 8.59137e-07 guanosine + 1.00763e-05 riboflavin + 0.00103945 citrate + 2.47028 PHB + 0.010512 Kdo2-lipid_A + 0.113109 O-antigen + 0.00542908 a_peptidoglycan_with_D,D_cross-links_(meso-diaminopimelate_containing) + 0.000903981 bacteriochlorophyll_a + 0.164082 phosphatidylglycerol + 0.000144714 thiamin_diphosphate + 0.000144714 tetrahydrofolate + 0.000144714 methoxyneurosporene + 0.000144714 putrescine + 0.000144714 biotin + 0.000144714 coenzyme_B12 + 0.000144714 protoheme_IX + 0.000144714 ubiquinol-10 + 0.000144714 siroheme + 0.000144714 5,10-methylenetetrahydrofolate + 0.000144714 pyridoxal_5′-phosphate + 0.000144714 10-formyl-tetrahydrofolate → 0.599258 diphosphate + 4.35149 H2O + 1 Biomass_Dshibae **Biomass-reaction_anaerobic**

Reaction name and equation
0.0309998 dTTP + 0.0542584 dGTP + 0.0285559 dATP + 0.0542767 dCTP + 0.0800826 ATP + 0.000294577 ADP + 0.144992 GTP + 0.0791003 UTP + 0.143511 CTP + 0.238199 L-proline + 0.261445 L-aspartate + 0.119688 L-lysine + 0.304458 L-glutamate + 0.380828 glycine + 0.449479 L-leucine + 0.323141 L-valine + 0.134608 L-glutamine + 0.0853919 L-histidine + 0.0924211 L-tyrosine + 0.115896 L-methionine + 0.161655 L-phenylalanine + 0.212845 L-serine + 0.101545 L-asparagine + 0.0611669 L-tryptophan + 0.0385789 L-cysteine + 0.214147 L-isoleucine + 0.246433 L-threonine + 0.303388 L-arginine + 0.569904 L-alanine + 0.0003588 GDP + 0.000196385 L-homocysteine + 0.000716538 L-citrulline + 0.00154808 D-fructose-6-phosphate + 0.000233538 D-ribose-5-phosphate + 0.000233538 D-xylulose-5-phosphate + 0.000567923 acetylphosphate + 9.97846e-05 guanine + 2.60077e-05 sn-glycerol-3-phosphate + 6.79384e-06 histidinol + 0.000198508 dihydroxyacetone_phosphate + 0.000321646 acetyl-CoA + 1.15708e-05 acetoacetyl-CoA + 0.00154808 beta-D-glucose-6-phosphate + 7.48384e-06 shikimate + 0.000748384 D-glycerate + 5.36077e-06 L-ornithine + 1.87892e-05 malonyl-CoA + 6.10384e-05 fumarate + 4.692e-06 dAMP + 2.82369e-06 propanoyl-CoA + 2.77061e-07 deoxyguanosine + 0.000160823 2-deoxy-alpha-D-ribose_5-phosphate + 8.54538e-06 cis-aconitate + 0.000191077 CMP + 0.002001 6-phospho-D-gluconate + 0.000235131 2-oxoglutarate + 0.000149146 AMP + 0.000610384 alpha-D-glucosamine-6-phosphate + 1.49677e-06 deoxyadenosine + 0.000200631 dTDP + 0.00154808 alpha-D-glucose_1-phosphate + 4.347e-05 N-acetyl-alpha-D-glucosamine_1-phosphate + 0.000302008 succinate + 0.00806769 fructose-1,6-bisphosphate + 4.416e-05 NADH + 0.000891692 (S)-malate + 0.00132692 UDP-alpha-D-glucose + 3.519e-06 adenosine_5′-phosphosulfate + 1.104e-06 NADP+ + 0.000727153 coenzyme_A + 0.000313154 N-carbamoyl-L-aspartate + 1.84708e-06 anthranilate + 6.4223e-05 NADPH + 0.000144369 IMP + 6.31615e-06 (S)-dihydroorotate + 1.25792e-05 GMP + 0.00135346 NAD+ + 9.76615e-05 S-adenosyl-L-methionine + 6.95307e-08 adenosine + 0.00490431 UDP-alpha-N-acetyl-D-glucosamine + 0.000136938 5-phospho-alpha-D-ribose_1-diphosphate + 2.77061e-05 4-hydroxybenzoate + 4.76631e-05 keto-phenylpyruvate + 9.76615e-05 phosphoenolpyruvate + 2.691e-05 dGMP + 0.000817384 3-phospho-D-glycerate + 9.1823e-05 FAD + 0.000123669 succinyl-CoA + 2.85023e-05 FMN + 0.000950076 UDP + 7.8023e-07 adenine + 2.29823e-05 N-acetyl-L-ornithine + 8.59846e-07 guanosine + 1.00846e-05 riboflavin + 0.00104031 citrate + 2.47231 PHB + 0.0105206 Kdo2-lipid_A + 0.113202 O-antigen + 0.00543356 a_peptidoglycan_with_D,D_cross-links_(meso-diaminopimelate_containing) + 0.164217 phosphatidylglycerol + 0.000144833 thiamin_diphosphate + 0.000144833 tetrahydrofolate + 0.000144833 methoxyneurosporene + 0.000144833 putrescine + 0.000144833 biotin + 0.000144833 coenzyme_B12 + 0.000144833 protoheme_IX + 0.000144833 ubiquinol-10 + 0.000144833 siroheme + 0.000144833 5,10-methylenetetrahydrofolate + 0.000144833 pyridoxal_5′-phosphate + 0.000144833 10-formyl-tetrahydrofolate → 0.599753 diphosphate + 4.35508 H2O + 1 Biomass_Dshibae
C4_photosynthetic_carbon_assimilation_cycle-2.7.9.1-PYRUVATEORTHOPHOSPHATE-DIKINASE-RXN
1 ATP + 1 phosphate + 1 pyruvate ↔ 1 AMP + 1 phosphoenolpyruvate + 1 diphosphate + 1 H+
CMP-KDO_biosynthesis-2.5.1.55-KDO-8PSYNTH-RXN
1 D-arabinose_5-phosphate + 1 phosphoenolpyruvate + 1 H2O → 1 3-deoxy-D-manno-octulosonate_8-phosphate + 1 phosphate
CMP-KDO_biosynthesis-2.7.7.38-CPM-KDOSYNTH-RXN
1 CTP + 1 3-deoxy-D-manno-octulosonate → 1 CMP-3-deoxy-D-manno-octulosonate + 1 diphosphate
CMP-KDO_biosynthesis-3.1.3.45-KDO-8PPHOSPHAT-RXN
1 3-deoxy-D-manno-octulosonate_8-phosphate + 1 H2O → 1 3-deoxy-D-manno-octulosonate + 1 phosphate
CMP-KDO_biosynthesis-5.3.1.13-DARAB5PISOM-RXN
1 D-arabinose_5-phosphate ↔ 1 D-ribulose-5-phosphate
CO2_fixation_in_Crenarchaeota-4.2.1.–RXN-11667
1 (S)-3-hydroxybutanoyl-CoA ↔ 1 crotonyl-CoA + 1 H2O
CO2_fixation_in_Crenarchaeota-4.2.1.–RXN-12566
1 (S)-3-hydroxybutanoyl-CoA → 1 crotonyl-CoA + 1 H2O
CO2_fixation_in_Crenarchaeota-6.4.1.3-PROPIONYL-COA-CARBOXY-RXN
1 ATP + 1 bicarbonate + 1 propanoyl-CoA → 1 ADP + 1 (S)-methylmalonyl-CoA + 1 phosphate + 1 H+
D-ribitol_Na+_symport
1 D-ribitol$_{ex}$ + 1 Na+$_{ex}$ → 1 Na+ + 1 D-ribitol
D-xylitol_Na+_symport
1 D-xylitol$_{ex}$ + 1 Na+$_{ex}$ → 1 Na+ + 1 D-xylitol
Degradation_of_sugar_acids-1.1.1.60-RXN0-5289
1 D-glycerate + 1 NAD+ ↔ 1 NADH + 1 H+ + 1 tartronate_semialdehyde
Degradation_of_sugar_acids-1.1.1.60-TSA-REDUCT-RXN_NAD

Reaction name and equation
1 D-glycerate + 1 NAD+ ⟵ 1 H+ + 1 tartronate_semialdehyde + 1 NADH
Degradation_of_sugar_acids-1.1.1.60-TSA-REDUCT-RXN_NADP
1 D-glycerate + 1 NADP+ ⟵ 1 H+ + 1 tartronate_semialdehyde + 1 NADPH
Entner_Doudoroff_pathway-4.1.2.14-KDPGALDOL-RXN
1 2-dehydro-3-deoxy-D-gluconate-6-phosphate → 1 D-glyceraldehyde-3-phosphate + 1 pyruvate
Entner_Doudoroff_pathway-4.2.1.12-PGLUCONDEHYDRAT-RXN
1 6-phospho-D-gluconate → 1 2-dehydro-3-deoxy-D-gluconate-6-phosphate + 1 H2O
Entner_Doudoroff_pathway-ALDOSE-1-EPIMERASE-RXN-spontaneous
1 alpha-D-glucose ↔ 1 beta-D-glucose
GDP-L-fucose_biosynthesis_I_(from_GDP-D-mannose)-1.1.1.271-1.1.1.271-RXN
1 GDP-L-fucose + 1 NADP+ ⟵ 1 GDP-4-dehydro-6-deoxy-D-mannose + 1 NADPH + 1 H+
KDO_transfer_to_lipid_IVA-2.4.99.12-KDOTRANS-RXN
1 CMP-3-deoxy-D-manno-octulosonate + 1 lipid_IVA ↔ 1 CMP + 1 alpha-Kdo-(2rarr6)-lipid_IVA + 1 H+
KDO_transfer_to_lipid_IVA-2.4.99.13-KDOTRANS2-RXN
1 CMP-3-deoxy-D-manno-octulosonate + 1 alpha-Kdo-(2rarr6)-lipid_IVA ↔ 1 CMP + 1 alpha-Kdo-(2→4)-alpha-Kdo-(2→6)-lipid_IVA + 1 H+
L-alanine_diffusion
1 L-alanine$_{ex}$ → 1 L-alanine
L-aspartate_diffusion
1 L-aspartate$_{ex}$ → 1 L-aspartate
L-glutamate_Na+_symport
1 L-glutamate$_{ex}$ + 1 Na+$_{ex}$ → 1 Na+ + 1 L-glutamate
L-glutamate_diffusion
1 L-glutamate$_{ex}$ → 1 L-glutamate
L-glutamine_diffusion
1 L-glutamine$_{ex}$ → 1 L-glutamine
L-lactaldehyde_degradation-1.2.1.22-LACTALDDEHYDROG-RXN
1 L-lactaldehyde + 1 NAD+ + 1 H2O → 1 (S)-lactate + 1 NADH + 2 H+
NAD_metabolism-1.6.1.2-1.6.1.2-RXN
1 NAD+ + 1 NADPH ↔ 1 NADH + 1 NADP+
NAD_metabolism-2.4.2.11-NICOTINATEPRIBOSYLTRANS-RXN
1 nicotinate_D-ribonucleotide + 1 diphosphate ⟵ 1 nicotinate + 1 H+ + 1 5-phospho-alpha-D-ribose_1-diphosphate
NAD_metabolism-2.7.1.23-NAD-KIN-RXN
1 H+ + 1 ATP + 1 NAD+ → 1 ADP + 1 NADP+
NAD_metabolism-2.7.7.18-NICONUCADENYLYLTRAN-RXN
1 ATP + 1 nicotinate_D-ribonucleotide + 1 H+ → 1 nicotinate_adenine_dinucleotide + 1 diphosphate
NAD_metabolism-6.3.1.5-NAD-SYNTH-NH3-RXN
2 H+ + 1 ammonia + 1 ATP + 1 nicotinate_adenine_dinucleotide → 1 AMP + 1 NAD+ + 1 diphosphate
NAD_metabolism-6.3.5.1-NAD-SYNTH-GLN-RXN
1 H+ + 1 ATP + 1 nicotinate_adenine_dinucleotide + 1 L-glutamine + 1 H2O → 1 AMP + 1 L-glutamate + 1 NAD+ + 1 diphosphate
Na+_proton_antiporter
1 Na+ + 2 H+$_{ex}$ → 1 Na+$_{ex}$ + 2 H+
O-antigen_synthesis–polymerization
1 dTDP-alpha-L-rhamnose → 1 H+ + 1 O-antigen + 1 dTDP
PHB_Na+_symport
1 PHB$_{ex}$ + 1 Na+$_{ex}$ → 1 Na+ + 1 PHB
RXN-10663-1.14.99.-
1 NADH + 1 |Palmitoyl-ACPs| → 1 NAD+ + 1 |Palmitoleoyl-ACPs|
UDP-GlcNAc_biosynthesis-5.4.2.10-5.4.2.10-RXN
1 D-glucosamine_1-phosphate ↔ 1 alpha-D-glucosamine-6-phosphate
UDP-N-acetyl-D-glucosamine_biosynthesis_I-2.3.1.157-2.3.1.157-RXN
1 acetyl-CoA + 1 D-glucosamine_1-phosphate → 1 coenzyme_A + 1 N-acetyl-alpha-D-glucosamine_1-phosphate + 1 H+
acetate_Na+_symport
1 acetate$_{ex}$ + 1 Na+$_{ex}$ → 1 Na+ + 1 acetate
acetate_fermentation-1.2.1.4-RXN0-3962
1 acetaldehyde + 1 NADP+ + 1 H2O → 1 acetate + 1 NADPH + 2 H+
acetate_fermentation-6.2.1.1-ACETATE–COA-LIGASE-RXN
1 acetate + 1 ATP + 1 coenzyme_A → 1 acetyl-CoA + 1 AMP + 1 diphosphate
acetyl-CoA_biosynthesis_(from_pyruvate)-1.2.4.1-RXN0-1134
1 H+ + 1 pyruvate + 1 lipoamide → 1 CO2 + 1 S-acetyldihydrolipoamide

Reaction name and equation
acetyl-CoA_biosynthesis_(from_pyruvate)-1.8.1.4-RXN0-1132
1 NAD+ + 1 dihydrolipoamide ↔ 1 NADH + 1 H+ + 1 lipoamide
acetyl-CoA_biosynthesis_(from_pyruvate)-2.3.1.12-RXN0-1133
1 acetyl-CoA + 1 dihydrolipoamide ↔ 1 coenzyme_A + 1 S-acetyldihydrolipoamide
acetyl_CoA_biosynthesis-1.2.1.18-RXN-2902
1 coenzyme_A + 1 malonate_semialdehyde + 1 NAD+ → 1 acetyl-CoA + 1 CO2 + 1 NADH
acetyl_CoA_biosynthesis-4.1.1.9-MALONYL-COA-DECARBOXYLASE-RXN
1 malonyl-CoA + 1 H+ ← 1 acetyl-CoA + 1 CO2
adenine_diffusion
1 adenine$_{ex}$ → 1 adenine
adenosylcobalamin_biosynthesis_I_(early_cobalt_insertion)-2.1.1.195-RXN-8764
1 cobalt-precorrin-5B + 1 S-adenosyl-L-methionine → 1 S-adenosyl-L-homocysteine + 1 cobalt-precorrin-6A + 2 H+
adenosylcobalamin_biosynthesis_I_(early_cobalt_insertion)-2.1.1.196-RXN-8767
1 cobalt-precorrin-7 + 2 H+ + 1 S-adenosyl-L-methionine → 1 S-adenosyl-L-homocysteine + 1 CO2 + 1 cobalt-precorrin-8x
adenosylcobalamin_biosynthesis_I_(early_cobalt_insertion)-3.7.1.12-RXN-8763
1 cobalt-precorrin-5A + 1 H2O → 1 acetaldehyde + 1 cobalt-precorrin-5B + 1 H+
adenosylcobalamin_biosynthesis_I_(early_cobalt_insertion)-6.3.5.11-RXN-8769
2 ATP + 1 cobyrinate + 2 L-glutamine + 2 H2O → 2 ADP + 1 cob(II)yrinate_a,c-diamide + 2 L-glutamate + 2 phosphate + 3 H+
adenosylcobalamin_biosynthesis_I_(early_cobalt_insertion)-cbiC-RXN-8768
1 cobalt-precorrin-8x → 1 cobyrinate
adenosylcobalamin_biosynthesis_I_(early_cobalt_insertion)-cbiJ-RXN-8765
1 cobalt-precorrin-6A + 1 NADPH + 1 H+ → 1 cobalt-precorrin-6B + 1 NADP+
aerobic_anoxygenic_photosynthesis–RC$_{ex}$ citation_and_electron_transfer
2 |Cytochromes-C2-Reduced| + 1 |Ubiquinones| + 2 photons + 2 H+ → 1 |Ubiquinols| + 2 |Cytochromes-C2-Oxidized|
aerobic_anoxygenic_photosynthesis–cytochrome_bc1
1 |Ubiquinols| + 2 |Cytochromes-C2-Oxidized| + 2 H+ → 1 |Ubiquinones| + 2 |Cytochromes-C2-Reduced| + 4 H+$_{ex}$
aerobic_respiration_–_electron_donor_II-1.10.2.2-1.10.2.2-RXN
2 |Cytochromes-C-Oxidized| + 1 |Ubiquinols| ↔ 2 H+ + 2 |Cytochromes-C-Reduced| + 1 |Ubiquinones|
aerobic_respiration_–_electron_donor_II-1.9.3.1-CYTOCHROME-C-OXIDASE-RXN
8 H+ + 1 oxygen + 4 |Cytochromes-C-Reduced| → 2 H2O + 4 |Cytochromes-C-Oxidized| + 4 H+$_{ex}$
alanine_metabolism-1.1.1.28-DLACTDEHYDROGNAD-RXN
1 (R)-lactate + 1 NAD+ ← 1 NADH + 1 H+ + 1 pyruvate
alanine_metabolism-1.1.1.59-3-HYDROXYPROPIONATE-DEHYDROGENASE-RXN
1 3-hydroxypropionate + 1 NAD+ → 1 malonate_semialdehyde + 1 NADH + 1 H+
alanine_metabolism-1.2.1.3-RXN-12331_NAD
1 3-aminopropanal + 1 H2O + 1 NAD+ ↔ 1 beta-alanine + 2 H+ + 1 NADH
alanine_metabolism-1.2.1.3-RXN-12331_NADP
1 3-aminopropanal + 1 H2O + 1 NADP+ ↔ 1 beta-alanine + 2 H+ + 1 NADPH
alanine_metabolism-1.3.1.2-1.3.1.2-RXN
1 5,6-dihydrouracil + 1 NADP+ ↔ 1 NADPH + 1 H+ + 1 uracil
alanine_metabolism-1.4.1.1-ALANINE-DEHYDROGENASE-RXN
1 L-alanine + 1 NAD+ + 1 H2O ↔ 1 ammonia + 1 NADH + 2 H+ + 1 pyruvate
alanine_metabolism-2.6.1.18-2.6.1.18-RXN
1 L-alanine + 1 malonate_semialdehyde ↔ 1 beta-alanine + 1 pyruvate
alanine_metabolism-2.6.1.21-D-ALANINE-AMINOTRANSFERASE-RXN
1 2-oxoglutarate + 1 D-alanine ↔ 1 D-glutamate + 1 pyruvate
alanine_metabolism-3.5.1.6-BETA-UREIDOPROPIONASE-RXN
1 3-ureidopropionate + 1 H+ + 1 H2O → 1 ammonia + 1 beta-alanine + 1 CO2
alanine_metabolism-3.5.2.2-DIHYDROPYRIMIDINASE-RXN
1 5,6-dihydrouracil + 1 H2O ↔ 1 3-ureidopropionate + 1 H+
alanine_metabolism-5.1.1.1-ALARACECAT-RXN
1 L-alanine ↔ 1 D-alanine
alpha-D-glucose_Na+_symport
1 alpha-D-glucose$_{ex}$ + 1 Na+$_{ex}$ → 1 Na+ + 1 alpha-D-glucose
alpha-D-xylopyranose_Na+_symport
1 alpha-D-xylopyranose$_{ex}$ + 1 Na+$_{ex}$ → 1 Na+ + 1 alpha-D-xylopyranose
alpha-L-rhamnose_Na+_symport
1 alpha-L-rhamnose$_{ex}$ + 1 Na+$_{ex}$ → 1 Na+ + 1 alpha-L-rhamnose
alpha-maltose_Na+_symport
1 alpha-maltose$_{ex}$ + 1 Na+$_{ex}$ → 1 Na+ + 1 alpha-maltose

Reaction name and equation
aminopropanol_phosphate_biosynthesis-4.1.1.81-4.1.1.81-RXN 1 L-threonine_O-3-phosphate → 1 CO2 + 1 (R)-1-amino-2-propanol_O-2-phosphate
aminopropanol_phosphate_biosynthesis-pduX-RXN-8626 1 ATP + 1 L-threonine → 1 ADP + 1 L-threonine_O-3-phosphate
ammonia_diffusion 1 ammonia$_{ex}$ → 1 ammonia
anaerobic_ubiquinone_biosynthesis-1.14.-.–RXN-9236 1 6-methoxy-3-methyl-2-all-trans-decaprenyl-1,4-benzoquinol + 1 H2O + 1 NADPH → 1 3-demethylubiquinol-10 + 1 NADP+ + 3 H+
anaerobic_ubiquinone_biosynthesis-1.14.13.–RXN-9232 1 2-decaprenylphenol + 1 NADPH + 1 H2O → 1 3-(all-trans-decaprenyl)benzene-1,2-diol + 1 NADP+ + 3 H+
anaerobic_ubiquinone_biosynthesis-1.14.13.–RXN-9234 1 2-methoxy-6-(all-trans-decaprenyl)phenol + 1 NADPH + 1 H2O → 1 2-methoxy-6-all_trans-decaprenyl-2-methoxy-1,4-benzoquinol + 1 NADP+ + 3 H+
anapleurotic_synthesis_of_oxalacetate-6.4.1.1-PYRUVATE-CARBOXYLASE-RXN 1 ATP + 1 bicarbonate + 1 pyruvate → 1 ADP + 1 oxaloacetate + 1 phosphate + 1 H+
arginine_metabolism-1.2.1.38-N-ACETYLGLUTPREDUCT-RXN 1 N-acetyl-L-glutamate_5-semialdehyde + 1 NADP+ + 1 phosphate ↔ 1 N-acetylglutamyl-phosphate + 1 NADPH + 1 H+
arginine_metabolism-2.3.1.1-N-ACETYLTRANSFER-RXN 1 acetyl-CoA + 1 L-glutamate → 1 N-acetyl-L-glutamate + 1 coenzyme_A + 1 H+
arginine_metabolism-2.3.1.35-GLUTAMATE-N-ACETYLTRANSFERASE-RXN 1 L-glutamate + 1 N-acetyl-L-ornithine → 1 N-acetyl-L-glutamate + 1 L-ornithine
arginine_metabolism-2.6.1.11-ACETYLORNTRANSAM-RXN 1 2-oxoglutarate + 1 N-acetyl-L-ornithine ↔ 1 N-acetyl-L-glutamate_5-semialdehyde + 1 L-glutamate
arginine_metabolism-2.7.2.8-ACETYLGLUTKIN-RXN 1 N-acetyl-L-glutamate + 1 ATP → 1 ADP + 1 N-acetylglutamyl-phosphate
arginine_metabolism-3.5.3.6-ARGININE-DEIMINASE-RXN 1 L-arginine + 1 H2O ↔ 1 ammonia + 1 L-citrulline + 1 H+
arginine_metabolism-4.3.1.12-ORNITHINE-CYCLODEAMINASE-RXN 1 L-ornithine → 1 ammonium + 1 L-proline
arginine_metabolism-6.3.5.5-CARBPSYN-RXN 2 ATP + 1 L-glutamine + 1 bicarbonate + 1 H2O → 2 ADP + 1 carbamoyl-phosphate + 1 L-glutamate + 1 phosphate + 2 H+
bacteriochlorophyll_a_biosynthesis-BchX-RXN-8786 1 3-hydroxyethylchlorophyllide_a + 2 H+ → 1 2-desacetyl-2-hydroxyethyl_bacteriochlorophyllide_a,
bacteriochlorophyll_a_biosynthesis-BchX-RXN-8792 1 ATP + 1 chlorophyllide_a + 1 H+ + 1 H2O → 1 ADP + 1 3-vinyl-bacteriochlorophyllide_a + 1 phosphate
bacteriochlorophyll_a_biosynthesis-BchY-RXN-8786 1 3-hydroxyethylchlorophyllide_a + 2 H+ → 1 2-desacetyl-2-hydroxyethyl_bacteriochlorophyllide_a,
bacteriochlorophyll_a_biosynthesis-BchY-RXN-8792 1 ATP + 1 chlorophyllide_a + 1 H+ + 1 H2O → 1 ADP + 1 3-vinyl-bacteriochlorophyllide_a + 1 phosphate
bacteriochlorophyll_a_biosynthesis-BchZ-RXN-8786 1 3-hydroxyethylchlorophyllide_a + 2 H+ → 1 2-desacetyl-2-hydroxyethyl_bacteriochlorophyllide_a,
bacteriochlorophyll_a_biosynthesis-BchZ-RXN-8792 1 ATP + 1 chlorophyllide_a + 1 H+ + 1 H2O → 1 ADP + 1 3-vinyl-bacteriochlorophyllide_a + 1 phosphate
bacteriochlorophyll_a_biosynthesis-bchC-RXN-8787 1 2-desacetyl-2-hydroxyethyl_bacteriochlorophyllide_a, → 1 bacteriochlorophyllide_a + 2 H+
bacteriochlorophyll_a_biosynthesis-bchF-RXN-8785 1 chlorophyllide_a + 1 H2O → 1 3-hydroxyethylchlorophyllide_a
bacteriochlorophyll_a_biosynthesis-bchF-RXN-8793 1 3-vinyl-bacteriochlorophyllide_a + 1 H2O → 1 2-desacetyl-2-hydroxyethyl_bacteriochlorophyllide_a,
bacteriochlorophyll_a_biosynthesis-bchG-RXN-8788 1 bacteriochlorophyllide_a + 1 all-trans-geranyl-geranyl_diphosphate + 1 H+ → 1 geranylgeranyl-bacteriochlorophyll_a + 1 diphosphate
bacteriochlorophyll_a_biosynthesis-bchP-RXN-8789 1 geranylgeranyl-bacteriochlorophyll_a + 1 NADPH + 1 H+ → 1 dihydrogeranylgeranyl-bacteriochlorophyll_a + 1 NADP+

Reaction name and equation
bacteriochlorophyll_a_biosynthesis-bchP-RXN-8790
1 dihydrogeranylgeranyl-bacteriochlorophyll_a + 1 NADPH + 1 H+ → 1 tetrahydrogeranylgeranyl-bacteriochlorophyll_a + 1 NADP+
bacteriochlorophyll_a_biosynthesis-bchP-RXN-8791
1 tetrahydrogeranylgeranyl-bacteriochlorophyll_a + 1 NADPH + 1 H+ → 1 bacteriochlorophyll_a + 1 NADP+
beta-D-fructofuranose_Na+_symport
1 beta-D-fructofuranose$_{ex}$ + 1 Na+$_{ex}$ → 1 Na+ + 1 beta-D-fructofuranose
beta-D-glucose_Na+_symport
1 beta-D-glucose$_{ex}$ + 1 Na+$_{ex}$ → 1 Na+ + 1 beta-D-glucose
beta-D-ribofuranose_Na+_symport
1 beta-D-ribofuranose$_{ex}$ + 1 Na+$_{ex}$ → 1 Na+ + 1 beta-D-ribofuranose
branched-chain_alpha-keto_acid_dehydrogenase_complex-1.8.1.4-RXN-7719
1 NAD+ + 1 dihydrolipoamide ↔ 1 NADH + 1 H+ + 1 lipoamide
carnitine_degradation_I-4.2.1.–RXN0-3561
1 L-carnitinyl-CoA → 1 crotonobetainyl-CoA + 1 H2O
chlorophyll_metabolism-1.14.13.81-RXN-5282
1 magnesium-protoporphyrin_IX_13-monomethyl_ester + 1 NADPH + 1 oxygen + 1 H+ → 1 131-hydroxy-magnesium-protoporphyrin_IX_13-monomethyl_ester + 1 NADP+ + 1 H2O
chlorophyll_metabolism-1.14.13.81-RXN-5283
1 131-hydroxy-magnesium-protoporphyrin_IX_13-monomethyl_ester + 1 NADPH + 1 oxygen + 1 H+ → 1 131-oxo-magnesium-protoporphyrin_IX_13-monomethyl_ester + 1 NADP+ + 2 H2O
chlorophyll_metabolism-1.14.13.81-RXN-5284
1 131-oxo-magnesium-protoporphyrin_IX_13-monomethyl_ester + 1 NADPH + 1 oxygen + 1 H+ → 1 divinyl_protochlorophyllide_a + 1 NADP+ + 2 H2O
chlorophyll_metabolism-1.3.1.33-RXN1F-10
1 chlorophyllide_a + 1 NADP+ ← 1 monovinyl_protochlorophyllide_a + 1 NADPH + 1 H+
chlorophyll_metabolism-1.3.1.75-RXN1F-72
1 divinyl_protochlorophyllide_a + 1 NADPH + 1 H+ → 1 monovinyl_protochlorophyllide_a + 1 NADP+
chlorophyll_metabolism-2.1.1.11-RXN-MG-PROTOPORPHYRIN-METHYLESTER-SYN
1 Mg-protoporphyrin + 1 S-adenosyl-L-methionine → 1 S-adenosyl-L-homocysteine + 1 magnesium-protoporphyrin_IX_13-monomethyl_ester
chlorophyll_metabolism-6.6.1.1-RXN1F-20
1 ATP + 1 Mg2+ + 1 protoporphyrin_IX + 1 H2O → 1 ADP + 1 Mg-protoporphyrin + 1 phosphate + 3 H+
chlorophyllide_a_biosynthesis_II-1.14.13.–RXN-8797
1 magnesium-protoporphyrin_IX_13-monomethyl_ester + 1 NADPH + 1 H2O → 1 131-hydroxy-magnesium-protoporphyrin_IX_13-monomethyl_ester + 1 NADP+ + 3 H+
chlorophyllide_a_biosynthesis_II-1.14.13.–RXN-8798
1 131-hydroxy-magnesium-protoporphyrin_IX_13-monomethyl_ester + 1 NADPH → 1 131-oxo-magnesium-protoporphyrin_IX_13-monomethyl_ester + 1 NADP+ + 3 H+
chlorophyllide_a_biosynthesis_II-1.14.13.–RXN-8799
1 131-oxo-magnesium-protoporphyrin_IX_13-monomethyl_ester + 1 NADPH → 1 divinyl_protochlorophyllide_a + 1 NADP+ + 3 H+
chorismate_metabolism-1.1.1.25-SHIKIMATE-5-DEHYDROGENASE-RXN
1 NADP+ + 1 shikimate ↔ 1 3-dehydroshikimate + 1 NADPH + 1 H+
chorismate_metabolism-2.5.1.19-2.5.1.19-RXN
1 phosphoenolpyruvate + 1 shikimate-3-phosphate ↔ 1 5-enolpyruvyl-shikimate-3-phosphate + 1 phosphate
chorismate_metabolism-2.5.1.54-DAHPSYN-RXN
1 D-erythrose-4-phosphate + 1 phosphoenolpyruvate + 1 H2O → 1 3-deoxy-D-arabino-heptulosonate-7-phosphate + 1 phosphate
chorismate_metabolism-2.7.1.71-SHIKIMATE-KINASE-RXN
1 ATP + 1 shikimate → 1 ADP + 1 H+ + 1 shikimate-3-phosphate
chorismate_metabolism-4.2.1.10-3-DEHYDROQUINATE-DEHYDRATASE-RXN
1 3-dehydroquinate ↔ 1 3-dehydroshikimate + 1 H2O
chorismate_metabolism-4.2.3.4-3-DEHYDROQUINATE-SYNTHASE-RXN
1 3-deoxy-D-arabino-heptulosonate-7-phosphate → 1 3-dehydroquinate + 1 phosphate
chorismate_metabolism-4.2.3.5-CHORISMATE-SYNTHASE-RXN
1 5-enolpyruvyl-shikimate-3-phosphate → 1 chorismate + 1 phosphate
cis-vaccenate_biosynthesis-RXN-9558
1 NADPH + 1 H+ + 1 |cis-vaccen-2-enoyl-ACPs| → 1 NADP+ + 1 |Cis-vaccenoyl-ACPs|
citrate_Na+_symport
1 citrate$_{ex}$ + 1 Na+$_{ex}$ → 1 Na+ + 1 citrate
citric_acid_cycle-1.1.1.42-ISOCITDEH-RXN

Reaction name and equation
1 NADP+ + 1 D-threo-isocitrate → 1 2-oxoglutarate + 1 CO2 + 1 NADPH
citric_acid_cycle-1.3.5.1-SUCCINATE-DEHYDROGENASE-UBIQUINONE-RXN
1 succinate + 1 |Ubiquinones| ↔ 1 fumarate + 1 |Ubiquinols|
citric_acid_cycle-1.3.99.1-SUCC-FUM-OXRED-RXN
1 succinate + 1 FAD ↔ 1 fumarate + 1 FADH2
citric_acid_cycle-2.3.3.1-CITSYN-RXN
1 acetyl-CoA + 1 oxaloacetate + 1 H2O ↔ 1 citrate + 1 coenzyme_A + 1 H+
citric_acid_cycle-2.3.3.9-MALSYN-RXN
1 acetyl-CoA + 1 glyoxylate + 1 H2O → 1 coenzyme_A + 1 (S)-malate + 1 H+
citric_acid_cycle-2.8.3.5-RXNI-2
1 acetoacetate + 1 succinyl-CoA ↔ 1 acetoacetyl-CoA + 1 succinate
citric_acid_cycle-4.1.3.1-ISOCIT-CLEAV-RXN
1 D-threo-isocitrate ↔ 1 glyoxylate + 1 succinate
citric_acid_cycle-4.1.3.34-RXN-7929
1 (3S)-citryl-CoA ↔ 1 acetyl-CoA + 1 oxaloacetate
citric_acid_cycle-4.2.1.2-FUMHYDR-RXN
1 (S)-malate ↔ 1 fumarate + 1 H2O
citric_acid_cycle-4.2.1.3-ACONITATEDEHYDR-RXN
1 citrate ↔ 1 cis-aconitate + 1 H2O
citric_acid_cycle-4.2.1.3-ACONITATEHYDR-RXN
1 cis-aconitate + 1 H2O ↔ 1 D-threo-isocitrate
citric_acid_cycle-6.2.1.5-SUCCCOASYN-RXN
1 ATP + 1 coenzyme_A + 1 succinate ↔ 1 ADP + 1 phosphate + 1 succinyl-CoA
coenzyme_A_metabolism-2.7.1.24-DEPHOSPHOCOAKIN-RXN
1 ATP + 1 dephospho-CoA → 1 ADP + 1 coenzyme_A + 1 H+
coenzyme_A_metabolism-2.7.1.33-PANTOTHENATE-KIN-RXN
1 ATP + 1 (R)-pantothenate → 1 D-4′-phosphopantothenate + 1 ADP + 1 H+
coenzyme_A_metabolism-2.7.7.3-PANTEPADENYLYLTRAN-RXN
1 ATP + 1 4′-phosphopantetheine + 1 H+ → 1 dephospho-CoA + 1 diphosphate
coenzyme_A_metabolism-4.1.1.36-P-PANTOCYSDECARB-RXN
1 H+ + 1 R-4′-phosphopantothenoyl-L-cysteine → 1 CO2 + 1 4′-phosphopantetheine
coenzyme_A_metabolism-6.3.2.5-P-PANTOCYSLIG-RXN
1 D-4′-phosphopantothenate + 1 CTP + 1 L-cysteine → 1 CMP + 1 diphosphate + 1 H+ + 1 R-4′-phosphopantothenoyl-L-cysteine
conversions-1.11.1.6-CATAL-RXN
2 hydrogen_peroxide → 1 oxygen + 2 H2O
conversions-2.1.1.64-RXN-9237
1 3-demethylubiquinol-10 + 1 S-adenosyl-L-methionine → 1 S-adenosyl-L-homocysteine + 1 ubiquinol-10 + 1 H+
conversions-3.6.1.–RXN0-385
1 dGTP + 1 H2O → 1 dGMP + 1 diphosphate + 1 H+
conversions-3.6.1.1-INORGPYROPHOSPHAT-RXN
1 diphosphate + 1 H2O → 2 phosphate + 1 H+
cyanate_degradation-4.2.1.1-RXN0-5224
1 bicarbonate + 1 H+ ↔ 1 CO2 + 1 H2O
cysteine_metabolism-2.3.1.30-SERINE-O-ACETTRAN-RXN
1 acetyl-CoA + 1 L-serine ↔ 1 O-acetyl-L-serine + 1 coenzyme_A
cysteine_metabolism-2.5.1.47-ACSERLY-RXN
1 O-acetyl-L-serine + 1 hydrogen_sulfide ↔ 1 acetate + 1 L-cysteine + 1 H+
cysteine_metabolism-2.5.1.49-ACETYLHOMOSER-CYS-RXN
1 O-acetyl-L-homoserine + 1 hydrogen_sulfide ↔ 1 acetate + 1 L-homocysteine + 1 H+
cytosine_diffusion
1 cytosine_{ex} → 1 cytosine
d-mannose_degradation-2.7.7.22-MANNPGUANYLTRANGDP-RXN
1 GDP + 1 alpha-D-mannose_1-phosphate + 1 H+ ↔ 1 GDP-alpha-D-mannose + 1 phosphate
d-mannose_degradation-4.2.1.47-GDPMANDEHYDRA-RXN
1 GDP-alpha-D-mannose → 1 GDP-4-dehydro-6-deoxy-D-mannose + 1 H2O
d-mannose_degradation-5.4.2.8-PHOSMANMUT-RXN
1 alpha-D-mannose_1-phosphate ↔ 1 D-mannose_6-phosphate
d-xylose_degradation-5.3.1.5-XYLISOM-RXN
1 alpha-D-xylopyranose ↔ 1 D-xylulose
dTDPLrhamnose_biosynthesis-1.1.1.133-DTDPDEHYRHAMREDUCT-RXN
1 dTDP-alpha-L-rhamnose + 1 NADP+ ↔ 1 dTDP-4-dehydro-6-deoxy-beta-L-mannose + 1 NADPH + 1 H+
dTDPLrhamnose_biosynthesis-2.7.7.24-DTDPGLUCOSEPP-RXN
1 alpha-D-glucose_1-phosphate + 1 H+ + 1 dTTP ↔ 1 dTDP-alpha-D-glucose + 1 diphosphate
dTDPLrhamnose_biosynthesis-4.2.1.46-DTDPGLUCDEHYDRAT-RXN

Reaction name and equation
1 dTDP-alpha-D-glucose ↔ 1 dTDP-4-dehydro-6-deoxy-alpha-D-glucose + 1 H2O
dTDPLrhamnose_biosynthesis-5.1.3.13-DTDPDEHYDRHAMEPIM-RXN
1 dTDP-4-dehydro-6-deoxy-alpha-D-glucose ↔ 1 dTDP-4-dehydro-6-deoxy-beta-L-mannose
de_novo_biosynthesis_of_pyrimidine_deoxyribonucleotides-1.17.4.1-CDPREDUCT-RXN
1 dCDP + 1 H2O + 1 |Ox-Thioredoxin| ← 2 H+ + 1 CDP + 1 |Red-Thioredoxin|
de_novo_biosynthesis_of_pyrimidine_deoxyribonucleotides-1.17.4.1-UDPREDUCT-RXN
1 dUDP + 1 H2O + 1 |Ox-Thioredoxin| ← 2 H+ + 1 UDP + 1 |Red-Thioredoxin|
degradation_of_hexoses-2.7.1.5-RHAMNULOKIN-RXN
1 ATP + 1 L-rhamnulose → 1 ADP + 1 H+ + 1 L-rhamnulose-1-phosphate
degradation_of_hexoses-4.1.2.19-RHAMNULPALDOL-RXN
1 L-rhamnulose-1-phosphate ↔ 1 dihydroxyacetone_phosphate + 1 L-lactaldehyde
degradation_of_hexoses-5.3.1.14-RHAMNISOM-RXN
1 alpha-L-rhamnose ↔ 1 L-rhamnulose
degradation_of_hexoses-5.3.1.8-MANNPISOM-RXN
1 D-mannose_6-phosphate ↔ 1 D-fructose-6-phosphate
degradation_of_pentoses-2.7.1.47-D-RIBULOKIN-RXN
1 ATP + 1 D-ribulose → 1 ADP + 1 H+ + 1 D-ribulose-5-phosphate
degradation_of_sugar_alcohols-1.1.1.56-RIBITOL-2-DEHYDROGENASE-RXN
1 NAD+ + 1 D-ribitol → 1 D-ribulose + 1 NADH + 1 H+
degradation_of_sugar_alcohols-1.1.1.9-D-XYLULOSE-REDUCTASE-RXN
1 NAD+ + 1 D-xylitol ↔ 1 D-xylulose + 1 NADH + 1 H+
degradation_of_sugar_alcohols-2.7.1.17-XYLULOKIN-RXN
1 ATP + 1 D-xylulose → 1 ADP + 1 H+ + 1 D-xylulose-5-phosphate
degradation_of_sugar_alcohols-2.7.1.30-GLYCEROL-KIN-RXN
1 ATP + 1 glycerol → 1 ADP + 1 sn-glycerol-3-phosphate + 1 H+
dimethylsulfoniopropionate_Na+_symport
1 dimethylsulfoniopropionate$_{ex}$ + 1 Na+$_{ex}$ → 1 Na+ + 1 dimethylsulfoniopropionate
ethanol_Na+_symport
1 ethanol$_{ex}$ + 1 Na+$_{ex}$ → 1 Na+ + 1 ethanol
ethanol_fermentation-1.1.1.1-ALCOHOL-DEHYDROG-RXN
1 ethanol + 1 NAD+ ↔ 1 acetaldehyde + 1 NADH + 1 H+
fatty_acid__elongation_–_unsaturated-4.2.1.60-FABAUNSATDEHYDR-RXN
1 |Beta-hydroxydecanoyl-ACPs| ↔ 1 H2O + 1 |Trans-D2-decenoyl-ACPs|
fatty_acid_biosynthesis_-_initial_steps_I-2.3.1.41-3-OXOACYL-ACP-SYNTH-BASE-RXN
1 ACETYL-ACP + 1 MALONYL-ACP → 1 ACP + 1 CO2 + 1 |Acetoacetyl-ACPs|
fatty_acid_biosynthesis_-_initial_steps_II_(plant)-2.3.1.180-2.3.1.180-RXN
1 acetyl-CoA + 1 MALONYL-ACP → 1 CO2 + 1 coenzyme_A + 1 |Acetoacetyl-ACPs|
fatty_acid_biosynthesis_-_initial_steps_II_(plant)-2.3.1.39-MALONYL-COA-ACP-TRANSACYL-RXN
1 ACP + 1 malonyl-CoA + 1 H+ ↔ 1 coenzyme_A + 1 MALONYL-ACP
fatty_acid_elongation_–_saturated-1.1.1.100-3-OXOACYL-ACP-REDUCT-RXN
1 NADP+ + 1 OH-ACYL-ACP ↔ 1 B-KETOACYL-ACP + 1 NADPH + 1 H+
fatty_acid_elongation_–_saturated-1.3.1.9-ENOYL-ACP-REDUCT-NADH-RXN
1 NAD+ + 1 |Saturated-Fatty-Acyl-ACPs| ← 1 NADH + 1 H+ + 1 TRANS-D2-ENOYL-ACP
fatty_acid_elongation_–_saturated-2.3.1.41-3-OXOACYL-ACP-SYNTH-RXN
1 MALONYL-ACP + 1 |Saturated-Fatty-Acyl-ACPs| → 1 ACP + 1 B-KETOACYL-ACP + 1 CO2
fatty_acid_elongation_–_saturated-4.2.1.–3-HYDROXYDECANOYL-ACP-DEHYDR-RXN
1 OH-ACYL-ACP ↔ 1 TRANS-D2-ENOYL-ACP + 1 H2O
flagellar_motor_proton_flux
1 H+$_{ex}$ → 1 H+
flavin_biosynthesis-1.1.1.193-RIBOFLAVINSYNREDUC-RXN
1 5-amino-6-(5-phospho-D-ribitylamino)uracil + 1 NADP+ ← 1 5-amino-6-(5-phospho-D-ribosylamino)uracil + 1 NADPH + 1 H+
flavin_biosynthesis-2.5.1.78-LUMAZINESYN-RXN
1 5-amino-6-(D-ribitylamino)uracil + 1 1-deoxy-L-glycero-tetrulose_4-phosphate → 1 6,7-dimethyl-8-(1-D-ribityl)lumazine + 1 phosphate + 1 H+ + 2 H2O
flavin_biosynthesis-2.5.1.9-RIBOFLAVIN-SYN-RXN
2 6,7-dimethyl-8-(1-D-ribityl)lumazine + 1 H+ → 1 5-amino-6-(D-ribitylamino)uracil + 1 riboflavin
flavin_biosynthesis-2.7.1.26-RIBOFLAVINKIN-RXN
1 ATP + 1 riboflavin → 1 ADP + 1 FMN + 1 H+
flavin_biosynthesis-2.7.7.2-FADSYN-RXN
1 ATP + 1 FMN + 2 H+ → 1 FAD + 1 diphosphate
flavin_biosynthesis-3.5.4.25-GTP-CYCLOHYDRO-II-RXN
1 GTP + 3 H2O → 1 2,5-diamino-6-(5-phospho-D-ribosylamino)pyrimidin-4(3H)-one + 1 formate + 1 diphosphate + 2 H+

Reaction name and equation
flavin_biosynthesis-3.5.4.26-RIBOFLAVINSYNDEAM-RXN
1 2,5-diamino-6-(5-phospho-D-ribosylamino)pyrimidin-4(3H)-one + 1 H2O → 1 ammonia + 1 5-amino-6-(5-phospho-D-ribosylamino)uracil
flavin_biosynthesis-4.1.99.12-DIOHBUTANONEPSYN-RXN
1 D-ribulose-5-phosphate → 1 1-deoxy-L-glycero-tetrulose_4-phosphate + 1 formate + 1 H+
flavin_biosynthesis-RIBOPHOSPHAT-RXN
1 5-amino-6-(5-phospho-D-ribitylamino)uracil + 1 H2O → 1 5-amino-6-(D-ribitylamino)uracil + 1 phosphate
formaldehyde_oxidation-1.1.1.284-RXN-2962_NAD
1 S-hydroxymethylglutathione + 1 NAD+ ↔ 1 S-formylglutathione + 1 H+ + 1 NADH
formaldehyde_oxidation-1.1.1.284-RXN-2962_NADP
1 S-hydroxymethylglutathione + 1 NADP+ ↔ 1 S-formylglutathione + 1 H+ + 1 NADPH
formaldehyde_oxidation-3.1.2.12-S-FORMYLGLUTATHIONE-HYDROLASE-RXN
1 S-formylglutathione + 1 H2O → 1 formate + 1 glutathione + 1 H+
formaldehyde_oxidation-RXN-2961-spontaneous
1 S-hydroxymethylglutathione ↔ 1 formaldehyde + 1 glutathione
fumarate_Na+_symport
1 fumarate$_{ex}$ + 1 Na+$_{ex}$ → 1 Na+ + 1 fumarate
glutamate_and_glutamine_metabolism-1.4.1.13-GLUTAMATESYN-RXN
2 L-glutamate + 1 NADP+ ← 1 2-oxoglutarate + 1 L-glutamine + 1 NADPH + 1 H+
glutamate_and_glutamine_metabolism-1.4.1.4-GLUTDEHYD-RXN
1 L-glutamate + 1 NADP+ + 1 H2O ↔ 1 2-oxoglutarate + 1 ammonia + 1 NADPH + 2 H+
glutamate_and_glutamine_metabolism-6.3.1.2-GLUTAMINESYN-RXN
1 ammonia + 1 ATP + 1 L-glutamate → 1 ADP + 1 L-glutamine + 1 phosphate
glutathione_metabolism-1.8.1.7-GLUTATHIONE-REDUCT-NADPH-RXN
2 glutathione + 1 NADP+ ← 1 NADPH + 1 glutathione_disulfide + 1 H+
glutathione_metabolism-6.3.2.2-GLUTCYSLIG-RXN
1 ATP + 1 L-cysteine + 1 L-glutamate → 1 ADP + 1 L-gamma-glutamylcysteine + 1 phosphate + 1 H+
glutathione_metabolism-6.3.2.3-GLUTATHIONE-SYN-RXN
1 ATP + 1 glycine + 1 L-gamma-glutamylcysteine → 1 ADP + 1 glutathione + 1 phosphate + 1 H+
glutathione_redox_reactions_I-1.11.1.9-GLUTATHIONE-PEROXIDASE-RXN
2 glutathione + 1 hydrogen_peroxide → 1 glutathione_disulfide + 2 H2O
glycerol_Na+_symport
1 glycerol$_{ex}$ + 1 Na+$_{ex}$ → 1 Na+ + 1 glycerol
glycerol_degradation_IV-1.1.5.3-RXN0-5258
1 sn-glycerol-3-phosphate + 1 |Ubiquinones| → 1 dihydroxyacetone_phosphate + 1 |Ubiquinols|
glycine_cleavage_complex-1.4.4.2-GCVP-RXN
1 glycine + 1 lipoamide → 1 AMINOMETHYLDIHYDROLIPOYL-GCVH + 1 CO2
glycine_cleavage_complex-1.8.1.4-RXN-8629
1 NAD+ + 1 dihydrolipoamide → 1 NADH + 1 H+ + 1 lipoamide
glycine_cleavage_complex-2.1.2.10-GCVT-RXN
1 AMINOMETHYLDIHYDROLIPOYL-GCVH + 1 tetrahydrofolate → 1 ammonia + 1 5,10-methylenetetrahydrofolate + 1 dihydrolipoamide
glycine_metabolism-1.1.3.15-RXN-969
1 glycolate + 1 oxygen → 1 glyoxylate + 1 hydrogen_peroxide
glycine_metabolism-1.4.3.19-1.4.3.19-RXN
1 glycine + 1 oxygen + 1 H2O → 1 ammonia + 1 glyoxylate + 1 hydrogen_peroxide + 1 H+
glycine_metabolism-2.6.1.45-SERINE–GLYOXYLATE-AMINOTRANSFERASE-RXN
1 glyoxylate + 1 L-serine → 1 glycine + 1 hydroxypyruvate
glycine_metabolism-2.6.1.45-SERINE-GLYOXYLATE-AMINOTRANSFERASE-RXN
1 glyoxylate + 1 L-serine → 1 glycine + 1 hydroxypyruvate
glycogen_metabolism-2.7.1.2-GLUCOKIN-RXN
1 ATP + 1 beta-D-glucose → 1 ADP + 1 beta-D-glucose-6-phosphate + 1 H+
glycogen_metabolism-5.4.2.2-PHOSPHOGLUCMUT-RXN
1 alpha-D-glucose_1-phosphate ↔ 1 alpha-D-glucose_6-phosphate
glycolate_Na+_symport
1 glycolate$_{ex}$ + 1 Na+$_{ex}$ → 1 Na+ + 1 glycolate
glycolate_and_glyoxylate_degradation-1.1.1.26-GLYCOLATE-REDUCTASE-RXN
1 glycolate + 1 NAD+ ↔ 1 glyoxylate + 1 NADH + 1 H+
glycolysis-1.2.1.12-GAPOXNPHOSPHN-RXN
1 D-glyceraldehyde-3-phosphate + 1 NAD+ + 1 phosphate ↔ 1 1,3-bisphospho-D-glycerate + 1 NADH + 1 H+
glycolysis-2.7.1.11-6PFRUCTPHOS-RXN
1 ATP + 1 D-fructose-6-phosphate → 1 ADP + 1 fructose-1,6-bisphosphate + 1 H+

Reaction name and equation
glycolysis-4.2.1.11-2PGADEHYDRAT-RXN
1 2-phospho-D-glycerate ↔ 1 phosphoenolpyruvate + 1 H2O
glycolysis-5.3.1.9-PGLUCISOM-RXN
1 beta-D-glucose-6-phosphate ↔ 1 D-fructose-6-phosphate
glycolysis-5.4.2.1-3PGAREARR-RXN
1 3-phospho-D-glycerate ↔ 1 2-phospho-D-glycerate
glyoxylate_Na+_symport
1 glyoxylate$_{ex}$ + 1 Na+$_{ex}$ → 1 Na+ + 1 glyoxylate
glyoxylate_diffusion
1 glyoxylate$_{ex}$ → 1 glyoxylate
guanosine_diffusion
1 guanosine$_{ex}$ → 1 guanosine
heme_biosynthesis_I-1.3.5.3-RXN0-6259
1 protoporphyrinogen_IX + 3 |Ubiquinones| → 1 protoporphyrin_IX + 3 |Ubiquinols|
heme_metabolism-1.3.3.4-PROTOPORGENOXI-RXN
3 oxygen + 1 protoporphyrinogen_IX → 3 hydrogen_peroxide + 1 protoporphyrin_IX
heme_metabolism-1.3.99.22-HEMN-RXN
1 coproporphyrinogen_III + 2 S-adenosyl-L-methionine → 2 CO2 + 2 5′-deoxyadenosine + 2 L-methionine + 1 protoporphyrinogen_IX
heme_metabolism-2.3.1.37-5-AMINOLEVULINIC-ACID-SYNTHASE-RXN
1 glycine + 1 H+ + 1 succinyl-CoA → 1 5-amino-levulinate + 1 CO2 + 1 coenzyme_A
heme_metabolism-2.5.1.61-OHMETHYLBILANESYN-RXN
4 porphobilinogen + 1 H2O ↔ 4 ammonia + 1 hydroxymethylbilane + 4 H+
heme_metabolism-4.1.1.37-UROGENDECARBOX-RXN
4 H+ + 1 uroporphyrinogen-III → 4 CO2 + 1 coproporphyrinogen_III
heme_metabolism-4.2.1.24-PORPHOBILSYNTH-RXN
2 5-amino-levulinate ↔ 1 porphobilinogen + 1 H+ + 2 H2O
heme_metabolism-4.2.1.75-UROGENIIISYN-RXN
1 hydroxymethylbilane ↔ 1 uroporphyrinogen-III + 1 H2O
heme_metabolism-4.99.1.1-PROTOHEMEFERROCHELAT-RXN
1 Fe2+ + 1 protoporphyrin_IX → 1 protoheme_IX + 2 H+
histidine_metabolism-1.1.1.23-HISTALDEHYD-RXN
1 histidinal + 1 NAD+ + 1 H2O → 1 L-histidine + 1 NADH + 2 H+
histidine_metabolism-1.1.1.23-HISTOLDEHYD-RXN
1 histidinol + 1 NAD+ ↔ 1 histidinal + 1 NADH + 1 H+
histidine_metabolism-2.4.2.–GLUTAMIDOTRANS-RXN
1 L-glutamine + 1 phosphoribulosylformimino-AICAR-P → 1 aminoimidazole_carboxamide_ribonucleotide + 1 D-erythro-imidazole-glycerol-phosphate + 1 L-glutamate + 1 H+
histidine_metabolism-2.4.2.17-ATPPHOSPHORIBOSYLTRANS-RXN
1 phosphoribosyl-ATP + 1 diphosphate ← 1 ATP + 1 5-phospho-alpha-D-ribose_1-diphosphate
histidine_metabolism-2.4.2.17-RXN-10968
1 phosphoribosyl-ATP + 1 diphosphate ← 1 ATP + 1 5-phospho-alpha-D-ribose_1-diphosphate
histidine_metabolism-2.6.1.9-HISTAMINOTRANS-RXN
1 L-glutamate + 1 imidazole_acetol-phosphate ↔ 1 2-oxoglutarate + 1 L-histidinol-phosphate
histidine_metabolism-2.7.6.1-PRPPSYN-RXN
1 ATP + 1 D-ribose-5-phosphate ↔ 1 AMP + 1 H+ + 1 5-phospho-alpha-D-ribose_1-diphosphate
histidine_metabolism-3.1.3.15-HISTIDPHOS-RXN
1 L-histidinol-phosphate + 1 H2O → 1 histidinol + 1 phosphate
histidine_metabolism-3.5.4.19-HISTCYCLOHYD-RXN
1 1-(5-phospho-D-ribosyl)-AMP + 1 H2O → 1 1-(5-phosphoribosyl)-5-[(5-phosphoribosylamino)methylideneamino]imidazole-4-carboxamide
histidine_metabolism-3.6.1.31-HISTPRATPHYD-RXN
1 phosphoribosyl-ATP + 1 H2O → 1 1-(5-phospho-D-ribosyl)-AMP + 1 diphosphate + 1 H+
histidine_metabolism-4.2.1.19-IMIDPHOSDEHYD-RXN
1 D-erythro-imidazole-glycerol-phosphate → 1 imidazole_acetol-phosphate + 1 H2O
histidine_metabolism-5.3.1.16-PRIBFAICARPISOM-RXN
1 1-(5-phosphoribosyl)-5-[(5-phosphoribosylamino)methylideneamino]imidazole-4-carboxamide → 1 phosphoribulosylformimino-AICAR-P
inosine_diffusion
1 inosine$_{ex}$ → 1 inosine
isoleucine_metabolism-1.1.1.86-ACETOOHBUTREDUCTOISOM-RXN
1 2,3-dihydroxy-3-methylvalerate + 1 NADP+ ↔ 1 2-aceto-2-hydroxy-butanoate + 1 NADPH + 1 H+

Reaction name and equation
isoleucine_metabolism-2.2.1.6-ACETOOHBUTSYN-RXN 1 2-oxobutanoate + 1 H+ + 1 pyruvate → 1 2-aceto-2-hydroxy-butanoate + 1 CO2
isoleucine_metabolism-2.6.1.42-BRANCHED-CHAINAMINOTRANSFERILEU-RXN 1 2-oxoglutarate + 1 L-isoleucine ↔ 1 2-keto-3-methyl-valerate + 1 L-glutamate
isoleucine_metabolism-4.2.1.9-DIHYDROXYMETVALDEHYDRAT-RXN 1 2,3-dihydroxy-3-methylvalerate → 1 2-keto-3-methyl-valerate + 1 H2O
isoprenid_biosynthesis-1.1.1.267-DXPREDISOM-RXN 1 2-C-methyl-D-erythritol-4-phosphate + 1 NADP+ ↔ 1 1-deoxy-D-xylulose_5-phosphate + 1 NADPH + 1 H+
isoprenid_biosynthesis-2.5.1.1-GPPSYN-RXN 1 dimethylallyl_diphosphate + 1 isopentenyl_diphosphate ↔ 1 geranyl_diphosphate + 1 diphosphate
isoprenid_biosynthesis-2.5.1.10-FPPSYN-RXN 1 isopentenyl_diphosphate + 1 geranyl_diphosphate ↔ 1 (2E,6E)-farnesyl_diphosphate + 1 diphosphate
isoprenid_biosynthesis-2.5.1.29-FARNESYLTRANSTRANSFERASE-RXN 1 isopentenyl_diphosphate + 1 (2E,6E)-farnesyl_diphosphate → 1 all-trans-geranyl-geranyl_diphosphate + 1 diphosphate
isoprenid_biosynthesis-2.5.1.32-2.5.1.32-RXN 2 all-trans-geranyl-geranyl_diphosphate → 1 prephytoene_diphosphate + 1 diphosphate
isoprenid_biosynthesis-2.7.1.148-2.7.1.148-RXN 1 4-(cytidine_5′-diphospho)-2-C-methyl-D-erythritol + 1 ATP → 1 2-phospho-4-(cytidine_5′-diphospho)-2-C-methyl-D-erythritol + 1 ADP + 1 H+
isoprenid_biosynthesis-2.7.7.60-2.7.7.60-RXN 1 2-C-methyl-D-erythritol-4-phosphate + 1 CTP + 1 H+ → 1 4-(cytidine_5′-diphospho)-2-C-methyl-D-erythritol + 1 diphosphate
isoprenid_biosynthesis-4.6.1.12-RXN0-302 1 2-phospho-4-(cytidine_5′-diphospho)-2-C-methyl-D-erythritol → 1 2-C-methyl-D-erythritol-2,4-cyclodiphosphate + 1 CMP
isoprenid_biosynthesis-5.3.3.2-IPPISOM-RXN 1 isopentenyl_diphosphate ↔ 1 dimethylallyl_diphosphate
leucine_metabolism-1.1.1.85-3-ISOPROPYLMALDEHYDROG-RXN 1 (2R,3S)-3-isopropylmalate + 1 NAD+ ↔ 1 (2S)-2-isopropyl-3-oxosuccinate + 1 NADH + 1 H+
leucine_metabolism-2.3.3.13-2-ISOPROPYLMALATESYN-RXN 1 2-oxoisovalerate + 1 acetyl-CoA + 1 H2O → 1 (2S)-2-isopropylmalate + 1 coenzyme_A + 1 H+
leucine_metabolism-2.6.1.42-BRANCHED-CHAINAMINOTRANSFERLEU-RXN 1 2-oxoglutarate + 1 L-leucine ↔ 1 4-methyl-2-oxopentanoate + 1 L-glutamate
leucine_metabolism-4.2.1.33-3-ISOPROPYLMALISOM-RXN 1 (2S)-2-isopropylmalate → 1 2-isopropylmaleate + 1 H2O
leucine_metabolism-4.2.1.33-RXN-8991 1 (2R,3S)-3-isopropylmalate ← 1 2-isopropylmaleate + 1 H2O
leucine_metabolism-RXN-7800-spontaneous 1 (2S)-2-isopropyl-3-oxosuccinate + 1 H+ → 1 4-methyl-2-oxopentanoate + 1 CO2
lipid-A-precursor_biosynthesis-2.3.1.129-UDPNACETYLGLUCOSAMACYLTRANS-RXN 1 UDP-alpha-N-acetyl-D-glucosamine + 1 |R-3-hydroxymyristoyl-ACPs| ↔ 1 ACP + 1 UDP-3-O-[(3R)-3-hydroxymyristoyl]-N-alpha-acetylglucosamine
lipid-A-precursor_biosynthesis-2.3.1.191-UDPHYDROXYMYRGLUCOSAMNACETYLTRANS-RXN 1 UDP-3-O-(3-hydroxymyristoyl)-alpha-D-glucosamine + 1 |R-3-hydroxymyristoyl-ACPs| ↔ 1 ACP + 1 UDP-2,3-bis[O-(3R)-3-hydroxymyristoyl]-alpha-D-glucosamine + 1 H+
lipid-A-precursor_biosynthesis-3.5.1.108-UDPACYLGLCNACDEACETYL-RXN 1 UDP-3-O-[(3R)-3-hydroxymyristoyl]-N-alpha-acetylglucosamine + 1 H2O → 1 acetate + 1 UDP-3-O-(3-hydroxymyristoyl)-alpha-D-glucosamine
lipid-A-precursor_biosynthesis-3.6.1.54-LIPIDXSYNTHESIS-RXN 1 UDP-2,3-bis[O-(3R)-3-hydroxymyristoyl]-alpha-D-glucosamine + 1 H2O → 1 2,3-bis[(3R)-3-hydroxymyristoyl]-alpha-D-glucosaminyl_1-phosphate + 2 H+ + 1 uridine-5′-phosphate
lipid_A_biosynthesis-2.4.1.182-LIPIDADISACCHARIDESYNTH-RXN 1 2,3-bis[(3R)-3-hydroxymyristoyl]-alpha-D-glucosaminyl_1-phosphate + 1 UDP-2,3-bis[O-(3R)-3-hydroxymyristoyl]-alpha-D-glucosamine → 1 lipid_A_disaccharide + 1 H+ + 1 UDP
lipid_A_biosynthesis-2.7.1.130-TETRAACYLDISACC4KIN-RXN 1 ATP + 1 lipid_A_disaccharide → 1 ADP + 1 lipid_IVA + 1 H+
lysine_metabolism-1.3.1.26-DIHYDROPICRED-RXN_NAD 1 (S)-2,3,4,5-tetrahydrodipicolinate + 1 NAD+ ← 1 (S)-2,3-dihydrodipicolinate + 1 H+ + 1 NADH

Reaction name and equation
lysine_metabolism-1.3.1.26-DIHYDROPICRED-RXN_NADP 1 (S)-2,3,4,5-tetrahydrodipicolinate + 1 NADP+ ← 1 (S)-2,3-dihydrodipicolinate + 1 H+ + 1 NADPH
lysine_metabolism-2.3.1.117-TETHYDPICSUCC-RXN 1 (S)-2,3,4,5-tetrahydrodipicolinate + 1 succinyl-CoA + 1 H2O ↔ 1 coenzyme_A + 1 N-succinyl-2-amino-6-ketopimelate
lysine_metabolism-2.6.1.17-SUCCINYLDIAMINOPIMTRANS-RXN 1 2-oxoglutarate + 1 N-succinyl-L,L-2,6-diaminopimelate ↔ 1 L-glutamate + 1 N-succinyl-2-amino-6-ketopimelate
lysine_metabolism-3.5.1.18-SUCCDIAMINOPIMDESUCC-RXN 1 N-succinyl-L,L-2,6-diaminopimelate + 1 H2O ↔ 1 L,L-diaminopimelate + 1 succinate
lysine_metabolism-4.1.1.20-DIAMINOPIMDECARB-RXN 1 meso-diaminopimelate + 1 H+ → 1 CO2 + 1 L-lysine
lysine_metabolism-4.2.1.52-DIHYDRODIPICSYN-RXN 1 L-aspartate-semialdehyde + 1 pyruvate ↔ 1 (S)-2,3-dihydrodipicolinate + 1 H+ + 2 H2O
lysine_metabolism-5.1.1.7-DIAMINOPIMEPIM-RXN 1 L,L-diaminopimelate ↔ 1 meso-diaminopimelate
metabolism_of_disaccharids-2.7.1.4-FRUCTOKINASE-RXN 1 ATP + 1 beta-D-fructofuranose → 1 ADP + 1 D-fructose-6-phosphate + 1 H+
methionine_metabolism-2.1.1.13-HOMOCYSMETB12-RXN 1 5-methyl-tetrahydrofolate + 1 L-homocysteine → 1 L-methionine + 1 tetrahydrofolate
methionine_metabolism-2.3.1.46-HOMSUCTRAN-RXN 1 L-homoserine + 1 succinyl-CoA → 1 coenzyme_A + 1 O-succinyl-L-homoserine
methionine_metabolism-2.5.1.48-O-SUCCHOMOSERLYASE-RXN 1 L-cysteine + 1 O-succinyl-L-homoserine → 1 L-cystathionine + 1 H+ + 1 succinate
methionine_metabolism-2.5.1.6-S-ADENMETSYN-RXN 1 ATP + 1 L-methionine + 1 H2O → 1 phosphate + 1 diphosphate + 1 S-adenosyl-L-methionine
methionine_metabolism-3.3.1.1-ADENOSYLHOMOCYSTEINASE-RXN 1 S-adenosyl-L-homocysteine + 1 H2O ↔ 1 adenosine + 1 L-homocysteine
methionine_metabolism-4.4.1.8-CYSTATHIONINE-BETA-LYASE-RXN 1 L-cystathionine + 1 H2O ↔ 1 ammonia + 1 L-homocysteine + 1 H+ + 1 pyruvate
methylerythritol_phosphate_pathway-1.17.1.2-ISPH2-RXN_NAD 1 isopentenyl_diphosphate + 1 H2O + 1 NAD+ ← 1 1-hydroxy-2-methyl-2-(E)-butenyl_4-diphosphate + 1 H+ + 1 NADH
methylerythritol_phosphate_pathway-1.17.1.2-ISPH2-RXN_NADP 1 isopentenyl_diphosphate + 1 H2O + 1 NADP+ ← 1 1-hydroxy-2-methyl-2-(E)-butenyl_4-diphosphate + 1 H+ + 1 NADPH
methylerythritol_phosphate_pathway-1.17.1.2-RXN0-884_NAD 1 dimethylallyl_diphosphate + 1 H2O + 1 NAD+ ← 1 1-hydroxy-2-methyl-2-(E)-butenyl_4-diphosphate + 1 H+ + 1 NADH
methylerythritol_phosphate_pathway-1.17.1.2-RXN0-884_NADP 1 dimethylallyl_diphosphate + 1 H2O + 1 NADP+ ← 1 1-hydroxy-2-methyl-2-(E)-butenyl_4-diphosphate + 1 H+ + 1 NADPH
methylerythritol_phosphate_pathway-1.17.7.1-RXN0-882 3 H+ + 1 1-hydroxy-2-methyl-2-(E)-butenyl_4-diphosphate + 1 H2O + 2 |Oxidized-flavodoxins| ← 1 2-C-methyl-D-erythritol-2,4-cyclodiphosphate + 2 |Reduced-flavodoxins|
methylglyoxal_degradation_V-1.1.2.3-L-LACTATE-DEHYDROGENASE-CYTOCHROME-RXN 1 (S)-lactate + 2 |Cytochromes-C-Oxidized| → 2 H+ + 1 pyruvate + 2 |Cytochromes-C-Reduced|
methylglyoxal_degradation_VI-1.1.2.4-D-LACTATE-DEHYDROGENASE-CYTOCHROME-RXN 1 (R)-lactate + 2 |Cytochromes-C-Oxidized| → 2 H+ + 1 pyruvate + 2 |Cytochromes-C-Reduced|
myo-inositol_Na+_symport 1 myo-inositol$_{ex}$ + 1 Na+$_{ex}$ → 1 Na+ + 1 myo-inositol
myo-inositol_biosynthesis-1.1.1.18-MYO-INOSITOL-2-DEHYDROGENASE-RXN 1 myo-inositol + 1 NAD+ → 1 2-keto-myo-inositol + 1 NADH + 1 H+
myo-inositol_degradation-2.7.1.92-5-DEHYDRO-2-DEOXYGLUCONOKINASE-RXN 1 ATP + 1 5-dehydro-2-deoxy-D-gluconate → 1 ADP + 1 5-dehydro-2-deoxy-D-gluconate_6-phosphate + 1 H+
myo-inositol_degradation-3.7.1.–R503-RXN 1 D-2,3-diketo-4-deoxy-epi-inositol + 1 H2O → 1 5-dehydro-2-deoxy-D-gluconate + 1 H+
myo-inositol_degradation-4.1.2.29-4.1.2.29-RXN 1 5-dehydro-2-deoxy-D-gluconate_6-phosphate → 1 dihydroxyacetone_phosphate + 1 malonate_semialdehyde

Reaction name and equation
myo-inositol_degradation-4.2.1.44-MYO-INOSOSE-2-DEHYDRATASE-RXN
1 2-keto-myo-inositol → 1 D-2,3-diketo-4-deoxy-epi-inositol + 1 H2O
nitrate_diffusion
1 $nitrate_{ex}$ → 1 nitrate
nitrate_reduction_I_(denitrification)-1.7.2.4-RXN-12130
1 N2 + 1 H2O + 2 |Cytochromes-C-Oxidized| ↔ 2 H+ + 1 nitrous_oxide + 2 |Cytochromes-C-Reduced|
nitrate_reduction_I_(denitrification)-1.7.2.5-NITRIC-OXIDE-REDUCTASE-RXN
1 nitrous_oxide + 1 H2O + 2 |Cytochromes-C-Oxidized| ↔ 2 nitric_oxide + 2 H+ + 2 |Cytochromes-C-Reduced|
oxidative_phosphorylation-3.6.3.14-ATPSYN-RXN
1 ATP + 3 H+ + 1 H2O ↔ 1 ADP + 1 phosphate + 4 $H+_{ex}$
oxidative_phosphorylation-3.6.3.27-3.6.3.27-RXN
1 ATP + 1 $phosphate_{ex}$ + 1 H2O → 1 ADP + 2 phosphate + 1 H+
pantothenate_biosynthesis-1.1.1.169-2-DEHYDROPANTOATE-REDUCT-RXN
1 (R)-pantoate + 1 NADP+ ← 1 2-dehydropantoate + 1 NADPH + 1 H+
pantothenate_biosynthesis-2.1.2.11-3-CH3-2-OXOBUTANOATE-OH-CH3-XFER-RXN
1 2-oxoisovalerate + 1 5,10-methylenetetrahydrofolate + 1 H2O ↔ 1 2-dehydropantoate + 1 tetrahydrofolate
pantothenate_biosynthesis-6.3.2.1-PANTOATE-BETA-ALANINE-LIG-RXN
1 ATP + 1 beta-alanine + 1 (R)-pantoate → 1 AMP + 1 (R)-pantothenate + 1 diphosphate + 1 H+
pentose_phosphate_pathway-1.1.1.49-GLU6PDEHYDROG-RXN
1 beta-D-glucose-6-phosphate + 1 NADP+ ↔ 1 6-phospho-D-glucono-1,5-lactone + 1 NADPH + 1 H+
pentose_phosphate_pathway-2.2.1.2-TRANSALDOL-RXN
1 D-sedoheptulose-7-phosphate + 1 D-glyceraldehyde-3-phosphate ↔ 1 D-erythrose-4-phosphate + 1 D-fructose-6-phosphate
pentose_phosphate_pathway-3.1.1.31-6PGLUCONOLACT-RXN
1 6-phospho-D-glucono-1,5-lactone + 1 H2O → 1 6-phospho-D-gluconate + 1 H+
pentose_phosphate_pathway-GLUCOSE-6-PHOSPHATE-1-EPIMERASE-RXN-spontaneous
1 alpha-D-glucose_6-phosphate ↔ 1 beta-D-glucose-6-phosphate
peptidoglycan_biosynthesis-1.1.1.158-UDPNACETYLMURAMATEDEHYDROG-RXN
1 NADP+ + 1 UDP-N-acetylmuramate ← 1 NADPH + 1 H+ + 1 UDP-N-acetylglucosamine-enolpyruvate
peptidoglycan_biosynthesis-2.5.1.7-UDPNACETYLGLUCOSAMENOLPYRTRANS-RXN
1 phosphoenolpyruvate + 1 UDP-alpha-N-acetyl-D-glucosamine → 1 phosphate + 1 UDP-N-acetylglucosamine-enolpyruvate
peptidoglycan_biosynthesis-3.6.1.27-UNDECAPRENYL-DIPHOSPHATASE-RXN
1 di-trans,octa-cis-undecaprenyl_diphosphate + 1 H2O → 1 ditrans,octacis-undecaprenyl_phosphate + 1 phosphate + 1 H+
peptidoglycan_biosynthesis-6.3.2.13-UDP-NACMURALGLDAPLIG-RXN
1 ATP + 1 meso-diaminopimelate + 1 UDP-N-acetylmuramoyl-L-alanyl-D-glutamate → 1 ADP + 1 phosphate + 1 H+ + 1 UDP-N-acetylmuramoyl-L-alanyl-D-glutamyl-meso-2,6-diaminopimelate
peptidoglycan_biosynthesis-6.3.2.4-DALADALALIG-RXN
1 ATP + 2 D-alanine → 1 ADP + 1 D-alanyl-D-alanine + 1 phosphate + 1 H+
peptidoglycan_biosynthesis-6.3.2.8-UDP-NACMUR-ALA-LIG-RXN
1 ATP + 1 L-alanine + 1 UDP-N-acetylmuramate → 1 ADP + 1 UDP-N-acetylmuramyl-L-Ala + 1 phosphate + 1 H+
peptidoglycan_biosynthesis-6.3.2.9-UDP-NACMURALA-GLU-LIG-RXN
1 ATP + 1 UDP-N-acetylmuramyl-L-Ala + 1 D-glutamate → 1 ADP + 1 phosphate + 1 H+ + 1 UDP-N-acetylmuramoyl-L-alanyl-D-glutamate
phenylalanine_metabolism-2.6.1.57-PHEAMINOTRANS-RXN
1 L-glutamate + 1 keto-phenylpyruvate ↔ 1 2-oxoglutarate + 1 L-phenylalanine
phenylalanine_metabolism-4.2.1.51-PREPHENATEDEHYDRAT-RXN
1 prephenate + 1 H+ → 1 CO2 + 1 keto-phenylpyruvate + 1 H2O
phenylalanine_metabolism-5.4.99.5-CHORISMATEMUT-RXN
1 chorismate ↔ 1 prephenate
phospholipid_biosynthesis_I-2.3.1.15-RXN-1381
1 sn-glycerol-3-phosphate + 1 |Cis-vaccenoyl-ACPs| → 1 1-cis-vaccenoyl-3-phosphate + 1 ACP
phospholipid_biosynthesis_I-2.3.1.51-1-ACYLGLYCEROL-3-P-ACYLTRANSFER-RXN
1 1-cis-vaccenoyl-3-phosphate + 1 |Cis-vaccenoyl-ACPs| → 1 1,2-di-cis-vaccenoyl-3-phosphate + 1 ACP
phospholipid_biosynthesis_I-2.7.7.41-RXN0-5515
1 CTP + 1 H+ + 1 1,2-di-cis-vaccenoyl-3-phosphate ↔ 1 diphosphate + 1 CDP-1,2-di-cis-vaccenoyl-3-phosphate

Reaction name and equation
phospholipid_biosynthesis_I-2.7.8.5-PHOSPHAGLYPSYN-RXN 1 CDP-1,2-di-cis-vaccenoyl-3-phosphate + 1 sn-glycerol-3-phosphate → 1 H+ + 1 CMP + 1 L-1-phosphatidylglycerol-phosphate
phospholipid_biosynthesis_I-3.1.3.27-PGPPHOSPHA-RXN 1 L-1-phosphatidylglycerol-phosphate + 1 H2O → 1 phosphate + 1 phosphatidylglycerol
photosynthesis-2.2.1.1-2TRANSKETO-RXN 1 D-erythrose-4-phosphate + 1 D-xylulose-5-phosphate ↔ 1 D-fructose-6-phosphate + 1 D-glyceraldehyde-3-phosphate
polyamine_pathway-4.1.1.17-ORNDECARBOX-RXN 1 L-ornithine + 1 H+ → 1 CO2 + 1 putrescine
polyhydroxybutyrate_biosynthesis-PhbC-RXN1-42 1 (R)-3-hydroxybutanoyl-CoA → 1 PHB + 1 coenzyme_A
polyhydroxybutyrate_degradation-3.1.1.75-3.1.1.75-RXN 1 PHB + 1 H2O → 1 (R)-3-hydroxybutanoate
proline_metabolism-1.2.1.41-GLUTSEMIALDEHYDROG-RXN 1 L-glutamate_gamma-semialdehyde + 1 NADP+ + 1 phosphate ← 1 L-glutamate-5-phosphate + 1 NADPH + 1 H+
proline_metabolism-1.5.1.12-PYRROLINECARBDEHYDROG-RXN 1 (S)-1-pyrroline-5-carboxylate + 1 NAD+ + 2 H2O → 1 L-glutamate + 1 NADH + 1 H+
proline_metabolism-1.5.1.2-PYRROLINECARBREDUCT-RXN_NAD 1 L-proline + 1 NAD+ ← 1 (S)-1-pyrroline-5-carboxylate + 2 H+ + 1 NADH
proline_metabolism-1.5.1.2-PYRROLINECARBREDUCT-RXN_NADP 1 L-proline + 1 NADP+ ← 1 (S)-1-pyrroline-5-carboxylate + 2 H+ + 1 NADPH
proline_metabolism-2.7.2.11-GLUTKIN-RXN 1 ATP + 1 L-glutamate → 1 ADP + 1 L-glutamate-5-phosphate
proline_metabolism-SPONTPRO-RXN-spontaneous 1 L-glutamate_gamma-semialdehyde ↔ 1 (S)-1-pyrroline-5-carboxylate + 1 H+ + 1 H2O
propionate_Na+_symport 1 propionate$_{ex}$ + 1 Na+$_{ex}$ → 1 Na+ + 1 propionate
purine_deoxyribonucleosides_degradation-2.4.2.1-DEOXYADENPHOSPHOR-RXN 1 deoxyadenosine + 1 phosphate ↔ 1 adenine + 1 2-deoxy-alpha-D-ribose_1-phosphate
purine_deoxyribonucleosides_degradation-2.4.2.1-DEOXYGUANPHOSPHOR-RXN 1 deoxyguanosine + 1 phosphate ↔ 1 2-deoxy-alpha-D-ribose_1-phosphate + 1 guanine
purine_metabolism-1.1.1.205-IMP-DEHYDROG-RXN 1 IMP + 1 NAD+ + 1 H2O ↔ 1 NADH + 1 H+ + 1 XMP
purine_metabolism-1.17.1.4-RXN-7682 1 hypoxanthine + 1 NAD+ + 1 H2O → 1 NADH + 1 H+ + 1 xanthine
purine_metabolism-1.17.1.4-RXN0-901 1 NAD+ + 1 H2O + 1 xanthine ↔ 1 NADH + 1 H+ + 1 urate
purine_metabolism-1.2.1.2-1.2.1.2-RXN 1 formate + 1 NAD+ → 1 CO2 + 1 NADH
purine_metabolism-2.1.2.3-AICARTRANSFORM-RXN 1 10-formyl-tetrahydrofolate + 1 aminoimidazole_carboxamide_ribonucleotide ↔ 1 phosphoribosyl-formamido-carboxamide + 1 tetrahydrofolate
purine_metabolism-2.4.2.1-ADENPHOSPHOR-RXN 1 adenosine + 1 phosphate ↔ 1 adenine + 1 alpha-D-ribose-1-phosphate
purine_metabolism-2.4.2.1-INOPHOSPHOR-RXN 1 inosine + 1 phosphate ↔ 1 hypoxanthine + 1 alpha-D-ribose-1-phosphate
purine_metabolism-2.4.2.1-RXN0-5199 1 guanosine + 1 phosphate ↔ 1 guanine + 1 alpha-D-ribose-1-phosphate
purine_metabolism-2.4.2.1-XANTHOSINEPHOSPHORY-RXN 1 phosphate + 1 xanthosine ↔ 1 alpha-D-ribose-1-phosphate + 1 xanthine
purine_metabolism-2.4.2.14-PRPPAMIDOTRANS-RXN 1 5-phospho-beta-D-ribosyl-amine + 1 L-glutamate + 1 diphosphate ← 1 L-glutamine + 1 5-phospho-alpha-D-ribose_1-diphosphate + 1 H2O
purine_metabolism-2.4.2.22-XANPRIBOSYLTRAN-RXN 1 diphosphate + 1 XMP ← 1 5-phospho-alpha-D-ribose_1-diphosphate + 1 xanthine
purine_metabolism-2.4.2.7-ADENPRIBOSYLTRAN-RXN 1 AMP + 1 diphosphate ← 1 adenine + 1 5-phospho-alpha-D-ribose_1-diphosphate
purine_metabolism-2.4.2.8-GUANPRIBOSYLTRAN-RXN 1 GMP + 1 diphosphate ← 1 guanine + 1 5-phospho-alpha-D-ribose_1-diphosphate
purine_metabolism-2.4.2.8-HYPOXANPRIBOSYLTRAN-RXN 1 IMP + 1 diphosphate ← 1 hypoxanthine + 1 5-phospho-alpha-D-ribose_1-diphosphate
purine_metabolism-2.7.4.3-ADENYL-KIN-RXN 1 AMP + 1 ATP ↔ 2 ADP
purine_metabolism-2.7.4.6-DADPKIN-RXN 1 ATP + 1 dADP → 1 ADP + 1 dATP

Reaction name and equation
purine_metabolism-2.7.4.6-DGDPKIN-RXN 1 ATP + 1 dGDP → 1 ADP + 1 dGTP
purine_metabolism-2.7.4.6-GDPKIN-RXN 1 ATP + 1 GDP → 1 ADP + 1 GTP
purine_metabolism-2.7.4.8-GUANYL-KIN-RXN 1 ATP + 1 GMP → 1 ADP + 1 GDP
purine_metabolism-3.1.3.5-AMP-DEPHOSPHORYLATION-RXN 1 AMP + 1 H2O → 1 adenosine + 1 phosphate
purine_metabolism-3.1.3.5-RXN-7609 1 GMP + 1 H2O → 1 guanosine + 1 phosphate
purine_metabolism-3.1.3.5-XMPXAN-RXN 1 H2O + 1 XMP → 1 phosphate + 1 xanthosine
purine_metabolism-3.1.5.1-DGTPTRIPHYDRO-RXN 1 dGTP + 1 H2O → 1 deoxyguanosine + 1 PPPi + 1 H+
purine_metabolism-3.2.2.4-AMP-NUCLEOSID-RXN 1 AMP + 1 H2O → 1 adenine + 1 D-ribose-5-phosphate
purine_metabolism-3.5.4.10-IMPCYCLOHYDROLASE-RXN 1 IMP + 1 H2O ↔ 1 phosphoribosyl-formamido-carboxamide
purine_metabolism-3.5.4.2-ADENINE-DEAMINASE-RXN 1 adenine + 1 H2O → 1 ammonia + 1 hypoxanthine
purine_metabolism-3.5.4.3-GUANINE-DEAMINASE-RXN 1 guanine + 1 H2O → 1 ammonia + 1 xanthine
purine_metabolism-3.5.4.4-ADENODEAMIN-RXN 1 adenosine + 1 H2O → 1 ammonia + 1 inosine
purine_metabolism-4.1.1.21-AIRCARBOXY-RXN 1 5-amino-1-(5-phospho-D-ribosyl)imidazole-4-carboxylate + 2 H+ ↔ 1 5-amino-1-(5-phospho-D-ribosyl)imidazole + 1 CO2
purine_metabolism-4.3.2.2-AICARSYN-RXN 1 5′-phosphoribosyl-4-(N-succinocarboxamide)-5-aminoimidazole ↔ 1 aminoimidazole_carboxamide_ribonucleotide + 1 fumarate
purine_metabolism-4.3.2.2-AMPSYN-RXN 1 adenylo-succinate ↔ 1 AMP + 1 fumarate
purine_metabolism-5.4.2.7-PPENTOMUT-RXN 1 alpha-D-ribose-1-phosphate ↔ 1 D-ribose-5-phosphate
purine_metabolism-6.3.2.6-SAICARSYN-RXN 1 ATP + 1 L-aspartate + 1 5-amino-1-(5-phospho-D-ribosyl)imidazole-4-carboxylate → 1 ADP + 1 5′-phosphoribosyl-4-(N-succinocarboxamide)-5-aminoimidazole + 1 phosphate + 1 H+
purine_metabolism-6.3.3.1-AIRS-RXN 1 5-phosphoribosyl-N-formylglycineamidine + 1 ATP → 1 5-amino-1-(5-phospho-D-ribosyl)imidazole + 1 ADP + 1 phosphate + 1 H+
purine_metabolism-6.3.4.13-GLYRIBONUCSYN-RXN 1 5-phospho-beta-D-ribosyl-amine + 1 ATP + 1 glycine → 1 5-phospho-ribosyl-glycineamide + 1 ADP + 1 phosphate + 1 H+
purine_metabolism-6.3.4.3-FORMATETHFLIG-RXN 1 ATP + 1 formate + 1 tetrahydrofolate → 1 10-formyl-tetrahydrofolate + 1 ADP + 1 phosphate
purine_metabolism-6.3.4.4-ADENYLOSUCCINATE-SYNTHASE-RXN 1 GTP + 1 IMP + 1 L-aspartate → 1 adenylo-succinate + 1 GDP + 1 phosphate + 2 H+
purine_metabolism-6.3.5.2-GMP-SYN-GLUT-RXN 1 ATP + 1 L-glutamine + 1 H2O + 1 XMP → 1 AMP + 1 L-glutamate + 1 GMP + 1 diphosphate + 2 H+
purine_metabolism-6.3.5.3-FGAMSYN-RXN 1 5′-phosphoribosyl-N-formylglycineamide + 1 ATP + 1 L-glutamine + 1 H2O → 1 5-phosphoribosyl-N-formylglycineamidine + 1 ADP + 1 L-glutamate + 1 phosphate + 1 H+
pyridoxal_5′-phosphate_biosynthesis-1.1.1.290-ERYTHRON4PDEHYDROG-RXN 1 erythronate-4-phosphate + 1 NAD+ → 1 2-oxo-3-hydroxy-4-phosphobutanoate + 1 NADH + 1 H+
pyridoxal_5′-phosphate_biosynthesis-1.2.1.72-ERYTH4PDEHYDROG-RXN 1 D-erythrose-4-phosphate + 1 NAD+ + 1 H2O → 1 erythronate-4-phosphate + 1 NADH + 2 H+
pyrimidine_metabolism-2.1.3.2-ASPCARBTRANS-RXN 1 carbamoyl-phosphate + 1 L-aspartate ↔ 1 N-carbamoyl-L-aspartate + 1 phosphate + 1 H+
pyrimidine_metabolism-2.4.2.10-OROPRIBTRANS-RXN 1 orotidine-5′-phosphate + 1 diphosphate ↔ 1 orotate + 1 5-phospho-alpha-D-ribose_1-diphosphate
pyrimidine_metabolism-2.4.2.9-URACIL-PRIBOSYLTRANS-RXN 1 diphosphate + 1 uridine-5′-phosphate ↔ 1 5-phospho-alpha-D-ribose_1-diphosphate + 1 uracil

Reaction name and equation
pyrimidine_metabolism-2.7.4.14-CMPKI-RXN
1 ATP + 1 CMP → 1 ADP + 1 CDP
pyrimidine_metabolism-2.7.4.14-RXN-12002
1 ATP + 1 uridine-5′-phosphate ↔ 1 ADP + 1 UDP
pyrimidine_metabolism-2.7.4.22-2.7.4.22-RXN
1 ATP + 1 uridine-5′-phosphate → 1 ADP + 1 UDP
pyrimidine_metabolism-2.7.4.6-CDPKIN-RXN
1 ATP + 1 CDP ↔ 1 ADP + 1 CTP
pyrimidine_metabolism-2.7.4.6-DCDPKIN-RXN
1 ATP + 1 dCDP → 1 ADP + 1 dCTP
pyrimidine_metabolism-2.7.4.6-DTDPKIN-RXN
1 ATP + 1 dTDP → 1 ADP + 1 dTTP
pyrimidine_metabolism-2.7.4.6-DUDPKIN-RXN
1 ATP + 1 dUDP → 1 ADP + 1 dUTP
pyrimidine_metabolism-2.7.4.6-UDPKIN-RXN
1 ATP + 1 UDP → 1 ADP + 1 UTP
pyrimidine_metabolism-2.7.4.9-DTMPKI-RXN
1 ATP + 1 dTMP → 1 ADP + 1 dTDP
pyrimidine_metabolism-3.5.2.3-DIHYDROOROT-RXN
1 (S)-dihydroorotate + 1 H2O ↔ 1 N-carbamoyl-L-aspartate + 1 H+
pyrimidine_metabolism-3.5.4.1-CYTDEAM-RXN
1 cytosine + 1 H2O → 1 ammonia + 1 uracil
pyrimidine_metabolism-3.5.4.13-DCTP-DEAM-RXN
1 dCTP + 1 H2O → 1 ammonia + 1 dUTP
pyrimidine_metabolism-3.6.1.23-DUTP-PYROP-RXN
1 dUTP + 1 H2O → 1 dUMP + 1 diphosphate + 1 H+
pyrimidine_metabolism-4.1.1.23-OROTPDECARB-RXN
1 orotidine-5′-phosphate + 1 H+ → 1 CO2 + 1 uridine-5′-phosphate
pyrimidine_metabolism-6.3.4.2-CTPSYN-RXN
1 ATP + 1 L-glutamine + 1 UTP + 1 H2O → 1 ADP + 1 CTP + 1 L-glutamate + 1 phosphate + 2 H+
pyrimidine_ribonucleotides_interconversion-3.6.1.15-RXN-12195
1 CTP + 1 H2O → 1 CDP + 1 phosphate + 1 H+
pyrimidine_ribonucleotides_interconversion-3.6.1.15-RXN-12196
1 UTP + 1 H2O → 1 phosphate + 1 H+ + 1 UDP
pyruvate_Na+_symport
1 pyruvate_{ex} + 1 Na+_{ex} → 1 Na+ + 1 pyruvate
ribose_degradation-2.7.1.15-RIBOKIN-RXN
1 ATP + 1 alpha-D-ribofuranose → 1 ADP + 1 H+ + 1 D-ribose-5-phosphate
ribose_degradation-RXN0-5305-spontaneous
1 beta-D-ribofuranose ↔ 1 alpha-D-ribofuranose
serine_metabolism-1.1.1.81-HYDROXYPYRUVATE-REDUCTASE-RXN_NAD
1 D-glycerate + 1 NAD+ ↔ 1 hydroxypyruvate + 1 H+ + 1 NADH
serine_metabolism-1.1.1.81-HYDROXYPYRUVATE-REDUCTASE-RXN_NADP
1 D-glycerate + 1 NADP+ ↔ 1 hydroxypyruvate + 1 H+ + 1 NADPH
serine_metabolism-1.1.1.81-RXN0-300
1 D-glycerate + 1 NADP+ ↔ 1 NADPH + 1 hydroxypyruvate + 1 H+
serine_metabolism-1.1.1.95-PGLYCDEHYDROG-RXN
1 3-phospho-D-glycerate + 1 NAD+ ↔ 1 3-phospho-hydroxypyruvate + 1 NADH + 1 H+
serine_metabolism-2.6.1.52-PSERTRANSAM-RXN
1 2-oxoglutarate + 1 3-phospho-L-serine ↔ 1 3-phospho-hydroxypyruvate + 1 L-glutamate
serine_metabolism-3.1.3.3-RXN0-5114
1 3-phospho-L-serine + 1 H2O → 1 phosphate + 1 L-serine
siroheme_biosynthesis-1.3.1.76-DIMETHUROPORDEHYDROG-RXN
1 precorrin-2 + 1 NAD+ ↔ 1 NADH + 2 H+ + 1 sirohydrochlorin
siroheme_biosynthesis-4.99.1.4-SIROHEME-FERROCHELAT-RXN
1 Fe2+ + 1 sirohydrochlorin ↔ 2 H+ + 1 siroheme
starch_degradation-3.2.1.20-RXN-2141
1 alpha-maltose + 1 H2O → 2 alpha-D-glucose
succinate_Na+_symport
1 succinate_{ex} + 1 Na+_{ex} → 1 Na+ + 1 succinate
sulfate_reduction-1.8.1.2-SULFITE-REDUCT-RXN
1 hydrogen_sulfide + 3 NADP+ + 3 H2O ↔ 3 NADPH + 5 H+ + 1 sulfite
sulfate_reduction-2.7.1.25-ADENYLYLSULFKIN-RXN
1 adenosine_5′-phosphosulfate + 1 ATP → 1 ADP + 1 phosphoadenosine-5′-phosphosulfate + 1 H+
sulfate_reduction-2.7.7.4-SULFATE-ADENYLYLTRANS-RXN

Reaction name and equation
1 ATP + 1 H+ + 1 sulfate → 1 adenosine_5′-phosphosulfate + 1 diphosphate
sulfate_reduction_I_(assimilatory)-1.8.4.8-1.8.4.8-RXN
1 adenosine_3′,5′-bisphosphate + 1 sulfite + 1 |Ox-Thioredoxin| ↔ 1 phosphoadenosine-5′-phosphosulfate + 1 |Red-Thioredoxin|
tetrahydrofolate_metabolism-1.5.1.3-DIHYDROFOLATEREDUCT-RXN
1 NADP+ + 1 tetrahydrofolate ← 1 7,8-dihydrofolate_monoglutamate + 1 NADPH + 1 H+
tetrahydrofolate_metabolism-2.5.1.15-H2PTEROATESYNTH-RXN
1 6-hydroxymethyl-dihydropterin_diphosphate + 1 4-aminobenzoate → 1 7,8-dihydropteroate + 1 diphosphate
tetrahydrofolate_metabolism-2.7.6.3-H2PTERIDINEPYROPHOSPHOKIN-RXN
1 6-hydroxymethyl-7,8-dihydropterin + 1 ATP → 1 AMP + 1 6-hydroxymethyl-dihydropterin_diphosphate + 1 H+
tetrahydrofolate_metabolism-3.5.1.10-FORMYLTHFDEFORMYL-RXN
1 10-formyl-tetrahydrofolate + 1 H2O → 1 formate + 1 H+ + 1 tetrahydrofolate
tetrahydrofolate_metabolism-3.5.4.16-GTP-CYCLOHYDRO-I-RXN
1 GTP + 1 H2O → 1 7,8-dihydroneopterin_triphosphate + 1 formate + 1 H+
tetrahydrofolate_metabolism-3.6.1.–DIHYDRONEOPTERIN-MONO-P-DEPHOS-RXN
1 7,8-dihydroneopterin_3′-phosphate + 1 H2O → 1 7,8-dihydro-D-neopterin + 1 phosphate
tetrahydrofolate_metabolism-3.6.1.–H2NEOPTERINP3PYROPHOSPHOHYDRO-RXN
1 7,8-dihydroneopterin_triphosphate + 1 H2O → 1 7,8-dihydroneopterin_3′-phosphate + 1 diphosphate + 1 H+
tetrahydrofolate_metabolism-4.1.2.25-H2NEOPTERINALDOL-RXN
1 7,8-dihydro-D-neopterin → 1 6-hydroxymethyl-7,8-dihydropterin + 1 glycolaldehyde
tetrahydrofolate_metabolism-6.3.2.12-DIHYDROFOLATESYNTH-RXN
1 7,8-dihydropteroate + 1 ATP + 1 L-glutamate → 1 ADP + 1 7,8-dihydrofolate_monoglutamate + 1 phosphate + 1 H+
thiamin_synthesis-2.8.1.–THIAZOLSYN2-RXN
1 H+ + 1 hydrogen_sulfide + 1 2-iminoacetate + 1 1-deoxy-D-xylulose_5-phosphate → 1 4-methyl-5-(2-phosphonooxyethyl)thiazole + 3 H2O + 1 CO2
thiamin_synthesis-4.1.99.19-RXN-11319
1 S-adenosyl-L-methionine + 1 L-tyrosine + 1 NADH → 1 H+ + 1 5′-deoxyadenosine + 1 4-methylphenol + 1 2-iminoacetate + 1 L-methionine + 1 NAD+
thioredoxin_pathway-1.8.1.9-THIOREDOXIN-REDUCT-NADPH-RXN
1 H+ + 1 NADP+ + 1 |Red-Thioredoxin| ← 1 NADPH + 1 |Ox-Thioredoxin|
threonine_metabolism-1.1.1.3-HOMOSERDEHYDROG-RXN_NAD
1 L-homoserine + 1 NAD+ ← 1 L-aspartate-semialdehyde + 1 H+ + 1 NADH
threonine_metabolism-1.1.1.3-HOMOSERDEHYDROG-RXN_NADP
1 L-homoserine + 1 NADP+ ← 1 L-aspartate-semialdehyde + 1 H+ + 1 NADPH
threonine_metabolism-1.2.1.11-ASPARTATE-SEMIALDEHYDE-DEHYDROGENASE-RXN
1 L-aspartate-semialdehyde + 1 NADP+ + 1 phosphate ↔ 1 L-aspartyl-4-phosphate + 1 NADPH + 1 H+
threonine_metabolism-2.3.1.–KETOBUTFORMLY-RXN
1 2-oxobutanoate + 1 coenzyme_A → 1 formate + 1 propanoyl-CoA
threonine_metabolism-2.7.1.39-HOMOSERKIN-RXN
1 ATP + 1 L-homoserine → 1 ADP + 1 O-phospho-L-homoserine + 1 H+
threonine_metabolism-2.7.2.4-ASPARTATEKIN-RXN
1 ATP + 1 L-aspartate → 1 ADP + 1 L-aspartyl-4-phosphate
threonine_metabolism-4.1.2.5-THREONINE-ALDOLASE-RXN
1 L-threonine → 1 acetaldehyde + 1 glycine
threonine_metabolism-4.2.3.1-THRESYN-RXN
1 O-phospho-L-homoserine + 1 H2O → 1 phosphate + 1 L-threonine
threonine_metabolism-4.3.1.19-THREDEHYD-RXN
1 L-threonine → 1 2-oxobutanoate + 1 ammonia + 1 H+
triphosphate-hydrolysis
1 PPPi + 1 H2O → 1 phosphate + 1 diphosphate
tryptophan_metabolism-2.4.2.18-PRTRANS-RXN
1 N-(5′-phosphoribosyl)-anthranilate + 1 diphosphate ← 1 anthranilate + 1 5-phospho-alpha-D-ribose_1-diphosphate
tryptophan_metabolism-4.1.1.48-IGPSYN-RXN
1 1-(o-carboxyphenylamino)-1′-deoxyribulose-5′-phosphate + 1 H+ → 1 CO2 + 1 (1S,2R)-1-C-(indol-3-yl)glycerol_3-phosphate + 1 H2O
tryptophan_metabolism-4.1.3.27-ANTHRANSYN-RXN
1 chorismate + 1 L-glutamine ↔ 1 anthranilate + 1 L-glutamate + 1 H+ + 1 pyruvate
tryptophan_metabolism-5.3.1.24-PRAISOM-RXN
1 N-(5′-phosphoribosyl)-anthranilate → 1 1-(o-carboxyphenylamino)-1′-deoxyribulose-5′-phosphate
tyrosine_metabolism-1.3.1.12-PREPHENATEDEHYDROG-RXN

Reaction name and equation
1 NAD+ + 1 prephenate → 1 CO2 + 1 NADH + 1 4-hydroxyphenylpyruvate
tyrosine_metabolism-2.6.1.57-TYRAMINOTRANS-RXN
1 2-oxoglutarate + 1 L-tyrosine ↔ 1 L-glutamate + 1 4-hydroxyphenylpyruvate
ubiquinone_biosynthesis-1.14.-.–RXN-9236
1 H+ + 1 6-methoxy-3-methyl-2-all-trans-decaprenyl-1,4-benzoquinol + 1 oxygen + 1 NADPH → 1 3-demethylubiquinol-10 + 1 H2O + 1 NADP+
ubiquinone_biosynthesis-4.1.3.40-CHORPYRLY-RXN
1 chorismate → 1 4-hydroxybenzoate + 1 pyruvate
uracil_diffusion
1 $uracil_{ex}$ → 1 uracil
urea_cycle-2.1.3.3-ORNCARBAMTRANSFER-RXN
1 carbamoyl-phosphate + 1 L-ornithine ↔ 1 L-citrulline + 1 phosphate + 1 H+
urea_cycle-2.7.2.2-CARBAMATE-KINASE-RXN
1 ammonia + 1 ATP + 1 CO2 ↔ 1 ADP + 1 carbamoyl-phosphate + 1 H+
urea_cycle-3.5.1.5-UREASE-RXN
1 urea + 1 H2O → 2 ammonia + 1 CO2
urea_cycle-6.3.4.5-ARGSUCCINSYN-RXN
1 ATP + 1 L-aspartate + 1 L-citrulline → 1 AMP + 1 L-arginino-succinate + 1 diphosphate + 1 H+
urea_diffusion
1 $urea_{ex}$ → 1 urea
valine_biosynthesis-1.1.1.86-ACETOLACTREDUCTOISOM-RXN
1 (R)-2,3-dihydroxy-3-methylbutanoate + 1 NADP+ ↔ 1 (S)-2-acetolactate + 1 NADPH + 1 H+
valine_biosynthesis-2.2.1.6-ACETOLACTSYN-RXN
1 H+ + 2 pyruvate → 1 (S)-2-acetolactate + 1 CO2
valine_biosynthesis-4.2.1.9-DIHYDROXYISOVALDEHYDRAT-RXN
1 (R)-2,3-dihydroxy-3-methylbutanoate → 1 2-oxoisovalerate + 1 H2O
vitamin_B12_metabolism-1.14.13.83-R321-RXN
1 precorrin-3A + 1 NADH + 1 oxygen + 1 H+ ↔ 1 precorrin-3B + 1 NAD+ + 1 H2O
vitamin_B12_metabolism-1.16.8.1-R343-RXN
2 cob(I)yrinate_a,c-diamide + 1 FMN + 3 H+ ← 2 cob(II)yrinate_a,c-diamide + 1 FMNH2
vitamin_B12_metabolism-1.3.1.54-1.3.1.54-RXN
1 precorrin-6B + 1 NADP+ ↔ 1 precorrin-6A + 1 NADPH + 1 H+
vitamin_B12_metabolism-2.1.1.–RXN-8766
1 cobalt-precorrin-6B + 1 S-adenosyl-L-methionine → 1 S-adenosyl-L-homocysteine + 1 cobalt-precorrin-7 + 1 H+
vitamin_B12_metabolism-2.1.1.107-RXN-8675
1 precorrin-1 + 1 S-adenosyl-L-methionine → 1 S-adenosyl-L-homocysteine + 1 precorrin-2
vitamin_B12_metabolism-2.1.1.107-UROPORIIIMETHYLTRANSA-RXN
1 S-adenosyl-L-methionine + 1 uroporphyrinogen-III ↔ 1 S-adenosyl-L-homocysteine + 1 precorrin-1 + 1 H+
vitamin_B12_metabolism-2.1.1.130-2.1.1.130-RXN
1 precorrin-2 + 1 S-adenosyl-L-methionine ↔ 1 S-adenosyl-L-homocysteine + 1 precorrin-3A + 1 H+
vitamin_B12_metabolism-2.1.1.131-2.1.1.131-RXN
1 precorrin-3B + 1 S-adenosyl-L-methionine ↔ 1 S-adenosyl-L-homocysteine + 1 precorrin-4 + 2 H+
vitamin_B12_metabolism-2.1.1.131-RXN-8761
1 cobalt-precorrin-3 + 1 H+ + 1 S-adenosyl-L-methionine → 1 S-adenosyl-L-homocysteine + 1 cobalt-precorrin-4
vitamin_B12_metabolism-2.1.1.132-2.1.1.132-RXN
1 precorrin-6B + 2 S-adenosyl-L-methionine → 2 S-adenosyl-L-homocysteine + 1 CO2 + 1 precorrin-8x + 2 H+
vitamin_B12_metabolism-2.1.1.133-2.1.1.133-RXN
1 precorrin-4 + 1 S-adenosyl-L-methionine ↔ 1 S-adenosyl-L-homocysteine + 1 precorrin-5 + 1 H+
vitamin_B12_metabolism-2.1.1.133-RXN-8762
1 cobalt-precorrin-4 + 1 S-adenosyl-L-methionine → 1 S-adenosyl-L-homocysteine + 1 cobalt-precorrin-5A
vitamin_B12_metabolism-2.1.1.151-RXN-8760
1 cobalt-precorrin-2 + 1 S-adenosyl-L-methionine → 1 S-adenosyl-L-homocysteine + 1 cobalt-precorrin-3 + 1 H+
vitamin_B12_metabolism-2.1.1.152-R322-RXN
1 precorrin-5 + 1 S-adenosyl-L-methionine + 1 H2O ↔ 1 acetate + 1 S-adenosyl-L-homocysteine + 1 precorrin-6A + 1 H+
vitamin_B12_metabolism-2.4.2.21-DMBPPRIBOSYLTRANS-RXN
1 5,6-dimethylbenzimidazole + 1 nicotinate_D-ribonucleotide → 1 alpha-ribazole-5′-phosphate + 1 nicotinate + 1 H+

Reaction name and equation
vitamin_B12_metabolism-2.5.1.17-R344-RXN
1 ATP + 1 cob(I)yrinate_a,c-diamide → 1 adenosyl-cobyrinate_a,c-diamide + 1 PPPi
vitamin_B12_metabolism-2.7.7.62-COBINPGUANYLYLTRANS-RXN
1 adenosyl-cobinamide_phosphate + 1 GTP + 1 H+ ↔ 1 adenosylcobinamide-GDP + 1 diphosphate
vitamin_B12_metabolism-2.7.8.26-COBALAMIN5PSYN-RXN
1 adenosylcobinamide-GDP + 1 alpha-ribazole-5′-phosphate → 1 H+ + 1 adenosylcobalamin_5′-phosphate + 1 GMP
vitamin_B12_metabolism-2.7.8.26-COBALAMINSYN-RXN
1 adenosylcobinamide-GDP + 1 alpha-ribazole ↔ 1 coenzyme_B12 + 1 GMP + 1 H+
vitamin_B12_metabolism-3.1.3.73-RIBAZOLEPHOSPHAT-RXN
1 alpha-ribazole-5′-phosphate + 1 H2O → 1 alpha-ribazole + 1 phosphate
vitamin_B12_metabolism-4.99.1.3-RXN-8759
1 Co2+ + 1 precorrin-2 → 1 cobalt-precorrin-2 + 4 H+
vitamin_B12_metabolism-5.4.1.2-5.4.1.2-RXN
1 precorrin-8x + 1 H+ ↔ 1 hydrogenobyrinate
vitamin_B12_metabolism-6.3.1.10-RXN-6261
1 ATP + 1 adenosyl-cobyrate + 1 (R)-1-amino-2-propanol_O-2-phosphate → 1 adenosyl-cobinamide_phosphate + 1 ADP + 1 phosphate + 1 H+
vitamin_B12_metabolism-6.3.5.10-R345-RXN
4 ATP + 1 adenosyl-cobyrinate_a,c-diamide + 4 L-glutamine + 4 H2O → 4 ADP + 1 adenosyl-cobyrate + 4 L-glutamate + 4 phosphate + 4 H+
vitamin_B12_metabolism-6.3.5.9-R341-RXN
2 ATP + 1 hydrogenobyrinate + 2 L-glutamine + 2 H2O → 2 ADP + 1 hydrogenobyrinate_a,c-diamide + 2 L-glutamate + 2 phosphate + 2 H+
vitamin_B12_metabolism-6.6.1.2-R342-RXN
1 ATP + 1 Co2+ + 1 hydrogenobyrinate_a,c-diamide + 1 H2O → 1 ADP + 1 cob(II)yrinate_a,c-diamide + 1 phosphate + 3 H+
vitamin_B1_metabolism-2.5.1.3-THI-P-SYN-RXN
1 4-amino-2-methyl-5-diphosphomethylpyrimidine + 1 H+ + 1 4-methyl-5-(2-phosphonooxyethyl)thiazole → 1 diphosphate + 1 thiamin_phosphate
vitamin_B1_metabolism-2.7.4.16-THI-P-KIN-RXN
1 ATP + 1 thiamin_phosphate → 1 ADP + 1 thiamin_diphosphate
vitamin_B1_metabolism-2.7.4.7-PYRIMSYN3-RXN
1 4-amino-2-methyl-5-phosphomethylpyrimidine + 1 ATP → 1 ADP + 1 4-amino-2-methyl-5-diphosphomethylpyrimidine
vitamin_B6_metabolism-1.1.1.262-1.1.1.262-RXN
1 4-phospho-hydroxy-L-threonine + 1 NAD+ → 1 (2S)-2-amino-3-oxo-4-phosphonooxybutanoate + 1 NADH + 2 H+
vitamin_B6_metabolism-1.4.3.5-PNPOXI-RXN
1 oxygen + 1 pyridoxine-5′-phosphate → 1 hydrogen_peroxide + 1 pyridoxal_5′-phosphate
vitamin_B6_metabolism-2.6.1.52-PSERTRANSAMPYR-RXN
1 2-oxo-3-hydroxy-4-phosphobutanoate + 1 L-glutamate ↔ 1 2-oxoglutarate + 1 4-phospho-hydroxy-L-threonine
vitamin_B6_metabolism-2.6.99.2-PDXJ-RXN
1 3-amino-1-hydroxyacetone-1-phosphate + 1 1-deoxy-D-xylulose_5-phosphate → 1 phosphate + 1 H+ + 1 pyridoxine-5′-phosphate + 2 H2O
vitamin_B6_metabolism-RXN-8447-spontaneous
1 (2S)-2-amino-3-oxo-4-phosphonooxybutanoate + 2 H+ → 1 3-amino-1-hydroxyacetone-1-phosphate + 1 CO2
xanthine_diffusion
1 $xanthine_{ex}$ → 1 xanthine
NITRATE-REDUCTASE-NADH-RXN-1.7.1.1
1 NAD+ + 1 nitrite + 1 H2O ← 1 NADH + 1 nitrate + 1 H+

INDEX AND ABBREVIATIONS

BIBLIOGRAPHY

Alexander K, Young IG (1978) Alternative hydroxylases for the aerobic and anaerobic biosynthesis of ubiquinone in Escherichia coli. *Biochemistry* **17**: 4750–5

Arkin IT, Xu H, Jensen MO, Arbely E, Bennett ER, Bowers KJ, Chow E, Dror RO, Eastwood MP, Flitman-Tene R, Gregersen BA, Klepeis JL, Kolossváry I, Shan Y, Shaw DE (2007) Mechanism of Na+/H+ antiporting. *Science New York NY* **317**: 799–803

Bennett BD, Kimball EH, Gao M, Osterhout R, Van Dien SJ, Rabinowitz JD (2009) Absolute metabolite concentrations and implied enzyme active site occupancy in Escherichia coli. *Nature chemical biology* **5**: 593–9

Berg HC (2003) The rotary motor of bacterial flagella. *Annual review of biochemistry* **72**: 19–54

Berghoff BA, Glaeser J, Nuss AM, Zobawa M, Lottspeich F, Klug G (2011) Anoxygenic photosynthesis and photooxidative stress: a particular challenge for Roseobacter. *Environmental microbiology* **13**: 775–91

Biebl H, Allgaier M, Tindall BJ, Koblizek M, Lünsdorf H, Pukall R, Wagner-Döbler I (2005) Dinoroseobacter shibae gen. nov., sp. nov., a new aerobic phototrophic bacterium isolated from dinoflagellates. *International journal of systematic and evolutionary microbiology* **55**: 1089–1096

Biebl H, Wagner-Döbler I (2006) Growth and bacteriochlorophyll a formation in taxonomically diverse aerobic anoxygenic phototrophic bacteria in chemostat culture: Influence of light regimen and starvation. *Process Biochemistry* **41**: 2153–2159

Bourqui R, Cottret L, Lacroix V, Auber D, Mary P, Sagot MF, Jourdan F (2007) Metabolic network visualization eliminating node redundance and preserving metabolic pathways. *BMC systems biology* **1**: 29

Brinkhoff T, Giebel HA, Simon M (2008) Diversity, ecology, and genomics of the Roseobacter clade: a short overview. *Archives of microbiology* **189**: 531–9

Buchan A, González JM, Moran MA (2005) Overview of the marine roseobacter lineage. *Applied and environmental microbiology* **71**: 5665–77

Burton AC (1939) The properties of the steady state compared to those of equilibrium as shown in characteristic biological behavior. *Journal of Cellular and Comparative Physiology* **14**: 327–349

Camacho C, Coulouris G, Avagyan V, Ma N, Papadopoulos J, Bealer K, Madden TL (2009) BLAST+: architecture and applications. *BMC bioinformatics* **10**: 421

Caspi R, Altman T, Dreher K, Fulcher Ca, Subhraveti P, Keseler IM, Kothari A, Krummenacker M, Latendresse M, Mueller La, Ong Q, Paley S, Pujar A, Shearer AG, Travers M, Weerasinghe D, Zhang P, Karp PD (2012) The MetaCyc database of metabolic pathways and enzymes and the BioCyc collection of pathway/genome databases. *Nucleic acids research* **40**: D742–53

Choi-Rhee E, Cronan JE (2005) A nucleosidase required for in vivo function of the S-adenosyl-L-methionine radical enzyme, biotin synthase. *Chemistry biology* **12**: 589–93

Covert MW, Schilling CH, Famili I, Edwards JS, Goryanin II, Selkov E, Palsson BO (2001) Metabolic modeling of microbial strains in silico. *Trends in Biochemical Sciences* **26**: 179–186

Curson ARJ, Todd JD, Sullivan MJ, Johnston AWB (2011) Catabolism of dimethylsulphoniopropionate: microorganisms, enzymes and genes. *Nature Reviews Microbiology*

DeJongh M, Formsma K, Boillot P, Gould J, Rycenga M, Best A (2007) Toward the automated generation of genome-scale metabolic networks in the SEED. *BMC bioinformatics* **8**: 139

Dickschat JS, Zell C, Brock NL (2010) Pathways and substrate specificity of DMSP catabolism in marine bacteria of the Roseobacter clade. *Chembiochem a European journal of chemical biology* **11**: 417–25

Doi M, Shioi Y (1991) Enhancement of denitrifying activity in cells of Roseobacter denitrificans grown aerobically in the light. *Plant and cell physiology* **32**: 365–370

Durot M, Bourguignon PY, Schachter V (2009) Genome-scale models of bacterial metabolism: reconstruction and applications. *FEMS microbiology reviews* **33**: 164–90

Ellson J, Gansner ER, Koutsofios E, North SC, Woodhull G (2004) Graphviz and dynagraph—static and dynamic graph drawing tools. *Graph Drawing Software* : 127–148

Feist AM, Henry CS, Reed JL, Krummenacker M, Joyce AR, Karp PD, Broadbelt LJ, Hatzimanikatis V, Palsson BO (2007) A genome-scale metabolic reconstruction for Escherichia coli K-12 MG1655 that accounts for 1260 ORFs and thermodynamic information. *Molecular systems biology* **3**: 121

Feist AM, Palsson BO (2010) The biomass objective function. *Current Opinion in Microbiology* **13**: 344–349

Fell DA, Small JR (1986) Fat synthesis in adipose tissue. An examination of stoichiometric constraints. *The Biochemical journal* **238**: 781–6

Fürch T, Preusse M, Tomasch J, Zech H, Wagner-Döbler I, Rabus R, Wittmann C (2009) Metabolic fluxes in the central carbon metabolism of Dinoroseobacter shibae and Phaeobacter gallaeciensis, two members of the marine Roseobacter clade. *BMC microbiology* **9**: 209

Geng H, Belas R (2010) Molecular mechanisms underlying roseobacter-phytoplankton symbioses. *Current opinion in biotechnology* **21**: 332–8

Gibson M, Gibson F, Doy C, Morgan P (1962) The Branch Point in the Biosynthesis of the Aromatic Amino-Acids. *Nature* **195**: 1173–1175

González JM, Kiene RP, Moran MA (1999) Transformation of sulfur compounds by an abundant lineage of marine bacteria in the alpha-subclass of the class Proteobacteria. *Applied and environmental microbiology* **65**: 3810–9

Gudmundsson S, Thiele I (2010) Computationally efficient flux variability analysis. *BMC bioinformatics* **11**: 489

Hagberg AA, Schult DA, Swart PJ (2008) Exploring network structure, dynamics, and function using NetworkX. In *Proceedings of the 7th Python in Science Conference (SciPy2008)*

Harashima K, Hayasaki J, Ikari T, Shiba T (1980) O2-stimulated synthesis of bacteriochlorophyll and carotenoids in marine bacteria. *Plant and Cell Physiology* **21**: 1283–1294

Heath AP, Bennett GN, Kavraki LE (2011) An algorithm for efficient identification of branched metabolic pathways. *Journal of computational biology a journal of computational molecular cell biology* **18**: 1575–97

Henry CS, DeJongh M, Best AA, Frybarger PM, Linsay B, Stevens RL (2010) High-throughput generation, optimization and analysis of genome-scale metabolic models. *Nature Biotechnology* **28**: 977–982

Holert J, Hahnke S, Cypionka H (2011) Influence of light and anoxia on chemiosmotic energy conservation in Dinoroseobacter shibae. *Environmental microbiology reports* **3**: 136–141

Imam S, Yilmaz S, Sohmen U, Gorzalski AS, Reed JL, Noguera DR, Donohue TJ (2011) iRsp1095: a genome-scale reconstruc-

tion of the Rhodobacter sphaeroides metabolic network. *BMC systems biology* **5**: 116

Jarosławski S, Duquesne K, Sturgis JN, Scheuring S (2009) High-resolution architecture of the outer membrane of the Gram-negative bacteria Roseobacter denitrificans. *Molecular microbiology* **74**: 1211–22

Johansen J, Pinhassi J, Blackburn N, Zweifel U, Hagström A (2002) Variability in motility characteristics among marine bacteria. *Aquatic Microbial Ecology* **28**: 229–237

Jurgenson CT, Begley TP, Ealick SE (2009) The Structural and Biochemical Foundations of Thiamin Biosynthesis. *Annual Review of Biochemistry* **78**: 569–603

Kanehisa M, Goto S, Sato Y, Furumichi M, Tanabe M (2012) KEGG for integration and interpretation of large-scale molecular data sets. *Nucleic acids research* **40**: D109–14

Karp PD, Paley SM, Krummenacker M, Latendresse M, Dale JM, Lee TJ, Kaipa P, Gilham F, Spaulding A, Popescu L, Altman T, Paulsen I, Keseler IM, Caspi R (2010) Pathway Tools version 13.0: integrated software for pathway/genome informatics and systems biology. *Briefings in bioinformatics* **11**: 40–79

Kauffman KJ, Prakash P, Edwards JS (2003) Advances in flux balance analysis. *Current Opinion in Biotechnology* **14**: 491–496

Kim PJ, Lee DY, Kim TY, Lee KH, Jeong H, Lee SY, Park S (2007) Metabolite essentiality elucidates robustness of Escherichia coli metabolism. *Proceedings of the National Academy of Sciences of the United States of America* **104**: 13638–42

Kim TY, Sohn SB, Kim YB, Kim WJ, Lee SY (2011) Recent advances in reconstruction and applications of genome-scale metabolic models. *Current opinion in biotechnology*

Kitano H (2002) Computational systems biology. *Nature* **420**: 206–10

Kjeldsen KR, Nielsen J (2009) In silico genome-scale reconstruction and validation of the Corynebacterium glutamicum metabolic network. *Biotechnology and bioengineering* **102**: 583–97

Klamt S, Grammel H, Straube R, Ghosh R, Gilles ED (2008) Modeling the electron transport chain of purple non-sulfur bacteria. *Molecular systems biology* **4**: 156

Kriek M, Martins F, Challand MR, Croft A, Roach PL (2007) Thiamine biosynthesis in Escherichia coli: identification of the intermediate and by-product derived from tyrosine. *Angewandte Chemie International ed in English* **46**: 9223–6

Lacroix V, Cottret L, Thébault P, Sagot MF (2008) An introduction to metabolic networks and their structural analysis. *IEEEACM transactions on computational biology and bioinformatics IEEE ACM* **5**: 594–617

Latendresse M, Krummenacker M, Trupp M, Karp PD (2012) Construction and completion of flux balance models from pathway databases. *Bioinformatics Oxford England* **28**: 388–96

Liu P, Geldmacher R (1977) On the deletion of nonplanar edges of a graph. In *Proc. 10th Southeastern Conference on Combinatorics, Graph Theory, and Computing*

Mahadevan R, Schilling C (2003) The effects of alternate optimal solutions in constraint-based genome-scale metabolic models. *Metabolic Engineering* **5**: 264–276

Meister M, Lowe G, Berg HC (1987) The proton flux through the bacterial flagellar motor. *Cell* **49**: 643–650

Mitchell JG, Pearson L, Bonazinga A, Dillon S, Khouri H, Paxinos R (1995) Long lag times and high velocities in the motility of natural assemblages of marine bacteria. *Applied and environmental microbiology* **61**: 877–82

Moran MA, Belas R, Schell MA, González JM, Sun F, Sun S, Binder BJ, Edmonds J, Ye W, Orcutt B, Howard EC, Meile

C, Palefsky W, Goesmann A, Ren Q, Paulsen I, Ulrich LE, Thompson LS, Saunders E, Buchan A (2007) Ecological genomics of marine Roseobacters. *Applied and environmental microbiology* **73**: 4559–69

Oberhardt Ma, Palsson BO, Papin Ja (2009) Applications of genome-scale metabolic reconstructions. *Molecular systems biology* **5**: 320

Orth JD, Conrad TM, Na J, Lerman Ja, Nam H, Feist AM, Palsson BO (2011) A comprehensive genome-scale reconstruction of Escherichia coli metabolism–2011. *Molecular systems biology* **7**: 535

Pagani I, Liolios K, Jansson J, Chen IMa, Smirnova T, Nosrat B, Markowitz VM, Kyrpides NC (2012) The Genomes OnLine Database (GOLD) v.4: status of genomic and metagenomic projects and their associated metadata. *Nucleic acids research* **40**: D571–9

Pey J, Prada J, Beasley JE, Planes FJ (2011) Path finding methods accounting for stoichiometry in metabolic networks. *Genome biology* **12**: R49

Puchałka J, Oberhardt Ma, Godinho M, Bielecka A, Regenhardt D, Timmis KN, Papin Ja, Martins dos Santos VaP (2008) Genome-scale reconstruction and analysis of the Pseudomonas putida KT2440 metabolic network facilitates applications in biotechnology. *PLoS computational biology* **4**: e1000210

Quester S, Schomburg D (2011) EnzymeDetector: an integrated enzyme function prediction tool and database. *BMC bioinformatics* **12**: 376

Riemer SA, Rex R, Schomburg D (submitted 2012) A metabolite-centric view on flux distributions in genome-scale metabolic models. *BMC Systems Biology*

Scheer M, Grote A, Chang A, Schomburg I, Munaretto C, Rother M, Söhngen C, Stelzer M, Thiele J, Schomburg D

(2011) BRENDA, the enzyme information system in 2011. *Nucleic acids research* **39**: D670–6

Schellenberger J, Lewis NE, Palsson BO (2011) Elimination of thermodynamically infeasible loops in steady-state metabolic models. *Biophysical journal* **100**: 544–53

Shapleigh JP (2011) Oxygen control of nitrogen oxide respiration, focusing on α-proteobacteria. *Biochemical Society transactions* **39**: 179–83

Sowa Y, Berry RM (2008) Bacterial flagellar motor. *Quarterly reviews of biophysics* **41**: 103–32

Taglicht D, Padan E, Schuldiner S (1993) Proton-sodium stoichiometry of NhaA, an electrogenic antiporter from Escherichia coli. *The Journal of biological chemistry* **268**: 5382–7

Thiele I, Palsson BO (2010) A protocol for generating a high-quality genome-scale metabolic reconstruction. *Nature Protocols* **5**: 93–121

Thomas Ma, Suntharalingam P, Pozzoli L, Devasthale A, Kloster S, Rast S, Feichter J, Lenton TM (2011) Rate of non-linearity in DMS aerosol-cloud-climate interactions. *Atmospheric Chemistry and Physics* **11**: 11175–11183

Tomasch J, Gohl R, Bunk B, Diez MS, Wagner-Döbler I (2011) Transcriptional response of the photoheterotrophic marine bacterium Dinoroseobacter shibae to changing light regimes. *The ISME journal* **5**: 1957–68

Vázquez J, González M, Murado M (2004) A new marine medium. *Enzyme and Microbial Technology* **35**: 385–392

Wagner-Döbler I, Ballhausen B, Berger M, Brinkhoff T, Buchholz I, Bunk B, Cypionka H, Daniel R, Drepper T, Gerdts G, Hahnke S, Han C, Jahn D, Kalhoefer D, Kiss H, Klenk HP, Kyrpides N, Liebl W, Liesegang H, Meincke L, *et al.* (2010) The complete genome sequence of the algal symbiont Dinoroseobacter shibae: a hitchhiker's guide to life in the sea. *The ISME journal* **4**: 61–77

Wagner-Döbler I, Biebl H (2006) Environmental biology of the marine Roseobacter lineage. *Annual review of microbiology* **60**: 255–80

Xiao N, Jiao N (2011) Formation of polyhydroxyalkanoate in aerobic anoxygenic phototrophic bacteria and its relationship to carbon source and light availability. *Applied and environmental microbiology* **77**: 7445–50

Yeliseev Aa, Kaplan S (1997) Anaerobic carotenoid biosynthesis in Rhodobacter sphaeroides 2.4.1: H2O is a source of oxygen for the 1-methoxy group of spheroidene but not for the 2-oxo group of spheroidenone. *FEBS Letters* **403**: 10–14

Yurkov VV, Beatty JT (1998) Aerobic anoxygenic phototrophic bacteria. *Microbiology and molecular biology reviews MMBR* **62**: 695–724